

**ON EFFICIENT ESTIMATION OF CONTROL CHART PARAMETERS  
FOR NORMAL AND AUTOCORRELATED PROCESSES**

BY

**ABDALJBBAR BABIKER ABDALJBBAR DAWOD**

A Thesis Presented to the  
DEANSHIP OF GRADUATE STUDIES

**KING FAHD UNIVERSITY OF PETROLEUM & MINERALS**

DHAHRAN, SAUDI ARABIA

In Partial Fulfillment of the  
Requirements for the Degree of

**MASTER OF SCIENCE**

In  
APPLIED STATISTICS


**MAY 2017**

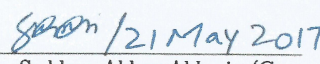
KING FAHD UNIVERSITY OF PETROLEUM & MINERALS  
DHAHRAN 31261. SAUDI ARABIA

DEANSHIP OF GRADUATE STUDIES

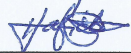
This thesis, written by **ABDALJBBARBABIKER ABDALJBBAR DAWOD** under the direction of his thesis adviser and approved by his thesis committee, has been presented to and accepted by the Dean of Graduate Studies, in partial fulfillment of the requirements for the degree of **MASTER OF SCIENCE IN APPLIED STATISTICS**.

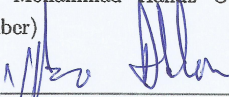
Thesis Committee

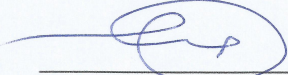
  
Dr. Marwan Al-Momani (Adviser)


  
Dr. Saddam Akbar Abbasi (Co-adviser)

  
Dr. Muhammad Riaz (Member)

  
Dr. Mohammad Hafidz Omar (Member)

  
Dr. Nasir Abbas (Member)

  
Dr. Hussein Al-Attas  
Department Chairman

  
Dr. Salam A. Zummo  
Dean of Graduate Studies

  
Date



©Dawod  
2017

*I dedicate this work to my family and many friends. A special feeling of gratitude to my loving parents, Babiker and Hawa whose words of encouragement and push for tenacity ring in my ears. My sisters have never left my side and are very special.*

# ACKNOWLEDGMENTS

All glorification and gratitude to Allah Almighty who has given me the power to accomplish this thesis.

I sincerely thank my supervisor, Dr. Marwan Al-Momani for his guidance, help and continuous encouragement. I am grateful to him for his advice and deep look during my study without which it would not have been possible to finish my thesis in time.

I would also like to thank my co-supervisor, Dr. Saddam Akbar Abbasi for his guidance, caring and providing me with a solution to all problems I had faced in the linear profile as well as the coefficient of variation control charts during the preparation of this work.

My thanks also go to the advisory committee members Dr. Muhammad Riaz, Dr. Mohammad Hafidz Omar and Dr. Nasir Abbas for their patience for reading the thesis and providing with useful suggestions and comments which have improved it.

My thanks extended to all faculty, staff members, and the graduate students in Department of Mathematics and Statistics. Also, I would like to acknowledge the King Fahd University of Petroleum and Minerals (KFUPM) for the scholarship to fulfill my M.Sc. study.

I must also thank my parents/sisters for their support, patience, love, sacrifices and prayers that have not stopped during all my life. All words of gratitude are unable to acknowledge their real contribution.

At the end, I will not forget to dedicate some of my efforts and prayers to my relatives who are settling in refugee camps and ask Allah Almighty to give them the peace.

# TABLE OF CONTENTS

ACKNOWLEDGEMENT	v
LIST OF TABLES	xi
LIST OF FIGURES	xvi
LIST OF SYMBOLS	xviii
ABSTRACT (ENGLISH)	xx
ABSTRACT (ARABIC)	xxii
<b>CHAPTER 1 INTRODUCTION AND LITERATURE REVIEW</b>	<b>1</b>
1.1 Introduction . . . . .	1
1.1.1 Restricted estimator . . . . .	5
1.1.2 Pretest estimator . . . . .	5
1.1.3 Shrinkage estimator . . . . .	6
1.1.4 Positive shrinkage estimator . . . . .	6
1.2 Literature Review . . . . .	7
1.2.1 GARCH model . . . . .	7
1.2.2 Linear Profiles . . . . .	8
1.2.3 CV Control chart in phase I . . . . .	9
1.3 Thesis Organization and Contributions . . . . .	9
<b>CHAPTER 2 SHRINKAGE ESTIMATION OF THE ARCH MODEL</b>	<b>12</b>

2.1	Introduction . . . . .	12
2.2	Preliminary definitions . . . . .	14
2.3	GARCH model . . . . .	17
2.4	Estimating ARCH(q) parameters . . . . .	21
2.4.1	Estimation of the parameter $\theta$ . . . . .	23
2.4.2	Estimation of $\sigma_0^2$ . . . . .	23
2.4.3	Estimation of the information matrices . . . . .	24
2.4.4	Asymptotic distribution of the OLS estimator . . . . .	25
2.5	Improved Estimation Strategies . . . . .	26
2.5.1	Restricted estimator . . . . .	26
2.5.2	Pretest estimator . . . . .	28
2.5.3	Shrinkage estimator . . . . .	29
2.5.4	Positive shrinkage estimator . . . . .	29
2.6	Asymptotic Results . . . . .	29
2.6.1	Joint normality of the unrestricted and restricted estimators	30
2.6.2	Asymptotic Bias and Quadratic Bias . . . . .	38
2.6.3	Quadratic Weighted risks . . . . .	41
2.7	Risk Analysis of the Estimators . . . . .	49
2.7.1	Comparison of $\hat{\theta}^U$ and $\hat{\theta}^R$ . . . . .	49
2.7.2	Comparison of $\hat{\theta}^{PT}$ and $\hat{\theta}^U$ . . . . .	52
2.7.3	Comparison of $\hat{\theta}^S$ and $\hat{\theta}^U$ . . . . .	53
2.7.4	Comparison of $\hat{\theta}^S$ and $\hat{\theta}^{S+}$ . . . . .	53
2.8	MSE-Matrix Analysis of the Estimator . . . . .	54
2.8.1	Comparison of $\hat{\theta}^R$ and $\hat{\theta}^U$ . . . . .	55
2.8.2	Comparison of $\hat{\theta}^{PT}$ and $\hat{\theta}^U$ . . . . .	56
2.8.3	Comparison of $\hat{\theta}^S$ and $\hat{\theta}^U$ . . . . .	59
2.8.4	Comparison of $\hat{\theta}^S$ and $\hat{\theta}^{S+}$ . . . . .	60
2.9	Numerical Studies . . . . .	61
2.9.1	Monte Carlo simulation experiments . . . . .	61
2.9.2	Application on Standard & Poor 500 (SP500) stock market	98



2.10 Conclusion . . . . .	102
<b>CHAPTER 3 ON EFFICIENT ESTIMATION STRATEGIES IN</b>	
<b>MONITORING OF LINEAR PROFILES</b>	<b>104</b>
3.1 Introduction . . . . .	104
3.2 Simple Linear regression model . . . . .	107
3.3 Efficient estimation strategies . . . . .	109
3.3.1 Slope parameter . . . . .	110
3.3.2 Intercept parameter . . . . .	113
3.3.3 Residuals . . . . .	115
3.4 Monitoring linear profile coefficients in phase II . . . . .	116
3.5 Performance evaluation of charts in phase II . . . . .	119
3.6 Discussion and comparative analysis . . . . .	121
3.7 Illustrative example . . . . .	138
3.7.1 Darcy law of single-phase flow . . . . .	138
3.7.2 multiphase flow . . . . .	140
3.7.3 Experimental setup and data description . . . . .	140
3.7.4 Implementation of $EWMA_R$ and $EWMA_{PT}$ charts . . . . .	143
3.8 Summary and conclusions . . . . .	144
<b>CHAPTER 4 THE PERFORMANCE OF PHASE I COEFFICIENT</b>	
<b>OF VARIATION CONTROL CHARTS FOR PROCESS MONI-</b>	
<b>TORING</b>	<b>147</b>
4.1 Introduction . . . . .	147
4.2 Monitoring of process CV in phase I . . . . .	149
4.2.1 Control chart structure . . . . .	151
4.3 Simulation study . . . . .	153
4.4 Results and discussion . . . . .	154
4.4.1 The effect of $n$ , CV ( $\gamma$ ) and $m$ on PTS . . . . .	158
4.4.2 Simulation experiment . . . . .	164
4.5 Real life example . . . . .	167

4.6	Summary and conclusion . . . . .	169
<b>CHAPTER 5 CONCLUSION AND FUTURE RESEARCH</b>		<b>171</b>
5.1	Future Research . . . . .	174
<b>APPENDICES</b>		<b>175</b>
A.1	Courant Theorem . . . . .	175
A.2	Adjustment Constants ( $d_2$ and $d_3$ ) . . . . .	176
<b>REFERENCES</b>		<b>177</b>
<b>VITAE</b>		<b>187</b>

# LIST OF TABLES

2.1	Simulated relative efficiency of the restricted, pretest and shrinkage estimators with respect to $\hat{\theta}^U$ when $n = 30, q = 8, m = 3$ . . . . .	69
2.2	Simulated relative efficiency of the restricted, pretest and shrinkage estimators with respect to $\hat{\theta}^U$ when $n = 30; q = 9, m = 4$ . . . . .	70
2.3	Simulated relative efficiency of the restricted, pretest and shrinkage estimators with respect to $\hat{\theta}^U$ when $n = 30; q = 10, m = 5$ . . . . .	71
2.4	Simulated relative efficiency of the restricted, pretest and shrinkage estimators with respect to $\hat{\theta}^U$ when $n = 30; q = 14, m = 9$ . . . . .	72
2.5	Simulated relative efficiency of the restricted, pretest and shrinkage estimators with respect to $\hat{\theta}^U$ when $n = 30; q = 17, m = 12$ . . . . .	73
2.6	Simulated relative efficiency of the restricted, pretest and shrinkage estimators with respect to $\hat{\theta}^U$ when $n = 30; q = 20, m = 15$ . . . . .	74
2.7	Simulated relative efficiency of the restricted, pretest and shrinkage estimators with respect to $\hat{\theta}^U$ when $n = 50; q = 8, m = 3$ . . . . .	75
2.8	Simulated relative efficiency of the restricted, pretest and shrinkage estimators with respect to $\hat{\theta}^U$ when $n = 50; q = 9, m = 4$ . . . . .	76
2.9	Simulated relative efficiency of the restricted, pretest and shrinkage estimators with respect to $\hat{\theta}^U$ when $n = 50; q = 10, m = 5$ . . . . .	77
2.10	Simulated relative efficiency of the restricted, pretest and shrinkage estimators with respect to $\hat{\theta}^U$ when $n = 50; q = 14, m = 9$ . . . . .	78
2.11	Simulated relative efficiency of the restricted, pretest and shrinkage estimators with respect to $\hat{\theta}^U$ when $n = 50; q = 17, m = 12$ . . . . .	79

2.12	Simulated relative efficiency of the restricted, pretest and shrinkage estimators with respect to $\hat{\theta}^U$ when $n = 50$ ; $q = 20$ , $m = 15$ . . . .	80
2.13	Simulated relative efficiency of the restricted, pretest and shrinkage estimators with respect to $\hat{\theta}^U$ when $n = 75$ ; $q = 8$ , $m = 3$ . . . .	81
2.14	Simulated relative efficiency of the restricted, pretest and shrinkage estimators with respect to $\hat{\theta}^U$ when $n = 75$ ; $q = 9$ , $m = 4$ . . . .	82
2.15	Simulated relative efficiency of the restricted, pretest and shrinkage estimators with respect to $\hat{\theta}^U$ when $n = 75$ ; $q = 10$ , $m = 5$ . . . .	83
2.16	Simulated relative efficiency of the restricted, pretest and shrinkage estimators with respect to $\hat{\theta}^U$ when $n = 75$ ; $q = 14$ , $m = 9$ . . . .	84
2.17	Simulated relative efficiency of the restricted, pretest and shrinkage estimators with respect to $\hat{\theta}^U$ when $n = 75$ ; $q = 17$ , $m = 12$ . . . .	85
2.18	Simulated relative efficiency of the restricted, pretest and shrinkage estimators with respect to $\hat{\theta}^U$ when $n = 75$ ; $q = 20$ , $m = 15$ . . . .	86
2.19	Simulated relative efficiency of the restricted, pretest and shrinkage estimators with respect to $\hat{\theta}^U$ when $n = 100$ ; $q = 8$ , $m = 3$ . . . .	87
2.20	Simulated relative efficiency of the restricted, pretest and shrinkage estimators with respect to $\hat{\theta}^U$ when $n = 100$ ; $q = 9$ , $m = 4$ . . . .	88
2.21	Simulated relative efficiency of the restricted, pretest and shrinkage estimators with respect to $\hat{\theta}^U$ when $n = 100$ ; $q = 10$ , $m = 5$ . . . .	89
2.22	Simulated relative efficiency of the restricted, pretest and shrinkage estimators with respect to $\hat{\theta}^U$ when $n = 100$ ; $q = 14$ , $m = 9$ . . . .	90
2.23	Simulated relative efficiency of the restricted, pretest and shrinkage estimators with respect to $\hat{\theta}^U$ when $n = 100$ ; $q = 17$ , $m = 12$ . . . .	91
2.24	Simulated relative efficiency of the restricted, pretest and shrinkage estimators with respect to $\hat{\theta}^U$ when $n = 100$ ; $q = 20$ , $m = 15$ . . . .	92
2.25	Simulated relative efficiency of the restricted, pretest and shrinkage estimators with respect to $\hat{\theta}^U$ when $n = 150$ ; $q = 8$ , $m = 3$ . . . .	93
2.26	Simulated relative efficiency of the restricted, pretest and shrinkage estimators with respect to $\hat{\theta}^U$ when $n = 150$ ; $q = 9$ , $m = 4$ . . . .	94

2.27	Simulated relative efficiency of the restricted, pretest and shrinkage estimators with respect to $\hat{\theta}^U$ when $n = 150$ ; $q = 10$ , $m = 5$ . . . . .	95
2.28	Simulated relative efficiency of the restricted, pretest and shrinkage estimators with respect to $\hat{\theta}^U$ when $n = 150$ ; $q = 14$ , $m = 9$ . . . . .	96
2.29	Simulated relative efficiency of the restricted, pretest and shrinkage estimators with respect to $\hat{\theta}^U$ when $n = 150$ ; $q = 17$ , $m = 12$ . . . . .	97
2.30	Simulated relative efficiency of the restricted, pretest and shrinkage estimators with respect to $\hat{\theta}^U$ when $n = 150$ ; $q = 20$ , $m = 15$ . . . . .	98
2.31	Relative MSE with respect to $\hat{\theta}^U$ for S&P500 stock market daily closing prices. . . . .	102
3.1	Control chart multiplier $L$ to fix $ARL_0 = 200$ for $EWMA_R$ and $EWMA_{PT}$ control charts with different values of $d$ . . . . .	120
3.2	ARL, MDRL and SDRL comparisons for $d = 0.95$ under intercept shifts from $\beta_0$ to $\beta_0 + \delta\sigma$ . . . . .	122
3.3	ARL, MDRL and SDRL comparisons for $d = 0.75$ under intercept shifts from $\beta_0$ to $\beta_0 + \delta\sigma$ . . . . .	123
3.4	ARL, MDRL and SDRL comparisons for $d = 0.5$ under intercept shifts from $\beta_0$ to $\beta_0 + \delta\sigma$ . . . . .	123
3.5	ARL, MDRL and SDRL comparisons for $d = 0.25$ under intercept shifts from $\beta_0$ to $\beta_0 + \delta\sigma$ . . . . .	124
3.6	ARL, MDRL and SDRL comparisons for $d = 0.1$ under intercept shifts from $\beta_0$ to $\beta_0 + \delta\sigma$ . . . . .	124
3.7	ARL, MDRL and SDRL comparisons for $d = 0.95$ under slope shifts from $\beta_1$ to $\beta_1 + \delta\sigma$ . . . . .	127
3.8	ARL, MDRL and SDRL comparisons for $d = 0.75$ under slope shifts from $\beta_1$ to $\beta_1 + \delta\sigma$ . . . . .	127
3.9	ARL, MDRL and SDRL comparisons for $d = 0.5$ under slope shifts from $\beta_1$ to $\beta_1 + \delta\sigma$ . . . . .	128

3.10	ARL, MDRL and SDRL comparisons for $d = 0.25$ under slope Shifts from $\beta_1$ to $\beta_1 + \delta\sigma$ . . . . .	128
3.11	ARL, MDRL and SDRL comparisons for $d = 0.1$ under slope Shifts from $\beta_1$ to $\beta_1 + \delta\sigma$ . . . . .	129
3.12	ARL, MDRL and SDRL comparisons for $d = 0.95$ under standard deviation shifts from $\sigma$ to $\gamma\sigma$ . . . . .	131
3.13	ARL, MDRL and SDRL comparisons for $d = 0.75$ under standard deviation shifts from $\sigma$ to $\gamma\sigma$ . . . . .	131
3.14	ARL, MDRL and SDRL comparisons for $d = 0.5$ under standard deviation shifts from $\sigma$ to $\gamma\sigma$ . . . . .	132
3.15	ARL, MDRL and SDRL comparisons for $d = 0.25$ under standard deviation shifts from $\sigma$ to $\gamma\sigma$ . . . . .	132
3.16	ARL, MDRL and SDRL comparisons for $d = 0.1$ under standard deviation shifts from $\sigma$ to $\gamma\sigma$ . . . . .	133
3.17	ARL, MDRL and SDRL comparisons for $d = 0.95$ under slope shifts from $\beta_1$ to $\beta_1 + \delta\sigma$ . . . . .	135
3.18	ARL, MDRL and SDRL comparisons for $d = 0.75$ under slope shifts from $\beta_1$ to $\beta_1 + \delta\sigma$ . . . . .	135
3.19	ARL, MDRL and SDRL comparisons for $d = 0.5$ under slope shifts from $\beta_1$ to $\beta_1 + \delta\sigma$ . . . . .	135
3.20	ARL, MDRL and SDRL comparisons for $d = 0.25$ under slope shifts from $\beta_1$ to $\beta_1 + \delta\sigma$ . . . . .	136
3.21	ARL, MDRL and SDRL comparisons for $d = 0.1$ under slope shifts from $\beta_1$ to $\beta_1 + \delta\sigma$ . . . . .	136
3.22	The values of the constant $L$ . . . . .	143
3.23	Control limits for each control chart . . . . .	144
4.1	Control chart multiplier $\mathbf{L}$ to fix FAP at 0.01 for all the control charts. . . . .	154

4.2	The effect of the size of subgroup in the PTS of $\tilde{W}$ with localized CV disturbances, $m = 30, \gamma_0 = 0.05$ . . . . .	159
4.3	The effect of the size of subgroup in the PTS of $\tilde{W}$ with diffuse symmetric CV disturbances, $m = 30, \gamma_0 = 0.05$ . . . . .	160
4.4	The values of the constant multipliers of die casting hot chamber process. . . . .	168
A.1	Control chart coefficients $d_2$ and $d_3$ for different CV control charts.	176

# LIST OF FIGURES

2.1	Simulated relative efficiency of the restricted, pretest and shrinkage estimators with respect to $\hat{\theta}^U$ when $m = 3$ and $q = 8$ and different sample sizes. . . . .	64
2.2	Simulated relative efficiency of the restricted, pretest and shrinkage estimators with respect to $\hat{\theta}^U$ when $m = 4$ and $q = 9$ and different sample sizes. . . . .	65
2.3	Simulated relative efficiency of the restricted, pretest and shrinkage estimators with respect to $\hat{\theta}^U$ when $m = 5$ and $q = 10$ and different sample sizes. . . . .	66
2.4	Simulated relative efficiency of the restricted, pretest and shrinkage estimators with respect to $\hat{\theta}^U$ when $m = 9$ and $q = 14$ and different sample sizes. . . . .	67
2.5	Simulated relative efficiency of the restricted, pretest and shrinkage estimators with respect to $\hat{\theta}^U$ when the sample size is $n = 150$ and different values of $q$ and $m$ . . . . .	68
3.1	ARL comparisons under intercept shifts from $\beta_0$ to $\beta_0 + \delta\sigma$ . . . .	125
3.2	ARL comparisons under intercept Shifts from $\beta_0$ to $\beta_0 + \delta\sigma$ . . . .	125
3.3	ARL comparisons under intercept Shifts from $\beta_0$ to $\beta_0 + \delta\sigma$ . . . .	126
3.4	ARL comparisons under slope Shifts from $\beta_1$ to $\beta_1 + \delta\sigma$ . . . . .	129
3.5	ARL comparisons under slope Shifts from $\beta_1$ to $\beta_1 + \delta\sigma$ . . . . .	130
3.6	ARL comparisons under slope Shifts from $\beta_1$ to $\beta_1 + \delta\sigma$ . . . . .	130
3.7	ARL comparisons under standard deviation shifts from $\sigma$ to $\gamma\sigma$ . .	133



3.8	ARL comparisons under standard deviation shifts from $\sigma$ to $\gamma\sigma$ . . .	134
3.9	ARL comparisons under standard deviation shifts from $\sigma$ to $\gamma\sigma$ . . .	134
3.10	ARL comparisons under slope Shifts from $\beta_1$ to $\beta_1 + \delta\sigma$ . . . . .	137
3.11	ARL comparisons under slope Shifts from $\beta_1$ to $\beta_1 + \delta\sigma$ . . . . .	137
3.12	ARL comparisons under slope Shifts from $\beta_1$ to $\beta_1 + \delta\sigma$ . . . . .	138
3.13	Darcy law of the flow of water through sand filter. . . . .	139
3.14	Two-phase experimental setup . . . . .	142
3.15	EWMA <sub>3</sub> . . . . .	145
3.16	$EWMA_R$ . . . . .	145
3.17	$EWMA_{PT}$ . . . . .	146
4.1	The PTS of CV charts with localized CV disturbances, $n = 5, \gamma_0 =$ .05 and $m = 30$ . . . . .	155
4.2	The PTS of CV charts with localized CV disturbances, $n = 10, \gamma_0 =$ .05 and $m = 30$ . . . . .	156
4.3	The PTS of the CV charts with diffuse symmetric CV disturbances, $n = 5, \gamma_0 = .05$ and $m = 30$ . . . . .	157
4.4	The PTS of the CV charts with diffuse symmetric CV disturbances, $n = 10, \gamma_0 = .05$ and $m = 30$ . . . . .	158
4.5	The effect of the CV ( $\gamma$ ) in the PTS of $\tilde{W}$ chart, $m = 30, n = 5$ . . .	162
4.6	The effect of the number of subgroups in the PTS of $\tilde{W}$ with $\gamma_0 =$ 0.05, $n = 5$ . . . . .	163
4.7	The effect of the number of subgroups in the PTS of $\tilde{W}$ with $\gamma_0 =$ 0.05, $n = 5$ . . . . .	164
4.8	The CV Control Charts of the numerical experiment with localized CV disturbances. . . . .	166
4.9	The CV Control Charts of the numerical experiment with diffuse symmetric CV disturbances. . . . .	166
4.10	The CV Control Charts of die casting hot chamber process. . . . .	169

# LIST OF SYMBOLS

$\beta, \theta$	Parameter vectors
$\beta^U, \hat{\theta}^U$	Unrestricted maximum likelihood estimator
$\beta_1^R, \hat{\theta}^R$	Restricted estimator
$\beta^{PT}, \hat{\theta}^{PT}$	Pretest estimator
$\beta^S, \hat{\theta}^S$	James-Stein (Shrinkage) estimator
$\beta^{S+}, \hat{\theta}^{S+}$	Positive shrinkage estimator
$Ch_{min}(A)$	Smallest characteristic root of the matrix $\mathbf{A}$
$Ch_{max}(A)$	Largest characteristic root of the matrix $\mathbf{A}$
$\Delta^2$	Non-centrality parameter
$\mathbf{I}$	Identity matrix
$\mathbf{I}(\cdot)$	Indicator function
$\mathbf{R}$	A $(q \times m)$ known matrix of rank $m$
$H_0$	Null hypothesis
$H_n$	A class of local alternatives
$G_m(\mathcal{L}_\alpha; \Delta^2)$	A non-central chi-square distribution function with $m$ -degrees of freedom and non-centrality parameter $\Delta^2$

$\mathbf{r}$	A $(m \times 1)$ vector of known constants
$\mathbf{L}(\cdot, \cdot)$	Quadratic loss function
$\mathbf{W}$	A $(q \times q)$ positive semidefinite matrix
$\mathbf{q}$	Number of parameters in the $\boldsymbol{\beta}, \boldsymbol{\theta}$ vector under the full model
$\mathbf{m}$	Number of parameters in the $\boldsymbol{\beta}, \boldsymbol{\theta}$ vector under the reduced model
$tr(\mathbf{A})$	Trace of the matrix $\mathbf{A}$
$\lambda$	Tuning parameter
$\mathcal{L}_n$	Test statistic
$\zeta$	A $(m \times 1)$ fixed vector in $\mathbb{R}^m$
$\Sigma_Y$	Variance covariance matrix of $\mathbf{Y}$
$\ \cdot\ $	Euclidean norm
$d$	The degree of distrust in the null hypothesis
$\gamma$	coefficient of variation
$W_i, V_i$	Estimated coefficient of variation

# THESIS ABSTRACT

**NAME:** Abdaljbbar Babiker Abdaljbbar Dawod

**TITLE OF STUDY:** On Efficient Estimation of Control Chart Parameters for Normal and Autocorrelated Processes

**MAJOR FIELD:** Applied Statistics

**DATE OF DEGREE:** MARCH 2017

The estimation technique of any statistical model's parameters has a vital role in the performance of the underlying model. Therefore, using these techniques might not be beneficial in some circumstances. In this thesis, we have proposed shrinkage estimation strategy for ARCH model, we also investigated the performance of the linear profile charts in Phase II under the restricted and pretest estimation strategies. Besides, we investigated the performance of the coefficient of variation (CV) control charts in phase I under different estimation strategies.

We have investigated the performance of our proposed methods using different measures including the mean square error, probability to signal and average run length properties. We have compared our results with the well-known conven-

tional methodologies under different settings. Our results showed that the proposed methods excel the existing methods under different conditions. In addition, we have used practical datasets from real world processes and implemented our proposed techniques to show their application in real processes.

## ملخص الرسالة

الاسم: عبدالجبار بابكر عبدالجبار داود  
عنوان الرسالة: تحسين تقدير معالم مخططات التحكم للعمليات الخطية و غير الخطية  
التخصص الرئيسي: الأحصاء التطبيقي  
تاريخ الدرجة: مايو 2017

طريقة تقدير معالم أي نموذج إحصائي له الأثر الكبير في جودة النموذج المعني. طرق التقدير المعروفة المستخدمة في نمذجة معظم الظواهر هي طرق تقليدية. هذه الطرق التقليدية ربما لا تكون مناسبة تحت بعض الظروف. في هذه الأطروحة، إقترحنا طريقة التقدير المنكمش لنموذج ARCH، أيضا تحققنا من أداء مخططات الظاهرة الخطية (linear profile) في المرحلة الثانية باستخدام طريقة التقدير المقيد (Restricted) و طريقة الإختبار الأولي. بجانب التحقق من إستخدام طرق التقدير المختلفة في أداء مخططات معامل الإختلاف في المرحلة الأولى.

قمنا بالتحقق من أداء الطرق المقترحة باستخدام مقاييس مختلفة تتضمن متوسط مربعات الخطأ، الإحتمالية للإشارة و متوسط طول المدى. قمنا بمقارنة نتائجنا مع بعض الطرق المعروفة تحت الظروف المختلفة. أظهرت النتائج أن الطرق المقترحة تتفوق على الطرق الموجودة تحت الظروف المختلفة. علاوة إلى ذلك، إستخدمنا بيانات حقيقة من عمليات واقعية و قمنا بتطبيق الطرق المقترحة عليها.

## CHAPTER 1

# INTRODUCTION AND LITERATURE REVIEW

### 1.1 Introduction

Statistical models are used to represent the relationship between the real world phenomena, consequently, practitioners will be able to study and investigate the characteristics of these relationships. As these models incorporate variant types of phenomena; some of these phenomena play the role of responses or dependent variables and the others represent the predictors or independent variables.

After the mid of the twentieth century, statistical science shown vast development and it has been adopted in most of the day-today's activities. For instance, among the most flourishing disciplines that use statistical modeling as a backbone are:

- **Financial markets:** statistics is used widely in the business industry as a

modeling tool for some phenomena such as, forecasting the volatility, inflation rate, foreign exchange rates, etc. A set of time series models are incorporated, such as Autoregressive Integrated Moving Average (ARIMA), Generalized Autoregressive Conditional Heteroscedastic (GARCH) and other models.

- **Quality control:** in manufacturing, statistics has been involved as a monitoring tool, it offers Statistical Process Control (SPC) approach to monitor and manage the assignable causes of variation in manufacturing or service. SPC has been applied in variant applications, such as medicine, business, engineering and social sciences. Control charts are the most widely used SPC toolkit, it is used to monitor location, dispersion, Coefficient of Variation (CV), intercept, slope, etc.

Generally, statistical models can be represented mathematically as

$$y = f(\mathbf{X}, \boldsymbol{\beta}) + \epsilon, \tag{1.1}$$

where  $\mathbf{y} = (y_1, \dots, y_n)$  is  $n \times 1$  vector of responses or outcomes of the phenomenon whose variation is being studied,  $X = (\mathbf{x}_1, \dots, \mathbf{x}_q)$  represent  $n \times q$  predictors or the inputs or causes,  $\boldsymbol{\beta} = (\beta_1, \dots, \beta_q)$  is an unknown  $q \times 1$  vector of parameters and  $\epsilon = (\epsilon_1, \dots, \epsilon_n)$  is  $n \times 1$  vector of unobserved error term. So, models explain the effects that the independent variables have on the dependent variables.



In order to perform statistical tests on the model's parameters in (1.1), the unknown quantities should be estimated. Usually, practitioners estimate the unknown parameters based on the sample information while, others use the sample and non-sample information. Finding a consistent model by using any non-sample information has a vital role in making inferences and predictions about the behaviour of estimators. The non-sample information is known by *uncertain prior information* (UPI), and injecting the UPIs into the estimators is known by *Bayesian statistical methods*.

When an estimator is obtained using sample information without any non-sample information, it is referred as unrestricted estimator (UE) and denoted by  $\beta^U$ . Usually in case of  $\beta^U$ , the corresponding model is recognized as a *full model*, because all the parameters are included even though some of them may not have a significant effect, in contrast, suppose that the UPI is available, and we believe some of the parameters are not important, in such cases, the UPI can be formulated in the form of the following linear hypothesis

$$H_0 : R\beta = \mathbf{r}, \tag{1.2}$$

where  $R$  is  $m \times q$  known matrix of rank( $m$ ) ( $m \leq q$ ),  $\mathbf{r}$  is an  $m \times 1$  vector of known constants,  $q$  is the total number of parameters in (1.1) and  $m$  is number of parameters with significant effect in (1.1).

A family of estimation strategies that involve the use of the non-sample information have been introduced in the literature, they outperform the traditional

estimators under particular conditions by considering the mean squared error and the risk of the estimators as criteria.

There has been many studies in the area of efficient estimation relying on the work of Bancroft (1944) and Hansen (1982) that was known by the preliminary test estimator that uses UPI in addition to the sample information. Then, Stein et al. (1956) introduced an improvement of the preliminary test of Bancroft, known as shrinkage estimator or Stein-rule for multivariate normal population that dominates the usual maximum likelihood estimator under the squared error loss criterion.

In this thesis we propose an improved estimation strategies for the parameters of some statistical models. We consider processes with constant variances as well as non-constant variances. In the state of processes with non-constant variances, we propose efficient estimators for some time series models, in particular, ARCH model. In addition to that, we investigate different estimators for the CV of a process with applications in control chart. Alternatively, under the state of constant variances processes we consider more efficient estimators of linear profile monitoring.

In the following subsections, we consider alternative estimation strategies of  $\beta$  when some UPIs are available.

### 1.1.1 Restricted estimator

When the UPI(s) is formulated as the hypothesis in (1.2), in which it shows that there are some of the given parameters are zeros or, there is a restriction on some parameters. Then, the estimated parameters under such UPI criteria is known as *restricted estimator* (R) and is denoted simply by  $\beta^R$ .

### 1.1.2 Pretest estimator

The pretest estimate of  $\beta$ , denoted by  $\beta^{PT}$  is defined by:

$$\beta^{PT} = \begin{cases} \beta^U, & \text{if } \mathcal{L}_n \geq \mathcal{L}_{n,\alpha}, \\ \beta^R, & \text{if } \mathcal{L}_n < \mathcal{L}_{n,\alpha}, \end{cases} \quad (1.3)$$

where  $\mathcal{L}_n$  is a suitable test statistics for testing the hypothesis in (1.2), and  $\mathcal{L}_{n,\alpha}$  as the  $\alpha$ -critical value from the distribution of  $\mathcal{L}_n$ .

The pretest estimator is a binary choice function, it chooses  $\beta^U$  if the null hypothesis is rejected and  $\beta^R$  if the test fails to reject the null hypothesis. Alternatively,  $\beta^{PT}$  can be written as follows,

$$\begin{aligned} \beta^{PT} &= \beta^R I(\mathcal{L} \leq \mathcal{L}_\alpha) + \beta^U I(\mathcal{L} > \mathcal{L}_\alpha) \\ &= \beta^U - (\beta^U - \beta^R) I(\mathcal{L} \leq \mathcal{L}_\alpha), \end{aligned} \quad (1.4)$$

where  $I(A)$  is an indicator function of the set A.

### 1.1.3 Shrinkage estimator

The shrinkage estimator of Stein et al. (1956), denoted by  $\beta^S$ , is defined by:

$$\beta^S = \beta^R + \left[1 - \frac{m-2}{\mathcal{L}_n}\right](\beta^U - \beta^R), m \geq 3. \quad (1.5)$$

It is clear that  $\beta^S$  is not a binary choice anymore, whether  $H_0$  is rejected or not, shrinkage estimator is a smoothed function of  $\beta^U$  and  $\beta^R$ . So,  $\beta^S$  does not represent a convex combination of the two choices, and suffers from a phenomena known as over-shrinkage, which happens when  $\mathcal{L}_n$  is smaller than  $(m-2)$  and hence, unexpected signs for some of the estimated parameters may be obtained.

### 1.1.4 Positive shrinkage estimator

A modified version of James-Stein estimator has been proposed by Stein (1966) to overcome the phenomena of over-shrinkage estimator, it is known as positive shrinkage part, denoted by  $\beta^{S+}$ , and defined by:

$$\beta^{S+} = \beta^U + \left[1 - \frac{m-2}{\mathcal{L}_n}\right]^+ (\beta^U - \beta^R), m \geq 3, \quad (1.6)$$

where  $Z^+ = \max(0, Z)$ .

More useful discussion about shrinkage strategies can be found in Bancroft (1944); Stein (1956); Khan and Hoque (2002); Khan et al. (2005); Saleh (2006); Ahmed et al. (2015); Al-Momani et al. (2016).

## 1.2 Literature Review

In the following subsections we give an introductory literature review of the topics we will discuss in the forthcoming chapters.

### 1.2.1 GARCH model

As volatility forecasting is an important financial matter, a precise and accurate volatility forecast is essential to traders, investors and financial analysts. Before 1980s econometricians were relying on ARIMA models to model the financial time series, whereas these models enforce some distributional constraints such as, linearity, normality and the constant variance. In contrast, many financial time series exhibit fat tails, leverage effect, long memory and variances change over time and large (small) changes tend to be followed by small (large) changes of either sign. Hence, financial time series violate the assumptions of ARIMA models. Engle (1982) was the pioneer who proposed a stationary non-linear model for the economical time series. He introduced Autoregressive Conditionally Heteroscedastic (ARCH) model, where it is the conditional variance of a series  $\{y_k\}$  that changes according to an autoregressive-type process.

Since the early of 1980s; ARCH model has been vastly adopted in the modeling of time series with non-constant conditional variance. Reasons that urged for the large usage of ARCH model in time series analysis are: the time-varying conditional variance of ARCH model provides a more natural measure of risk and uncertainty, in addition, the statistical properties of ARCH model appear

to provide a parsimonious and accurate characteristics of a lot of economic time series. Engle's model recognizes the difference between the unconditional and the conditional variance by allowing the latter to change over time as a function of past errors. For more details see Engle (1982); Bollerslev (1986).

### 1.2.2 Linear Profiles

Many studies have been carried out to improve control charts for linear profiling, for example, Kang and Albin (2000) introduced two control chart structures to monitor a semiconductor manufacturing that was formulated as a simple linear regression with known coefficients. They used multivariate  $T^2$  chart and EWMA/Range(R) chart (i.e., EWMA chart in conjunction with R chart to monitor the mean and the variation respectively). Their charts based on the bivariate normality assumptions of the least square estimators. Kim et al. (2003) proposed a control chart as combination of three univariate EWMA charts to monitor the intercept, slope and the standard deviation in phase II simultaneously as the run length coming from the first chart to signal. The idea behind using simultaneous monitoring of the three charts is that at least one of three parameters would directly affects the state of the process. They transformed the predictor variable to give an average zero, that will get rid of the dependency between the intercept and the slope. Hence, having a control chart for each parameter led to easier diagnosis of the process change than the control chart of Kang and Albin (2000).

### **1.2.3 CV Control chart in phase I**

Many researchers have contributed in the development of the CV control charts structures, for example Kang et al. (2007) were the pioneers who introduced Shewhart control charts to monitor the CV. Hong et al. (2008) proposed EWMA control chart as an improvement of Kang et al. (2007) method, their results showed a significant improvement in the detection of small shifts. Castagliola et al. (2011) suggested two one-sided EWMA charts based on the squared CV as the monitoring statistic, it showed an improvement compared to the chart proposed by Hong et al. (2008). Calzada and Scariano (2013) suggested a control chart for monitoring CV which performed better than the method of Kang et al. (2007).

## **1.3 Thesis Organization and Contributions**

In this thesis, we elaborate the problem of finding efficient estimators in different environments as it has a central importance in all statistical models. We extend the general framework of the restricted, preliminary test, shrinkage estimation strategies in some time series models and linear profile when UPI is available. We also study the characteristics of different CV estimator and their impact in the performance of CV control charts in phase I.

The highlights of our contribution in this thesis are organized and summarized as follow

Chapter 2 is dedicated to apply the shrinkage estimation strategies on the ARCH model. This chapter was organized as follows: We list some the preliminary def-

initions of some conceptual terminologies that will be used in the forthcoming sections, with a definition of ARCH model and some related formulas. Next, We discuss the parameters estimation. Then we introduced the concept of restricted, pretest and shrinkage estimations of ARCH model. Hence, we derive the asymptotic properties of the estimators and compare their performances using the risk analysis and the mean square error in the next one. A simulation study was conducted to assure the analytical results. A conclusion is provided at the end of this chapter.

In chapter 3, we consider restricted and pretest estimation strategies for the simple linear regression with applications in the linear profiling. At the beginning of this chapter we introduced terminologies and assumptions of the simple linear regression. We propose the restricted and pretest estimations of simple linear regression model. Based on those estimators, we construct the limits of our control charts. We propose the strategy of performance evaluation of the different control charting structures via the average run length (ARL). We conduct extensive simulation study and discuss the results of our proposed estimators. A real world example was considered to assure our simulated results. We close this chapter by a summary and conclusion.

In Chapter 4, we study the performance of different CV control charts for process monitoring in phase I. We give a brief introduction and literature review of the CV control charts. Different estimators of CV have been used to construct control charts to monitor the CV in phase I. We illustrate the steps of our simulation



study, then we report our results and the associated discussion. A real world example is considered as a case study for our simulated results. Finally, we wrap up the chapter by reporting the most important findings of the chapter with the associated recommendation.

In Chapter 5, we summarize the results of the thesis and present recommendations for the future work.

The contributions in this dissertation are summarized as follows:

1. We propose the restricted, pretest, and shrinkage estimators for estimating the volatility in ARCH model. We indicate the importance of using the prior information in producing a sub-model, which carefully represents the data, and reduces the model complexity.
2. Analytical results on the risks and biases of the restricted, pretest, shrinkage and full model estimators are derived in terms of distributional biases and risks. The mean squared error matrices of these estimators are also derived and compared analytically and numerically with respect to the OLS estimator.
3. We utilize the restricted and pretest estimators to estimate the parameters of simple linear profile, then drive the control charts for linear profile monitoring. Then, we investigate the performance of the control charts for linear profile monitoring in phase II.
4. Finally, we investigate the effect of different CV estimators in the performance of the CV control charts in phase I.

## CHAPTER 2

# SHRINKAGE ESTIMATION OF THE ARCH MODEL

### 2.1 Introduction

Modeling and forecasting financial markets is a motivating and urging issue for both the investors and researchers. Financial markets are extremely manipulated by a number of factors such as, interest rates, political issues, inflation rates, foreign exchange rates, etc. In particular, stock markets are characterized by uncertainty. Hence, the phenomena is volatile and complex to be forecasted as these manipulation factors have serious consequences on the financial markets.

McNees (1980) reported that the inherited randomness or uncertainty associated with different forecasting regimes vary immensely overtime. He also documented that the large and small errors tend to cluster together in contiguous regimes.

Therefore, a model with a forecasted variance that may change overtime is needed.

At the beginning of the 1960s, many researchers were keen to study the changes in variance, but they were using informal procedures to tackle this problem. For example, Fama (1965) used recursive estimates of the variance overtime. Klein (1977) obtained an estimation of variance by constructing the five-period moving variance about the ten-period moving-mean of annual inflation rate. Khan (1977) utilized the notion of variability rather than variance and used the absolute value of the first difference of the inflation rate. Engle (1983) compared the empirical work of using time-series to measure shifts in the variance overtime with the ARCH estimates for U.S. data.

Tsay (2002) reported that ARCH model encounters weaknesses and drawbacks with some types of economical time series as: the assumption that positive and negative shocks have the same effects on the volatility, because it depends on the square of the previous shocks. Second, it only provides a way to describe the behavior of the conditional variance but it gives no indication about what causes such behavior to occur. Also, the model is likely to over-predict the volatility because it responds slowly to large isolated shocks to the return series.

To overcome the weaknesses and drawbacks of ARCH model, Bollerslev & Taylor (1986) independently generalized Engel's model to Generalized ARCH (GARCH)

as more realistic. The model had inspired the researchers to develop more sophisticated models for modeling the volatility of the financial time series (e.g., EGARCH, GJR-GARCH, F-CHARCH and etc). For more details about sophisticated models, the reader is referred to Fama (1965); Engle and Bollerslev (1986); Bollerslev (1986); Taylor (1986); Satchell and Knight (2002); Francq and Zikoïan (2010).

The rest of the chapter is organized as follows: Section 2.2 contains preliminary definitions of some conceptual terminologies that will be used in the forthcoming sections. Section 2.3 presents the definition of ARCH model and some related formulas. Section 2.4 discusses the parameters estimation of ARCH model. Section 2.5 is dedicated to introduce the concept of restricted, pretest and shrinkage estimations of ARCH model. We derive the asymptotic properties of the estimators in Section 2.6. We compare the performance of the estimators using the risk analysis and the mean square error in Section 2.7 and 2.8, respectively. We conduct extensive simulation study for our selected model and demonstrate the application of the proposed estimators in real life problems in Section 2.9. We close this chapter by conclusion in Section 2.10.

## **2.2 Preliminary definitions**

In this section and the next one, we will list some definitions from Francq and Zikoïan (2010), that will be used in the forthcoming parts of this chapter.

**Definition 2.1** The process  $\{Y_t\}$  is said to be strictly stationary if the vectors  $(y_1, \dots, y_k)$  and  $(y_{1+h}, \dots, y_{k+h})$  have the same joint distribution,  $\forall K, h \in \mathbb{N}$ .

**Definition 2.2** The process  $\{Y_t\}$  is said to be second-order stationary if:

1.  $E(y_t^2) < \infty, \forall t \in \mathbb{Z}$ ,
2.  $E(y_t) < m, \forall t \in \mathbb{Z}$ ,
3.  $\text{cov}(y_t, y_{t+h}) = \gamma_y(h), \forall t, h \in \mathbb{Z}$ ,

where  $\gamma_y(h)$  is called the autocovariance of  $y$  at time  $h$ .

**Remark 1** Autocorrelation function (ACF) of  $\{y_t\}$  is defined by

$$\rho_y(h) = \frac{\gamma_y(h)}{\gamma_y(0)},$$

where  $\gamma_y(h)$  is the autocovariance between  $y_t$  at  $y_{t+h}$  and  $t + h$ ,

and  $\gamma_y(0)$  is the autocovariance of  $y_t$  at time zero.

**Definition 2.3** If  $\{r_t\}$  is a financial time series, e.g, asset prices, stock index, exchange rate, share prices, etc. Instead of analyzing  $(r_t)$  which is often display non-stationary we take  $\log(r_t)$ ,

$$y_t = \log\left(\frac{r_t}{r_{t-1}}\right) = \log\left(1 + \frac{r_t - r_{t-1}}{r_{t-1}}\right), \quad t = 0, \dots, n,$$

and by Taylor-expansion about zero,  $y_t \approx \frac{r_t - r_{t-1}}{r_{t-1}}$ .

**Definition 2.4** A time series  $\{y_t\}$  is said to be white noise if its observations are uncorrelated and has a constant variance.

**Definition 2.5** A time series  $\{y_t\}$  is a weak white noise process if it is second-order stationary with mean zero and ACF given by

$$\rho(h) = \begin{cases} 1, & \text{when } h = 0, \\ 0, & \text{when } h \neq 0. \end{cases}$$

**Definition 2.6** An Autoregressive model of order  $q$  ( $AR(q)$ ) represents a type of random process, where it describes a certain time-varying processes in manufacturing, medicine, economics, etc. The model specifies that the output variable depends linearly on its own previous values with additional stochastic term.

$$y_t = \mu + \phi_1 y_{t-1} + \dots + \phi_q y_{t-q} + \epsilon_t.$$

**Definition 2.7 (Martingale difference)** Let  $\{Z_i\}$  be a  $K$ -dimensional stochastic process ( $K \geq 0$ ) and let  $x_i \in Z_i$  (with  $x_i = z_i$  if  $k=1$ ). The stochastic process  $\{x_i\}$  is a martingale with respect to  $\{z_i\}$ .

$$E(X_i | Z_{i-1}, Z_{i-2}, \dots) = X_{i-1}, \quad \text{for } i = \dots, -1, 0, 1, \dots$$

If  $\{X_i\}$  is a martingale with respect to  $\{Z_i\}$  for every  $X_i \in Z_i$  then we simply say that  $\{Z_i\}$  is a martingale.

**Definition 2.8 (Nonanticipative solution)** The process  $\{y_t\}$  such that  $y_t$  is measurable function of the variable  $\eta_{t-s}, s \geq 0$ . For such process  $\sigma_t$  is independent

of the  $\sigma$ -field generated by  $\{\eta_{t+h}, h \geq 0\}$  and  $y_t$  is independent of the  $\sigma$ -field generated by  $\{\eta_{t+h}, h \geq 0\}$ .

**Definition 2.9 Invertibility** *A time series model is invertible if it can be written as AR model. The essential concept is whether the innovations/noises can be inverted into a representation of past observations. Alternatively, An  $n \times n$  square matrix  $A$  is called invertible (also nonsingular or non-degenerate) if there exists an  $n \times n$  square matrix  $B$  such that*

$$AB = BA = I_n$$

*The thesis mainly deals with invertible matrices.*

## 2.3 GARCH model

Generalized Autoregressive Conditional Heteroscedasticity (GARCH) model. Here we introduce the GARCH model, and consider the existence of strictly stationary solution to this model.

**Definition 2.10** *A process  $\{Y_t\}$  is called strong GARCH( $p, q$ ) process with respect to  $\varepsilon_t$  if*

$$\sqrt{y_t} = \sigma_t \varepsilon_t, \tag{2.1}$$

$$\sigma_t^2 = \omega + \sum_{i=0}^q \alpha_i y_{t-i} + \sum_{j=0}^p \beta_j \sigma_{t-i}^2, \tag{2.2}$$

where  $\epsilon_t$  is the error term, distributed independently and identically with mean 0 and variance 1,  $\omega > 0$ ,  $\alpha_i \geq 0$ ,  $\beta_j \geq 0$  are unknown constants,  $\forall i=1, \dots, q$  and  $j=1, \dots, p$ , and  $\sigma_t^2 = \text{Var}(\sqrt{y_t}|\sqrt{y_{t-1}})$ .

The process  $\{Y_t\}$  can be represented in a matrix form as

$$\mathbf{Y}_t = \mathbf{b}_t + A_t \mathbf{Y}_{t-1}, \quad (2.3)$$

where

$$\mathbf{Y}_t = \begin{bmatrix} y_t \\ \vdots \\ y_{t-q+1} \\ \sigma_t^2 \\ \vdots \\ \sigma_{t-p+1}^2 \end{bmatrix} \in \mathbb{R}^{p+q}, \quad \mathbf{b}_t = \begin{bmatrix} \omega \epsilon_t^2 \\ 0 \\ \vdots \\ \omega \\ 0 \\ \vdots \\ 0 \end{bmatrix} \in \mathbb{R}^{p+q},$$



$$\text{and } A_t = \begin{bmatrix} \alpha_1 \epsilon_t^2 & \alpha_2 \epsilon_t^2 & \dots & \alpha_q \epsilon_t^2 & \beta_1 \epsilon_t^2 & \dots & \beta_p \epsilon_t^2 \\ 1 & 0 & \dots & 0 & 0 & \dots & 0 \\ 0 & 1 & \dots & 0 & 0 & \dots & 0 \\ \dots & \ddots & \dots & \dots & \ddots & \dots & \\ 0 & 1 & \dots & 0 & 0 & \dots & 0 \\ \alpha_1 & \dots & \alpha_q & \beta_1 & \dots & \beta_p & \\ 0 & \dots & 0 & 1 & 0 & \dots & 0 \\ 0 & \dots & 0 & 0 & 1 & \dots & 0 \\ \vdots & \ddots & \vdots & \vdots & \vdots & \ddots & 0 \\ 0 & \dots & 0 & 0 & 0 & \dots & 0 \end{bmatrix} \in \mathbb{R}^{(p+q)(p+q)}.$$

**Definition 2.11** *The necessary and sufficient condition for the existence of a strictly stationary solution to GARCH( $p, q$ ) is that  $\gamma < 0$ , where  $\gamma$  is the top lyapunov exponent of the sequence  $(A_t), t \in \mathbb{Z}$  defined in the matrices representation of GARCH model. When strictly stationary solution exists, it is unique.*

$$\gamma = \lim_{t \rightarrow \infty} \frac{1}{t} \log \|A_t A_{t-1} \dots A_1\|.$$

*If the GARCH model hold the following two conditions*

$$\omega > 0, \sum_{i=1}^q \alpha_i + \sum_{j=1}^p \beta_j < 1,$$

*then it is called a second-order stationary and the unique strictly stationary solu-*

tion of the model is weak white noise.

In this thesis we will focus on a special case of  $GARCH(p, q)$  when  $p = 0$ , the model is known as Autoregressive Conditional Heteroscedasticity (ARCH) model. That is,  $GARCH(0, q)$  is equivalent to  $ARCH(q)$ . The  $ARCH(q)$  is given by

$$\sqrt{y_t} = \sigma_t \epsilon_t, \quad (2.4)$$

$$\sigma_t^2 = \omega + \sum_{i=1}^q \alpha_i y_{t-i}, \quad (2.5)$$

where  $\epsilon_t, \omega, \alpha_i, \sigma^2$  are the same as in Definition 2.10.

$ARCH(q)$  can be represented in a matrix form as follows

$$\mathbf{Y}_t = \mathbf{b}_t + A_t \mathbf{Y}_{t-1}, \quad (2.6)$$

$$\text{where } \mathbf{Y}_t = \begin{bmatrix} y_t \\ \vdots \\ y_{t-q+1} \end{bmatrix} \in \mathbb{R}^q, \mathbf{b}_t = \begin{bmatrix} \omega \epsilon_t^2 \\ \vdots \\ 0 \end{bmatrix} \in \mathbb{R}^q,$$

and

$$A_t = \begin{bmatrix} \alpha_1 \epsilon_t^2 & \alpha_2 \epsilon_t^2 & \dots & \alpha_q \epsilon_t^2 \\ 1 & 0 & \dots & 0 \\ 0 & 1 & \dots & 0 \\ \vdots & \ddots & \dots & \vdots \\ 0 & 1 & \dots & 0 \\ \alpha_1 & \dots & \dots & \alpha_q \end{bmatrix} \in \mathbb{R}^{q \times q}.$$

Similarly, if ARCH(q) holds the conditions  $\omega > 0$  and  $\sum_{i=1}^q \alpha_i < 1$  then, the uniquely strictly stationary solution of the model is a weak white noise.

## 2.4 Estimating ARCH(q) parameters

Following Francq and Zakoian (2010), the Ordinary least squares (OLS) method will be used to estimate the parameters of ARCH(q). OLS method uses the autoregressive representation on the squares of the observed process and no distributional assumptions are needed for the error term ( $\epsilon_t$ ).

By using Definition 2.6, the AR(q) representation can be obtained by applying some mathematical transformations as follows

$$u_t = y_t - \sigma_t^2, \tag{2.7}$$

where  $(u_t, \mathcal{F}_t)$  is the sequence containing a martingale difference when  $E(y_t) =$

$\sigma_t^2 < \infty$ , denoting by  $\mathcal{F}_t$  the  $\sigma$ -field generated by  $\{y_s : s \leq t\}$

By substituting  $\sigma_t^2$  from Equation (2.7) in Equation (2.5), we get

$$\begin{aligned} y_t - u_t &= \omega + \sum_{i=1}^q \alpha_i y_{t-i}, \\ y_t &= \omega + \sum_{i=1}^q \alpha_i y_{t-i} + u_t. \end{aligned} \quad (2.8)$$

The true parameter will be denoted by  $\boldsymbol{\theta}_0$ , where  $\boldsymbol{\theta}_0 = (\omega, \alpha_1, \dots, \alpha_q)'$ .

Assume we observe  $\sqrt{y_1}, \dots, \sqrt{y_n}$ , observations of length  $n$  from a process  $\{Y_t\}$  and considering  $\sqrt{y_0}, \dots, \sqrt{y_{1-q}}$  as initial values of the process, these initial values can be chosen to be zeros. By introducing the vector  $\mathbf{Y}_{t-1} = (1, y_{t-1}, \dots, y_{t-q})'$ , we can rewrite Equation (2.8) as a linear system as follows

$$y_t = \mathbf{Y}_{t-1}' \boldsymbol{\theta}_0 + u_t, \quad t = 1, \dots, n, \quad (2.9)$$

and in a matrix format as

$$\mathbf{Y} = \mathbf{X} \boldsymbol{\theta}_0 + \mathbf{U}, \quad (2.10)$$

where

$$\mathbf{Y} = \begin{bmatrix} y_1 \\ \vdots \\ y_n \end{bmatrix}_{n \times 1}, \quad \mathbf{X} = \begin{bmatrix} 1 & y_0 & \cdots & y_{-q+1} \\ \vdots & \vdots & \ddots & \vdots \\ 1 & y_{n-1} & \cdots & y_{n-q} \end{bmatrix}_{n \times q} = \begin{bmatrix} \mathbf{Y}'_0 \\ \vdots \\ \mathbf{Y}'_{n-1} \end{bmatrix}_{n \times 1}, \quad \mathbf{U} = \begin{bmatrix} u_1 \\ \vdots \\ u_n \end{bmatrix}_{n \times 1}.$$

### 2.4.1 Estimation of the parameter $\theta$

Assuming  $\mathbf{X}$  is of full rank;  $X'X$  is invertible, then the OLS estimator is given by

$$\hat{\theta}^U = \operatorname{argmin} \|\mathbf{Y} - X\theta\|^2 = (X'X)^{-1}X'\mathbf{Y}. \quad (2.11)$$

OLS estimator of  $\theta$  is known as the *best linear unbiased estimator* (BLUE). In the forthcoming sections we will refer to this estimator as the *unrestricted estimator* (UE) or simply by  $\hat{\theta}^U$ .

### 2.4.2 Estimation of $\sigma_0^2$

Assuming that  $\epsilon_t$  follows normal distribution with mean 0 and variance  $\sigma_0^2$  and with the following conditions:

1.  $\{Y_t\}$  is nonanticipative strictly stationary solution of the ARCH model in (2.4).
2.  $E(y_t) < +\infty$ .
3.  $P(y_t = 1) \neq 1$ .
4.  $E(y_t^2) < +\infty$ ,

The first assumption guarantee that the series is convergent. The second assumption guarantee the existence of the variance. Assumption 3 that the law of  $y_t$  is non-degenerate allows us to identify the parameters. We need assumption 4 for the asymptotic normality of the OLS estimator that the fourth moment is exist.

Then  $\sigma_0^2$  is estimated by  $\hat{\sigma}_0^2$ , where

$$\begin{aligned}\hat{\sigma}_0^2 &= \frac{1}{n-q-1} \|\mathbf{Y} - X\hat{\boldsymbol{\theta}}\|^2 \\ &= \frac{1}{n-q-1} \sum_{t=1}^n \left\{ y_t - \hat{\omega} - \sum_{i=1}^q \hat{\alpha}_i y_{t-i} \right\}^2,\end{aligned}\tag{2.12}$$

where  $\hat{\omega}, \hat{\alpha}_1, \dots, \hat{\alpha}_q$  are estimated by Equation (2.11).

### 2.4.3 Estimation of the information matrices

Following Francq and Zikoian (2010) define  $\mathbf{A}$  &  $\mathbf{B}$  as

$$\mathbf{A} = E(\mathbf{Y}_{t-1} \mathbf{Y}'_{t-1}), \quad \mathbf{B} = E(\sigma_t^4 \mathbf{Y}_{t-1} \mathbf{Y}'_{t-1}),$$

where

1.  $\mathbf{A}$  &  $\mathbf{B}$  have the same length  $q \times q$ .
2.  $\mathbf{A}$  &  $\mathbf{B}$  are invertible.

Then, the estimates of  $\mathbf{A}$  &  $\mathbf{B}$  denoted by  $\hat{\mathbf{A}}, \hat{\mathbf{B}}$  are respectively given by:

$$\hat{\mathbf{A}} = \frac{1}{n} \sum_{t=1}^n \mathbf{Y}_{t-1} \mathbf{Y}'_{t-1},\tag{2.13}$$

$$\hat{\mathbf{B}} = \frac{1}{n} \sum_{t=1}^n \hat{\sigma}_t^4 \mathbf{Y}_{t-1} \mathbf{Y}'_{t-1},\tag{2.14}$$

where  $\hat{\sigma}_t^2 = \mathbf{Y}'_{t-1} \hat{\boldsymbol{\theta}}^U$ . The fourth order moment of process  $\epsilon_t = \frac{\sqrt{y_t}}{\sigma_t}$ , is  $E(\epsilon_t^4)$ ; that is also consistently estimated by  $\hat{\mu}_4 = \frac{1}{n} \sum_{i=1}^n \frac{y_t^2}{\hat{\sigma}_t^4}$ .

## 2.4.4 Asymptotic distribution of the OLS estimator

Weiss (1986) was one of the pioneer who discussed the properties of maximum likelihood and least squares estimates of the parameters of ARCH models, and also the properties of various tests of the model that are available. He did not assume that the errors are normally distributed. Another attractive way to estimate consistent and efficient estimators for ARCH model was introduced by Rich et al. (1991), they utilized the generalized method of moments of Hansen (1982) and considering the asymptotic normal distribution. Francq et al. (2004) and Francq and Zakoïan (2012) had proved the consistency and asymptotic normality of OLS. In this subsection, we list two theorems by Francq and Zakoïan (2010) about the consistency and the asymptotic normality of OLS estimator for  $\boldsymbol{\theta}$ .

**Theorem 2.1** (*Francq and Zakoïan, 2010*) **Consistency of OLS of ARCH model:** *If  $\hat{\boldsymbol{\theta}}^U$  is a sequence of estimators satisfying the OLS solution for ARCH under the assumptions (1)-(4) in Section 2.4.2, then*

$$\hat{\boldsymbol{\theta}}^U \xrightarrow{P} \boldsymbol{\theta}, \hat{\sigma}^2 \xrightarrow{P} \sigma^2 \text{ as } n \rightarrow \infty, \quad (2.15)$$

*that is  $\hat{\boldsymbol{\theta}}^U$  is a consistent estimator for  $\boldsymbol{\theta}$*

**Theorem 2.2** (*Francq and Zakoïan, 2010*) *Referring to  $A$  &  $B$  given in equation (2.13) and (2.14), we have*

$$\sqrt{n}(\hat{\boldsymbol{\theta}}^U - \boldsymbol{\theta}) \xrightarrow{L} \mathcal{N}_q\left(\mathbf{0}, (\hat{\mu}_4 - 1)A^{-1}BA^{-1}\right), \quad (2.16)$$

where  $\hat{\mu}_4 = E(\epsilon_t^4)$ ,  $\hat{\boldsymbol{\theta}}^U$  has asymptotic multivariate normal distribution, and  $L$  denotes convergence in distribution.

## 2.5 Improved Estimation Strategies

In this section we will consider different estimation methods of  $\boldsymbol{\theta}$  when some UPIs are available. The UPIs states that there is a set of linear restrictions on these coefficients. Hence, the resulting estimation methods are functions of the unrestricted estimator and the restricted estimator.

### 2.5.1 Restricted estimator

The UPI(s) can be formulated as a hypothesis, some parameters are nuisance.

Suppose that the UPI is given by th hypothesis in (1.2)

Under the restrictions given in (1.2), the method uses Lagrange Multiplier for each restriction. The method minimizes the following function,

$$f(X, \boldsymbol{\theta}) = (\mathbf{Y} - X\boldsymbol{\theta})'(\mathbf{Y} - X\boldsymbol{\theta}) - \lambda'(r - R\boldsymbol{\theta}), \quad (2.17)$$

with respect to  $\boldsymbol{\theta}$  and  $\lambda$  as follows:

$$\begin{aligned} f(X, \boldsymbol{\theta}) &= \mathbf{Y}'\mathbf{Y} - \boldsymbol{\theta}X'\mathbf{Y} - \mathbf{Y}'X\boldsymbol{\theta} + \boldsymbol{\theta}'X'X\boldsymbol{\theta} + \lambda'(r - R\boldsymbol{\theta}) \\ &= \mathbf{Y}'\mathbf{Y} - 2\boldsymbol{\theta}X'\mathbf{Y} + \boldsymbol{\theta}'X'X\boldsymbol{\theta} + \lambda'(r - R\boldsymbol{\theta}). \end{aligned}$$



$$\frac{\partial f(X, \boldsymbol{\theta})}{\partial \boldsymbol{\theta}} = -2X'\mathbf{Y} + 2X'X\boldsymbol{\theta} + \lambda'R = 0. \quad (2.18)$$

$$\frac{\partial f(X, \boldsymbol{\theta})}{\partial \lambda} = R\boldsymbol{\theta} - r = 0. \quad (2.19)$$

By multiplying Equation (2.18) by  $R(X'X)^{-1}$ , and solve the equation for  $\lambda$ .

$$-2R(X'X)^{-1}X'\mathbf{Y} + 2R(X'X)^{-1}(X'X)\boldsymbol{\theta} + R(X'X)^{-1}\lambda'R = 0.$$

$$\begin{aligned} R(X'X)^{-1}\lambda'R &= 2R(X'X)^{-1}X'\mathbf{Y} - 2R\boldsymbol{\theta} \\ &= 2R\hat{\boldsymbol{\theta}}^U - 2R\boldsymbol{\theta}. \end{aligned}$$

$$\begin{aligned} \lambda &= (R(X'X)^{-1}\lambda'R)^{-1}(2R\hat{\boldsymbol{\theta}}^U - 2R\boldsymbol{\theta}) \\ &= 2(R(X'X)^{-1}\lambda'R)^{-1}(R\hat{\boldsymbol{\theta}}^U - r). \end{aligned} \quad (2.20)$$

then substituting  $\lambda$  from (2.20) in (2.18), to obtain

$$-2X'\mathbf{Y} + 2X'X\boldsymbol{\theta} + R'[-2(R(X'X)^{-1}R')^{-1}(r - R\boldsymbol{\theta})] = 0.$$

$$X'X\boldsymbol{\theta} = X'\mathbf{Y} - R'[R(X'X)^{-1}R']^{-1}(r - R\boldsymbol{\theta}).$$

$$\begin{aligned} \hat{\boldsymbol{\theta}}^R &= (X'X)^{-1}X'\mathbf{Y} + (X'X)^{-1}R'[R(X'X)^{-1}R']^{-1}(r - R\boldsymbol{\theta}) \\ &= \hat{\boldsymbol{\theta}}^U - (X'X)^{-1}R'[R(X'X)^{-1}R']^{-1}(R\boldsymbol{\theta} - r). \end{aligned} \quad (2.21)$$

The estimator in Equation (2.21) is the restricted estimator ( $\hat{\boldsymbol{\theta}}^R$ ), it is a biased estimator for  $\boldsymbol{\theta}$  unless the restriction given in Equation (1.2) is true.

**Theorem 2.3** *The wald test statistic for testing the hypothesis in Equation (1.2) is given by*

$$\begin{aligned}\mathcal{L}_n &= (R\hat{\boldsymbol{\theta}}^U - r)'[R(\text{Var}(\hat{\boldsymbol{\theta}}^U))R']^{-1}(R\hat{\boldsymbol{\theta}}^U - r) \\ &= (R\hat{\boldsymbol{\theta}}^U - r)'[\sigma^2 R(X'X)^{-1}R']^{-1}(R\hat{\boldsymbol{\theta}}^U - r) \\ &= \frac{(R\hat{\boldsymbol{\theta}}^U - r)'[R(X'X)^{-1}R']^{-1}(R\hat{\boldsymbol{\theta}}^U - r)}{\hat{\sigma}^2},\end{aligned}\tag{2.22}$$

where  $\hat{\sigma}^2$  is estimated in Equation (2.12) and it can be shown that  $\mathcal{L}_n \xrightarrow{L} \chi^2(m)$ .

## 2.5.2 Pretest estimator

The pretest estimate of  $\boldsymbol{\theta}$ , denoted by  $\hat{\boldsymbol{\theta}}^{PT}$  is defined by:

$$\hat{\boldsymbol{\theta}}^{PT} = \begin{cases} \hat{\boldsymbol{\theta}}^U, & \text{if } \mathcal{L}_n \geq \mathcal{L}_{n,\alpha}, \\ \hat{\boldsymbol{\theta}}^R, & \text{if } \mathcal{L}_n < \mathcal{L}_{n,\alpha}, \end{cases}\tag{2.23}$$

where  $\mathcal{L}_n$  as given in Equation (2.22), and  $\mathcal{L}_{n,\alpha}$  as the  $\alpha$ -critical value from the distribution of  $\mathcal{L}_n$ .

The pretest can be written as

$$\begin{aligned}\hat{\boldsymbol{\theta}}^{PT} &= \hat{\boldsymbol{\theta}}^R I(\mathcal{L} \leq \mathcal{L}_\alpha) + \hat{\boldsymbol{\theta}}^U I(\mathcal{L} > \mathcal{L}_\alpha) \\ &= \hat{\boldsymbol{\theta}}^U - (\hat{\boldsymbol{\theta}}^U - \hat{\boldsymbol{\theta}}^R)I(\mathcal{L} \leq \mathcal{L}_\alpha),\end{aligned}\tag{2.24}$$

### 2.5.3 Shrinkage estimator

The shrinkage estimator ( $\hat{\boldsymbol{\theta}}^S$ ) is defined by:

$$\hat{\boldsymbol{\theta}}^S = \hat{\boldsymbol{\theta}}^R + \left[1 - \frac{m-2}{\mathcal{L}_n}\right] (\hat{\boldsymbol{\theta}}^U - \hat{\boldsymbol{\theta}}^R), m \geq 3. \quad (2.25)$$

Which is a continuous smoothed-function of  $\hat{\boldsymbol{\theta}}^U$  and  $\hat{\boldsymbol{\theta}}^R$

### 2.5.4 Positive shrinkage estimator

It is a modified version of James-Stein estimator and defined by:

$$\hat{\boldsymbol{\theta}}^{S+} = \hat{\boldsymbol{\theta}}^U + \left[1 - \frac{m-2}{\mathcal{L}_n}\right]^+ (\hat{\boldsymbol{\theta}}^U - \hat{\boldsymbol{\theta}}^R), m \geq 3, \quad (2.26)$$

where  $Z^+ = \max(0, Z)$ .

## 2.6 Asymptotic Results

In this section we will study the asymptotic behavior of the proposed estimators,  $\hat{\boldsymbol{\theta}}^U, \hat{\boldsymbol{\theta}}^R, \hat{\boldsymbol{\theta}}^{PT}, \hat{\boldsymbol{\theta}}^S, \hat{\boldsymbol{\theta}}^{S+}$ . We will show that the restricted and unrestricted estimators are jointly asymptotically normal. In addition, we will define and extract expressions for the asymptotic distributional quadratic bias, the asymptotic mean squared error matrix, and the asymptotic quadratic risk of the estimators relying on the joint normality of  $\hat{\boldsymbol{\theta}}^U$  and  $\hat{\boldsymbol{\theta}}^R$ .

## 2.6.1 Joint normality of the unrestricted and restricted estimators

The asymptotic distribution of all the estimators under the hypothesis (1.2) are the same. Hence, we will study the asymptotic properties under a class of local alternatives that is given by

$$H_{(n)} : R\boldsymbol{\theta} = r + \frac{\boldsymbol{\xi}}{\sqrt{n}}, \quad (2.27)$$

where  $\boldsymbol{\xi}$  is a  $q \times 1$  fixed vector in  $\mathbb{R}^q$ . If we set  $\boldsymbol{\xi} = 0$ , then the local alternative becomes as in (1.2), which is the linear hypothesis representing the candidate null subspace.

Some distributional results involving the estimators  $\hat{\boldsymbol{\theta}}^U$  and  $\hat{\boldsymbol{\theta}}^R$  are given in the following theorem.

**Theorem 2.4** *Under the local alternatives in (2.27) and the regularity conditions (1) – (4) appeared in Section (2.4.2), and assuming that*

$$\left( \frac{(X'_{q \times n} X_{n \times q})}{n} \right) \xrightarrow{P} C_{q \times q}, \quad (2.28)$$

as  $n \rightarrow \infty$ , where  $C$  is positive definite matrix (p.d.m). Then, we have

$$(1) \quad T_n^{(1)} = \sqrt{n}(\hat{\boldsymbol{\theta}}^U - \boldsymbol{\theta}) \xrightarrow{L} T^{(1)} \sim \mathcal{N}_q\left(0, \sigma^2 C^{-1}\right)$$

$$(2) \quad T_n^{(2)} = \sqrt{n}(\hat{\boldsymbol{\theta}}^R - \boldsymbol{\theta}) \xrightarrow{L} T^{(2)} \sim \mathcal{N}_q\left(-\boldsymbol{\delta}, \sigma^2[C^{-1} - A]\right)$$

$$(3) \quad T_n^{(3)} = \sqrt{n}(\hat{\boldsymbol{\theta}}^U - \hat{\boldsymbol{\theta}}^R) \xrightarrow{L} T^{(3)} \sim \mathcal{N}_q\left(\boldsymbol{\delta}, \sigma^2 A\right)$$

$$(4) \quad \begin{bmatrix} T_n^{(1)} \\ R\hat{\boldsymbol{\theta}}^U - r \end{bmatrix} \xrightarrow{L} \begin{bmatrix} T^{(1)} \\ R\boldsymbol{\theta} - r \end{bmatrix} \sim \mathcal{N}_{2q}\left(\begin{pmatrix} 0 \\ R\boldsymbol{\theta} - r \end{pmatrix}, \sigma^2 \begin{bmatrix} C^{-1} & C^{-1}R' \\ RC^{-1} & RC^{-1}R' \end{bmatrix}\right)$$

$$(5) \quad \begin{bmatrix} T_n^{(1)} \\ T_n^{(3)} \end{bmatrix} \xrightarrow{L} \begin{bmatrix} T^{(1)} \\ T^{(3)} \end{bmatrix} \sim \mathcal{N}_{2q}\left(\begin{bmatrix} 0 \\ \boldsymbol{\delta} \end{bmatrix}, \sigma^2 \begin{bmatrix} C^{-1} & A \\ A & A \end{bmatrix}\right)$$

$$(6) \quad \begin{bmatrix} T_n^{(2)} \\ T_n^{(3)} \end{bmatrix} \xrightarrow{L} \begin{bmatrix} T^{(2)} \\ T^{(3)} \end{bmatrix} \sim \mathcal{N}_{2q}\left(\begin{bmatrix} -\boldsymbol{\delta} \\ \boldsymbol{\delta} \end{bmatrix}, \sigma^2 \begin{bmatrix} C^{-1} - A & 0 \\ 0 & A \end{bmatrix}\right),$$

where,  $A = C^{-1}R'[RC^{-1}R']^{-1}RC^{-1}$ ,  $\boldsymbol{\delta} = C^{-1}R'[RC^{-1}R']^{-1}(R\boldsymbol{\theta} - r)$ .

**Proofs:**

1. The proof follows from Francq et al. (2004); Francq and Zakoïan (2012);

Weiss (1986).

2.

$$\begin{aligned} T_n^{(2)} &= \sqrt{n}(\hat{\boldsymbol{\theta}}^R - \boldsymbol{\theta}) = \sqrt{n}\{\hat{\boldsymbol{\theta}}^U + C^{-1}R'[RC^{-1}R']^{-1}(r - R\hat{\boldsymbol{\theta}}^U) - \boldsymbol{\theta}\} \\ &= \sqrt{n}(\hat{\boldsymbol{\theta}}^U - \boldsymbol{\theta}) + \sqrt{n}\{C^{-1}R'[RC^{-1}R']^{-1}(r - R\hat{\boldsymbol{\theta}}^U)\} \\ &= \sqrt{n}(\hat{\boldsymbol{\theta}}^U - \boldsymbol{\theta}) - \sqrt{n}\{C^{-1}R'[RC^{-1}R']^{-1}(R(\hat{\boldsymbol{\theta}}^U - \boldsymbol{\theta}) \\ &\quad + R\boldsymbol{\theta} - r)\} \\ &= \sqrt{n}(\hat{\boldsymbol{\theta}}^U - \boldsymbol{\theta}) - C^{-1}R'[RC^{-1}R']^{-1}R\sqrt{n}(\hat{\boldsymbol{\theta}}^U - \boldsymbol{\theta}) + \end{aligned}$$

$$\begin{aligned}
& C^{-1}R'[RC^{-1}R']^{-1}\sqrt{n}(R\boldsymbol{\theta} - r) \\
&= T_n^{(1)} + C^{-1}R'[RC^{-1}R']^{-1}RT_n^{(1)} - C^{-1}R'[RC^{-1}R']^{-1}\sqrt{n}(R\boldsymbol{\theta} - r) \\
&= \left[ I_q - C^{-1}R'[RC^{-1}R']^{-1}R \right] T_n^{(1)} - \sqrt{n}\{C^{-1}R'[RC^{-1}R']^{-1}(R\boldsymbol{\theta} - r)\},
\end{aligned}$$

where  $\mathbf{I}$  is the identity matrix.

$T_n^{(2)}$  is a linear combination in  $T_n^{(1)}$ , that can be represented in a matrix format as,  $T_n^{(2)} = A_2T_n^{(1)} - \mathbf{B}_2$ , where  $A_2$  and  $\mathbf{B}_2$  are given as follow

$$A_2 = \left[ I_q - C^{-1}R'[RC^{-1}R']^{-1}R \right]_{q \times q}, \mathbf{B}_2 = \left[ C^{-1}R'[RC^{-1}R']^{-1}(R\boldsymbol{\theta} - r) \right]_{q \times 1}.$$

From Theorem (2.4) part (1), as  $n \rightarrow \infty$ ,  $T_n^{(2)} \xrightarrow{L} T^{(2)}$  and by Slutsky's Theorem,

$$T_n^{(2)} \xrightarrow{L} T^{(2)} \sim \mathcal{N}_q\left(\boldsymbol{\mu}^{(2)}, \boldsymbol{\Sigma}^{(2)}\right), \quad (2.29)$$

with  $\boldsymbol{\mu}^{(2)}$  and  $\boldsymbol{\Sigma}^{(2)}$  are given by

$$\begin{aligned}
\boldsymbol{\mu}^{(2)} &= -C^{-1}R'[RC^{-1}R']^{-1}(R\boldsymbol{\theta} - r) \\
&= -\boldsymbol{\delta}, \\
\boldsymbol{\Sigma}^{(2)} &= \sigma^2C^{-1} - 2\sigma^2A + C^{-1}R'[RC^{-1}R']^{-1}R\sigma^2C^{-1}[RC^{-1}R']^{-1}RC^{-1} \\
&= \sigma^2[C^{-1} - 2A + A] \\
&= \sigma^2[C^{-1} - A].
\end{aligned}$$

3.

$$\begin{aligned}
T_n^{(3)} &= \sqrt{n}(\hat{\boldsymbol{\theta}}^U - \hat{\boldsymbol{\theta}}^R) \\
&= \sqrt{n}\left(\hat{\boldsymbol{\theta}}^U - [\hat{\boldsymbol{\theta}}^U + C^{-1}R'[RC^{-1}R']^{-1}(r - R\boldsymbol{\theta})]\right) \\
&= \sqrt{n}\left(C^{-1}R'[RC^{-1}R']^{-1}(\hat{\boldsymbol{\theta}}^U - r)\right) \\
&= \sqrt{n}\left(C^{-1}R'[RC^{-1}R']^{-1}(R(\hat{\boldsymbol{\theta}}^U - \boldsymbol{\theta}) + R\boldsymbol{\theta} - r)\right) \\
&= C^{-1}R'[RC^{-1}R']^{-1}R\sqrt{n}(\hat{\boldsymbol{\theta}}^U - \boldsymbol{\theta}) + C^{-1}R'[RC^{-1}R']^{-1}(R\boldsymbol{\theta} - r) \\
&= \left[C^{-1}R'[RC^{-1}R']^{-1}R\right]T_n^{(1)} + C^{-1}R'[RC^{-1}R']^{-1}(R\boldsymbol{\theta} - r).
\end{aligned}$$

$T_n^{(3)}$  is a linear combination in  $T_n^{(1)}$ . It can be represented in a matrix format as  $T_n^{(3)} = A_3T_n^{(1)} + \mathbf{B}_3$ , where  $A_3$  and  $\mathbf{B}_3$  are given as,

$$A_3 = \left[C^{-1}R'[RC^{-1}R']^{-1}R\right]_{q \times q}, \mathbf{B}_3 = \left[C^{-1}R'[RC^{-1}R']^{-1}(R\boldsymbol{\theta} - r)\right]_{q \times 1}.$$

Therefore, as  $T_n^{(1)}$  is normally distributed, by Theorem (2.4) part (1),  $T_n^{(3)} \xrightarrow{L} T^{(3)}$ , and by Slutsky's Theorem we get the following result

$$T_n^{(3)} \xrightarrow{L} T^{(3)} \sim \mathcal{N}_q\left(\boldsymbol{\mu}^{(3)}, \boldsymbol{\Sigma}^{(3)}\right). \quad (2.30)$$

The mean  $\boldsymbol{\mu}^{(3)}$  and the variance  $\boldsymbol{\Sigma}^{(3)}$  are given as follow:

$$\begin{aligned}
\boldsymbol{\mu}^{(3)} &= C^{-1}R'[RC^{-1}R']^{-1}(R\boldsymbol{\theta} - r) \\
&= \boldsymbol{\delta}.
\end{aligned}$$

$$\begin{aligned}\boldsymbol{\Sigma}^{(3)} &= \sigma^2 C^{-1} R' [RC^{-1}R']^{-1} RC^{-1} \\ &= \sigma^2 A.\end{aligned}$$

4.  $T_n^{(1)}$  and  $Z = R\hat{\boldsymbol{\theta}}^U - r$  are a linear combination on  $T_n^{(1)}$ , their equations can be represented in a matrix format  $T = A_4 T_n^{(1)} + B_4$  as follow:

$$\begin{aligned}\begin{bmatrix} T_n^{(1)} \\ Z \end{bmatrix} &= \begin{bmatrix} \sqrt{n}(\hat{\boldsymbol{\theta}}^U - \boldsymbol{\theta}) \\ \sqrt{n}(R\hat{\boldsymbol{\theta}}^U - r) \end{bmatrix} = \begin{bmatrix} \sqrt{n}(\hat{\boldsymbol{\theta}}^U - \boldsymbol{\theta}) \\ \sqrt{n}(R(\hat{\boldsymbol{\theta}}^U - \boldsymbol{\theta}) + R\boldsymbol{\theta} - r) \end{bmatrix} \\ &= \begin{bmatrix} \sqrt{n}(\hat{\boldsymbol{\theta}}^U - \boldsymbol{\theta}) \\ \sqrt{n}(R(\hat{\boldsymbol{\theta}}^U - \boldsymbol{\theta})) \end{bmatrix} + \begin{bmatrix} \mathbf{0}_q \\ (R\boldsymbol{\theta} - r) \end{bmatrix} \\ &= \begin{bmatrix} \mathbf{I}_q \\ \mathbf{I}_m \end{bmatrix} \sqrt{n}(\hat{\boldsymbol{\theta}}^U - \boldsymbol{\theta}) + \begin{bmatrix} \mathbf{0}_q \\ (R\boldsymbol{\theta} - r) \end{bmatrix} \\ &= \begin{bmatrix} \mathbf{I}_q \\ \mathbf{I}_m \end{bmatrix} T_n^{(1)} + \begin{bmatrix} \mathbf{0}_q \\ (R\boldsymbol{\theta} - r) \end{bmatrix}.\end{aligned}$$

where  $\mathbf{0}$  is a  $q \times 1$  vector of zeros.  $A_4$  and  $B_4$  are given as follow,

$$A_4 = \begin{bmatrix} \mathbf{I}_q \\ \mathbf{I}_m \end{bmatrix}_{(q+m) \times q}, \quad B_4 = \begin{bmatrix} \mathbf{0}_q \\ R\boldsymbol{\theta} - r \end{bmatrix}_{(q+m) \times 1}.$$

Therefore, by Theorem (2.4) part (1) and Slutsky's Theorem. We get the



following result,

$$\begin{bmatrix} T_n^{(1)} \\ R\hat{\boldsymbol{\theta}}^U - h \end{bmatrix} \xrightarrow{L} \begin{bmatrix} T^{(1)} \\ R\boldsymbol{\theta} - h \end{bmatrix} \sim \mathcal{N}_{2q}(\boldsymbol{\mu}^{(4)}, \boldsymbol{\Sigma}^{(4)}). \quad (2.31)$$

The joint distribution follows multivariate normal with mean  $\boldsymbol{\mu}^{(4)}$  and variance-covariance matrix  $\boldsymbol{\Sigma}^{(4)}$  are given as follow:

$$\boldsymbol{\mu}^{(4)} = \begin{bmatrix} \mathbf{0} \\ R\boldsymbol{\theta} - r \end{bmatrix},$$

$$\boldsymbol{\Sigma}^{(4)} = \sigma^2 \begin{bmatrix} C^{-1} & C^{-1}R' \\ RC^{-1} & RC^{-1}R' \end{bmatrix}.$$

5.  $T_n^{(1)}$  and  $T_n^{(3)}$  are a linear combination in  $T_n^{(1)}$ , and their equations can be represent in a matrix format  $T_n^{12} = A_5 T_n^{(1)} + B_5$  as follows:

$$\begin{bmatrix} T_n^{(1)} \\ T_n^{(3)} \end{bmatrix} = \begin{bmatrix} \sqrt{n}(\hat{\boldsymbol{\theta}}^U - \boldsymbol{\theta}) \\ \sqrt{n}((\hat{\boldsymbol{\theta}}^U - \hat{\boldsymbol{\theta}}^R)) \end{bmatrix}.$$

From Theorem (2.4) part (3),  $T_n^{(3)}$  can be represented as

$$\begin{aligned} T_n^{(3)} &= [C^{-1}R'[RC^{-1}R']^{-1}R]T_n^{(1)} - C^{-1}R'[RC^{-1}R']^{-1}\xi \\ &= \begin{bmatrix} I_q \\ C^{-1}R'[RC^{-1}R']^{-1}R \end{bmatrix} T_n^{(1)} - \begin{bmatrix} \boldsymbol{\theta} \\ C^{-1}R'[RC^{-1}R']^{-1}\xi \end{bmatrix}, \end{aligned}$$

where  $A_3$  and  $B_3$  are given as follow

$$\mathbf{A}_5 = \begin{bmatrix} I_q \\ C^{-1}R'[RC^{-1}R']^{-1}R \end{bmatrix}_{(2q) \times q}, \mathbf{B}_5 = \begin{bmatrix} \boldsymbol{\theta} \\ C^{-1}R'[RC^{-1}R']^{-1}\xi \end{bmatrix}_{(2q) \times 1}.$$

As  $T_n^{(1)}$  and  $T_n^{(3)}$  are linear combinations on  $T_n^{(1)}$ , by Theorem (2.4) and Slutsky's Theorem. We get the following result,

$$\begin{bmatrix} T_n^{(1)} \\ T_n^{(3)} \end{bmatrix} \xrightarrow{L} \begin{bmatrix} T^{(1)} \\ T^{(3)} \end{bmatrix} \sim \mathcal{N}_{2q}(\boldsymbol{\mu}^{(5)}, \boldsymbol{\Sigma}^{(5)}). \quad (2.32)$$

The joint distribution follows multivariate normal with mean  $\boldsymbol{\mu}^{(5)}$  and variance-covariance matrix  $\boldsymbol{\Sigma}^{(5)}$  that are given as follow

$$\boldsymbol{\mu}^{(5)} = \begin{bmatrix} \mathbf{0} \\ C^{-1}R'[RC^{-1}R']^{-1}(R\boldsymbol{\theta} - r) \end{bmatrix} = \begin{bmatrix} \mathbf{0} \\ -\boldsymbol{\delta} \end{bmatrix}.$$

$$\boldsymbol{\Sigma}^{(5)} = \sigma^2 \begin{bmatrix} C^{-1} & A \\ A & A \end{bmatrix}.$$

6.  $T_n^{(2)}$  and  $T_n^{(3)}$  are linear combinations on  $T_n^{(1)}$ , and their equations can be represent in a matrix format  $T_n^{23} = A_6 T_n^{(1)} + B_6$  as follows

$$\begin{bmatrix} T_n^{(2)} \\ T_n^{(3)} \end{bmatrix} = \begin{bmatrix} \sqrt{n}(\hat{\boldsymbol{\theta}}^R - \boldsymbol{\theta}) \\ \sqrt{n}((\hat{\boldsymbol{\theta}}^U - \hat{\boldsymbol{\theta}}^R)) \end{bmatrix}$$

$$\begin{aligned}
&= \begin{bmatrix} [\mathbf{I}_q - C^{-1}R'[RC^{-1}R']^{-1}R]\hat{\boldsymbol{\theta}}^U + [C^{-1}R'[RC^{-1}R']^{-1}(r - R\boldsymbol{\theta})] \\ [C^{-1}R'[RC^{-1}R']^{-1}R]\hat{\boldsymbol{\theta}}^U - C^{-1}R'[RC^{-1}R']^{-1}(R\boldsymbol{\theta} - r) \end{bmatrix} \\
&= \begin{bmatrix} \mathbf{I}_q - C^{-1}R'[RC^{-1}R']^{-1}R \\ C^{-1}R'[RC^{-1}R']^{-1}R \end{bmatrix} T_n^{(1)} + \begin{bmatrix} C^{-1}R'[RC^{-1}R']^{-1}(r - R\boldsymbol{\theta}) \\ C^{-1}R'[RC^{-1}R']^{-1}(R\boldsymbol{\theta} - r) \end{bmatrix},
\end{aligned}$$

where  $A_6$  and  $B_6$  are given as follow

$$\begin{aligned}
A_6 &= \begin{bmatrix} \mathbf{I}_q - C^{-1}R'[RC^{-1}R']^{-1}R \\ C^{-1}R'[RC^{-1}R']^{-1}R \end{bmatrix}_{(2q) \times (2q)}, \\
B_6 &= \begin{bmatrix} -C^{-1}R'[RC^{-1}R']^{-1}(R\boldsymbol{\theta} - r) \\ C^{-1}R'[RC^{-1}R']^{-1}(R\boldsymbol{\theta} - r) \end{bmatrix}_{(2q) \times 1}.
\end{aligned}$$

As  $T_n^{(2)}$  and  $T_n^{(3)}$  are linear combination in  $T_n^{(1)}$ , by Theorem (2.4) part (1) and Slutsky's Theorem. We get the following result,

$$\begin{bmatrix} T_n^{(2)} \\ T_n^{(3)} \end{bmatrix} \xrightarrow{L} \begin{bmatrix} T^{(2)} \\ T^{(3)} \end{bmatrix} \sim \mathcal{N}_{2q}(\boldsymbol{\mu}^{(6)}, \boldsymbol{\Sigma}^{(6)}). \quad (2.33)$$

The joint distribution follows multivariate normal with mean  $\boldsymbol{\mu}^{(6)}$  and variance-covariance matrix  $\boldsymbol{\Sigma}^{(6)}$  that are given as follow:

$$\boldsymbol{\mu}^{(6)} = \begin{bmatrix} -C^{-1}R'[RC^{-1}R']^{-1}(R\boldsymbol{\theta} - r) \\ C^{-1}R'(RC^{-1}R')^{-1}(R\boldsymbol{\theta} - r) \end{bmatrix} = \begin{bmatrix} -\boldsymbol{\delta} \\ \boldsymbol{\delta} \end{bmatrix}.$$

$$\Sigma^{(6)} = \sigma^2 \begin{bmatrix} C^{-1} - A & 0 \\ 0 & A \end{bmatrix}.$$

## 2.6.2 Asymptotic Bias and Quadratic Bias

In this subsection we will define and extract the asymptotic distributional bias and quadratic bias. Assuming local alternatives in (2.27), and under the assumptions of Theorem (2.4), the asymptotic distributional bias  $b_i(\hat{\boldsymbol{\theta}}^*)$ , and quadratic bias  $B_i(\hat{\boldsymbol{\theta}}^*)$ , where  $\hat{\boldsymbol{\theta}}^* \in \{\hat{\boldsymbol{\theta}}^U, \hat{\boldsymbol{\theta}}^R, \hat{\boldsymbol{\theta}}^{PT}, \hat{\boldsymbol{\theta}}^S, \hat{\boldsymbol{\theta}}^{S+}\}$  are given in the following theorem.

**Theorem 2.5** *Under the assumptions of Theorem (2.4) and the local alternatives in (2.27), we have*

$$\begin{aligned} (1) \quad b_1(\hat{\boldsymbol{\theta}}^U) &= 0, B_1(\hat{\boldsymbol{\theta}}^U) = 0. \\ (2) \quad b_2(\hat{\boldsymbol{\theta}}^R) &= -C^{-1}R'[RC^{-1}R']^{-1}(R\boldsymbol{\theta} - r) = -\boldsymbol{\delta}, \\ B_2(\hat{\boldsymbol{\theta}}^R) &= \frac{\boldsymbol{\delta}'C\boldsymbol{\delta}}{\sigma^2} = \Delta^2. \\ (3) \quad b_3(\hat{\boldsymbol{\theta}}^R) &= C^{-1}R'[RC^{-1}R']^{-1}(R\boldsymbol{\theta} - r)G_{m+2}(\chi_m^2(\alpha); \Delta^2) \\ &= -\boldsymbol{\delta}G_{m+2}(\chi_m^2(\alpha); \Delta^2), \\ B_3(\hat{\boldsymbol{\theta}}^{PT}) &= \Delta^2[G_{m+2}(\chi_m^2(\alpha); \Delta^2)]^2. \\ (4) \quad b_4(\hat{\boldsymbol{\theta}}^S) &= -(m-2)(C^{-1}\acute{R}[RC^{-1}R']^{-1}(R\boldsymbol{\theta} - r))E(\chi_{m+2}^{-2}(\Delta^2)) \\ &= -(m-2)\boldsymbol{\delta}E(\chi_{m+2}^{-2}(\Delta^2)), \\ B_4(\hat{\boldsymbol{\theta}}^S) &= (m-2)^2\Delta^2[E(\chi_{m+2}^{-2}(\Delta^2))]^2. \\ (5) \quad b_5(\hat{\boldsymbol{\theta}}^{S+}) &= C^{-1}R'[RC^{-1}R']^{-1}(R\boldsymbol{\theta} - r) \end{aligned}$$

$$\begin{aligned}
&= -\boldsymbol{\delta}\{(m-2)E[[\chi_m^{-2}(\Delta^2)]^{-1}I(\chi_m^{-2}(\Delta^2) \leq (m-2))] \\
&\quad -d_1E[\chi_m^{-2}(\Delta^2)]^{-1} - G_{m+2}(\chi_m^2(\alpha); \Delta^2)\}, \\
B_5(\hat{\boldsymbol{\theta}}^{S+}) &= \Delta^2\{(m-2)E[[\chi_m^{-2}(\Delta^2)]^{-1}I(\chi_m^{-2}(\Delta^2) \leq (m-2))] \\
&\quad - (m-2)E[\chi_m^{-2}(\Delta^2)]^{-1} - G_{m+2}(\chi_m^2(\alpha); \Delta^2)\},
\end{aligned}$$

where  $\Delta^2$  is the non-centrality parameter,  $G_m(\mathcal{L}_\alpha; \Delta^2)$  is the non-central chi-square distribution function with  $q$ -degrees of freedom and non-centrality parameter  $\Delta^2$ .

**Proofs:**

$$(1) \quad b_1(\hat{\boldsymbol{\theta}}^U) = E(T^{(1)}) = 0, \text{ by Theorem (2.4) part (1).}$$

$$(2) \quad b_2(\hat{\boldsymbol{\theta}}^R) = E(T^{(2)}) = -C^{-1}R'[RC^{-1}R']^{-1}(R\boldsymbol{\theta} - r) = -\boldsymbol{\delta},$$

by Theorem (2.4) part (2).

$$B_2(\hat{\boldsymbol{\theta}}^R) = \Delta^2.$$

$$\begin{aligned}
(3) \quad \sqrt{n}(\hat{\boldsymbol{\theta}}^{PT} - \boldsymbol{\theta}) &= \sqrt{n}\left(\hat{\boldsymbol{\theta}}^U - (\hat{\boldsymbol{\theta}}^U - \hat{\boldsymbol{\theta}}^R)I(\mathcal{L} \leq \mathcal{L}_\alpha) - \boldsymbol{\theta}\right) \\
&= \sqrt{n}(\hat{\boldsymbol{\theta}}^U - \boldsymbol{\theta}) - \sqrt{n}(\hat{\boldsymbol{\theta}}^U - \hat{\boldsymbol{\theta}}^R)I(\mathcal{L} \leq \mathcal{L}_\alpha) \\
&= T_n^{(1)} + \left(\sqrt{n}(X'X)^{-1}R'[RC^{-1}R']^{-1} \right. \\
&\quad \left. (r - R\boldsymbol{\theta})I(\mathcal{L} \leq \mathcal{L}_\alpha)\right),
\end{aligned}$$

As  $n \rightarrow \infty$ , with Slutsky's Theorem we have  $\mathcal{L}_n \xrightarrow{L} \mathcal{L} \sim \chi_m^2$  and  $\mathcal{L}_{n,\alpha} \xrightarrow{L} \mathcal{L} \sim$

$\chi_m^2(\alpha)$  then,

$$\begin{aligned}
\sqrt{n}(\hat{\boldsymbol{\theta}}^{PT} - \boldsymbol{\theta}) &= C^{-1}R'[RC^{-1}R']^{-1}(r - R\boldsymbol{\theta})G_{m+2}(\chi_m^2(\alpha); \Delta^2) \\
&= -\boldsymbol{\delta}G_{m+2}(\chi_m^2(\alpha); \Delta^2) \\
B_3(\hat{\boldsymbol{\theta}}^{PT}) &= \Delta^2[G_{m+2}(\chi_m^2(\alpha); \Delta^2)]^2.
\end{aligned}$$

(4) Note that,

$$\begin{aligned}
\sqrt{n}(\hat{\boldsymbol{\theta}}^S - \boldsymbol{\theta}) &= \sqrt{n}(\hat{\boldsymbol{\theta}}^U - \boldsymbol{\theta} - (m-2)((\hat{\boldsymbol{\theta}}^U - \hat{\boldsymbol{\theta}}^R))\mathcal{L}_n^{-1}) \\
&= \sqrt{n}(\hat{\boldsymbol{\theta}}^U - \boldsymbol{\theta}) - (m-2)\sqrt{n}((\hat{\boldsymbol{\theta}}^U - \hat{\boldsymbol{\theta}}^R))\mathcal{L}_n^{-1} \\
&= T_n^{(1)} - (m-2)T_n^{(3)}\mathcal{L}_n^{-1} \\
&= -m(m-2)\boldsymbol{\delta}E(G_{m+2}(\chi_m^2(\alpha); \Delta^2)). \\
B_4(\hat{\boldsymbol{\theta}}^S) &= m^2(m-2)^2\Delta^2E[(\chi_{m+2}^{-2}(\Delta^2))]^2.
\end{aligned}$$

(5) Also, note that

$$\begin{aligned}
\sqrt{n}(\hat{\boldsymbol{\theta}}^{S+} - \boldsymbol{\theta}) &= \sqrt{n}(\hat{\boldsymbol{\theta}}^S - \boldsymbol{\theta}) - \sqrt{n}[(\hat{\boldsymbol{\theta}}^U - \hat{\boldsymbol{\theta}}^R)I(\mathcal{L}_n \leq (m-2))] \\
&\quad + (m-2)\sqrt{n}[(\hat{\boldsymbol{\theta}}^U - \hat{\boldsymbol{\theta}}^R))\mathcal{L}_n^{-1}I\mathcal{L}_n \leq (m-2)].
\end{aligned}$$

The first term is given by (4), the second term equals  $\boldsymbol{\delta}(G_{m+2}(\chi_m^2(\alpha); \Delta^2))$  and the third term can be written as

$$\boldsymbol{\delta}(m-2)E[[\chi_m^{-2}(\Delta^2)]^{-1}I(\chi_m^{-2}(\Delta^2) \leq (m-2))]$$

Hence,

$$\begin{aligned}
\sqrt{n}(\hat{\boldsymbol{\theta}}^{S^+} - \boldsymbol{\theta}) &= \boldsymbol{\delta}G_{m+2}(\chi_m^2(\alpha); \Delta^2) - \boldsymbol{\delta}(G_{m+2}(\chi_m^2(\alpha); \Delta^2)) - \\
&\quad \boldsymbol{\delta}(m-2)E[[\chi_m^{-2}(\Delta^2)]^{-1}I(\chi_m^{-2}(\Delta^2) \leq (m-2))] \\
&= -\boldsymbol{\delta}\{(m-2)E[[\chi_m^{-2}(\Delta^2)]^{-1}I(\chi_m^{-2}(\Delta^2) \leq (m-2))] \\
&\quad -(m-2)E[\chi_m^{-2}(\Delta^2)]^{-1} - G_{m+2}(\chi_m^2(\alpha); \Delta^2)\}. \\
B(\hat{\boldsymbol{\theta}}^{S^+}) &= \Delta^2\{(m-2)E[[\chi_m^{-2}(\Delta^2)]^{-1}I(\chi_m^{-2}(\Delta^2) \leq (m-2))] \\
&\quad -(m-2)E[\chi_m^{-2}(\Delta^2)]^{-1} - G_{m+2}(\chi_m^2(\alpha); \Delta^2)\}.
\end{aligned}$$

### 2.6.3 Quadratic Weighted risks

In this subsection we will extract the asymptotic quadratic weighted risks and the asymptotic mean squared error matrix. For any estimator  $\hat{\boldsymbol{\theta}}^*$  of  $\boldsymbol{\theta}$ , define the quadratic loss as

$$\begin{aligned}
L(\hat{\boldsymbol{\theta}}^*, \boldsymbol{\theta}) &= n(\hat{\boldsymbol{\theta}}^* - \boldsymbol{\theta})'W(\hat{\boldsymbol{\theta}}^* - \boldsymbol{\theta}), \\
&= tr\left\{W(n(\hat{\boldsymbol{\theta}}^* - \boldsymbol{\theta})(\hat{\boldsymbol{\theta}}^* - \boldsymbol{\theta})')\right\}, \tag{2.34}
\end{aligned}$$

where  $W$  is a positive semidefinite matrix of order  $q \times q$ , and  $tr(\mathbf{A})$  is the trace of the matrix  $\mathbf{A}$ . In the context of statistical estimation, the risk involved in estimating a particular parameter is a measure of the degree to which the estimate is likely to be inaccurate.

The asymptotic mean squared error matrix  $M(\hat{\boldsymbol{\theta}}^*)$ , is given by

$$M(\hat{\boldsymbol{\theta}}^*) = E(n(\hat{\boldsymbol{\theta}}^* - \boldsymbol{\theta})'(\hat{\boldsymbol{\theta}}^* - \boldsymbol{\theta})), \quad (2.35)$$

and the asymptotic quadratic risk (AQR), is defined as

$$\begin{aligned} R(\hat{\boldsymbol{\theta}}^*, W) &= E[n(\hat{\boldsymbol{\theta}}^* - \boldsymbol{\theta})'W(\hat{\boldsymbol{\theta}}^* - \boldsymbol{\theta})] \\ &= \text{tr}[WM(\hat{\boldsymbol{\theta}}^*)]. \end{aligned} \quad (2.36)$$

The asymptotic quadratic weighted risks and the asymptotic mean squared error matrices are given in the following theorem.

**Theorem 2.6** *Under the assumptions of Theorem (2.4), we have*

$$\begin{aligned} (1) \quad M_1(\hat{\boldsymbol{\theta}}^U) &= \sigma^2 C^{-1}, \\ R_1(\hat{\boldsymbol{\theta}}^U, W) &= \sigma^2 \text{tr}(WC^{-1}). \\ (2) \quad M_2(\hat{\boldsymbol{\theta}}^R) &= \sigma^2 [C^{-1} - A] + \boldsymbol{\delta}\boldsymbol{\delta}', \\ R_2(\hat{\boldsymbol{\theta}}^R, W) &= \sigma^2 \text{tr}(WA) + \boldsymbol{\delta}W\boldsymbol{\delta}'. \\ (3) \quad M_3(\hat{\boldsymbol{\theta}}^{PT}) &= \sigma^2 [C^{-1} - AG_{m+2}(\chi_m^2(\alpha); \Delta^2)] + \boldsymbol{\delta}\boldsymbol{\delta}'\{2G_{m+2}(\chi_m^2(\alpha); \Delta^2) \\ &\quad - G_{m+4}(\chi_m^2(\alpha); \Delta^2)\}, \\ R_3(\hat{\boldsymbol{\theta}}^{PT}, W) &= \sigma^2 \text{tr}(WC^{-1}) - \sigma^2 \text{tr}(WA)G_{m+2}(\chi_m^2(\alpha); \Delta^2) + \\ &\quad 2\boldsymbol{\delta}W\boldsymbol{\delta}'\{G_{m+2}(\chi_m^2(\alpha); \Delta^2) - G_{m+4}(\chi_m^2(\alpha); \Delta^2)\}. \\ (4) \quad M_4(\hat{\boldsymbol{\theta}}^S) &= \sigma^2 C^{-1} - (m-2)\sigma^2 A\{2E[\chi_{m+4}^{-4}(\Delta^2)] - (m-2) \end{aligned}$$



$$\begin{aligned}
& E[\chi_{m+2}^{-4}(\Delta^2)]\} + (m-2)(m+2)\boldsymbol{\delta}\boldsymbol{\delta}'E[\chi_{m+4}^{-4}(\Delta^2)], \\
R_4(\hat{\boldsymbol{\theta}}^S, W) &= \sigma^2 \text{tr}(WC^{-1}) - \sigma^2(m-2)\text{tr}(WA) \times \{2E[\chi_{m+4}^{-4}(\Delta^2)] - (m \\
& -2)E[\chi_{m+2}^{-4}(\Delta^2)]\} + (m-2)(m+2)\boldsymbol{\delta}W\boldsymbol{\delta}'E[\chi_{m+4}^{-4}(\Delta^2)]. \\
(5) \quad M_5(\hat{\boldsymbol{\theta}}^{S+}) &= M_4(\hat{\boldsymbol{\theta}}^S) - \sigma^2 AE[(1 - (m-2)\chi_{(m+2)}^2(\Delta^2))^2 I(\chi_{(m+2)}^2(\Delta^2) \\
& < (m-2))] + \boldsymbol{\delta}\boldsymbol{\delta}' \left\{ 2E[(1 - (m-2)\chi_{m+2}^{-2}(\Delta^2))I(\chi_{m+2}^{-2}(\Delta^2) \\
& < (m-2)) - E[(1 - (m-2)\chi_{m+4}^{-2}(\Delta^2))^2(\chi_{m+4}^2(\Delta^2) \\
& < (m-2))] \right\}, \\
R_5(\hat{\boldsymbol{\theta}}^{S+}, W) &= R_4(\hat{\boldsymbol{\theta}}^S, W) - \sigma^2(C^{-1} - A)E[(1 - (m-2)\chi_{m+2}^{-2}(\Delta^2))^2 \\
& I(\chi_{m+2}^{-2}(\Delta^2) < (m-2))] + \boldsymbol{\delta}W\boldsymbol{\delta}' \left\{ 2E[(1 - (m-2)\chi_{m+4}^2(\Delta^2)) \\
& I(\chi_{m+4}^2(\Delta^2) < (m-2))] - E[(1 - (m-2)\chi_{m+4}^{-2}(\Delta^2))^2 \\
& I(\chi_{m+4}^2(\Delta^2) < (m-2))] \right\}.
\end{aligned}$$

**Proofs:**

1. Note that

$$n(\hat{\boldsymbol{\theta}}^U - \boldsymbol{\theta})(\hat{\boldsymbol{\theta}}^U - \boldsymbol{\theta})' = T_n^{(1)}T_n^{(1)'}$$

Therefore, by Theorem (2.4) part (1) we have

$$\begin{aligned}
M_1(\hat{\boldsymbol{\theta}}^U) &= E[n(\hat{\boldsymbol{\theta}}^U - \boldsymbol{\theta})(\hat{\boldsymbol{\theta}}^U - \boldsymbol{\theta})'] = \sigma^2 C^{-1} \\
R_1(\hat{\boldsymbol{\theta}}^U, W) &= \text{tr}(W(\sigma^2 C^{-1})) = \sigma^2 \text{tr}(WC^{-1}).
\end{aligned}$$

2. Also note that

$$n(\hat{\boldsymbol{\theta}}^R - \boldsymbol{\theta})(\hat{\boldsymbol{\theta}}^R - \boldsymbol{\theta})' = T_n^{(2)}T_n^{(2)'}$$

Then, by Theorem (2.4) part (2) we have

$$\begin{aligned} M_2(\hat{\boldsymbol{\theta}}^R) &= E[n(\hat{\boldsymbol{\theta}}^R - \boldsymbol{\theta})(\hat{\boldsymbol{\theta}}^R - \boldsymbol{\theta})'] \\ &= E\{n\{(\hat{\boldsymbol{\theta}}^U - \boldsymbol{\theta}) - C^{-1}\dot{R}[RC^{-1}R']^{-1}(R\boldsymbol{\theta} - r)\} \\ &\quad \{(\hat{\boldsymbol{\theta}}^U - \boldsymbol{\theta}) - C^{-1}\dot{R}[RC^{-1}R']^{-1}(R\boldsymbol{\theta} - r)\}'\} \\ &= \sigma^2C^{-1} + C^{-1}R'[RC^{-1}R']^{-1}E\{(R\hat{\boldsymbol{\theta}}^U - r)(R\hat{\boldsymbol{\theta}}^U - r)'\} \times \\ &\quad [RC^{-1}R']^{-1}RC^{-1} - 2C^{-1}R'[RC^{-1}R']^{-1} \times E\{(R\hat{\boldsymbol{\theta}}^U - r) \\ &\quad (R\hat{\boldsymbol{\theta}}^U - r)'\} \\ &= \sigma^2C^{-1} + C^{-1}R'[RC^{-1}R']^{-1}\{\sigma^2(RC^{-1}R') + (R\boldsymbol{\theta} - r)(R\boldsymbol{\theta} \\ &\quad - r)'\} \times [RC^{-1}R']^{-1}RC^{-1} - 2\sigma^2C^{-1}R'[RC^{-1}R']^{-1}RC^{-1} \\ &= \sigma^2C^{-1} - \sigma^2C^{-1}R'[RC^{-1}R']^{-1}RC^{-1} + \boldsymbol{\delta}\boldsymbol{\delta}' \\ &= \sigma^2[C^{-1} - A] + \boldsymbol{\delta}\boldsymbol{\delta}'. \end{aligned}$$

$$R_2(\hat{\boldsymbol{\theta}}^R, W) = \sigma^2\text{tr}(W(C^{-1} - A)) + \boldsymbol{\delta}W\boldsymbol{\delta}'$$

3.

$$\begin{aligned} n(\hat{\boldsymbol{\theta}}^{PT} - \boldsymbol{\theta})(\hat{\boldsymbol{\theta}}^{PT} - \boldsymbol{\theta})' &= n\{(\hat{\boldsymbol{\theta}}^U - \boldsymbol{\theta}) - (\hat{\boldsymbol{\theta}}^U - \hat{\boldsymbol{\theta}}^R)I(\mathcal{L}_n < \mathcal{L}_{n,\alpha})\} \{ \\ &\quad (\hat{\boldsymbol{\theta}}^U - \boldsymbol{\theta}) - (\hat{\boldsymbol{\theta}}^U - \hat{\boldsymbol{\theta}}^R)I(\mathcal{L}_n < \mathcal{L}_{n,\alpha})\}' \\ &= n(\hat{\boldsymbol{\theta}}^U - \boldsymbol{\theta})(\hat{\boldsymbol{\theta}}^U - \boldsymbol{\theta})' + n[(\hat{\boldsymbol{\theta}}^U - \hat{\boldsymbol{\theta}}^R)(\hat{\boldsymbol{\theta}}^U - \hat{\boldsymbol{\theta}}^R)'] \end{aligned}$$

$$\begin{aligned}
& I^2(\mathcal{L}_n < \mathcal{L}_{n,\alpha})] - 2n[(\hat{\boldsymbol{\theta}}^U - \boldsymbol{\theta})(\hat{\boldsymbol{\theta}}^U - \hat{\boldsymbol{\theta}}^R) \\
& I(\mathcal{L}_n < \mathcal{L}_{n,\alpha})] \\
& = T_n^{(1)}T_n^{(1)'} + T_n^{(3)}T_n^{(3)'}I^2(\mathcal{L}_n < \mathcal{L}_{n,\alpha}). \quad (2.37)
\end{aligned}$$

From Saleh (2006); Al-Momani (2013), as  $n \rightarrow \infty$ ,  $M_3(\hat{\boldsymbol{\theta}}^{PT})$  is given as

$$\begin{aligned}
M_3(\hat{\boldsymbol{\theta}}^{PT}) & = E\left(T_n^{(1)}T_n^{(1)'} + T_n^{(3)}T_n^{(3)'}I^2(\mathcal{L}_n < \mathcal{L}_{n,\alpha})\right) \\
& = E_1 + E_2 + E_3.
\end{aligned}$$

The first term is given by Theorem (2.4) part (1),

$$\begin{aligned}
E_1 & = E(T^{(1)}T^{(1)'}) = \sigma^2 C^{-1} \\
E_2 & = E(T^{(3)}T^{(3)'}I^2(\mathcal{L}_n < \mathcal{L}_{n,\alpha}; \Delta^2)) \\
& = \sigma^2 AG_{m+2}(\chi_m^2(\alpha); \Delta^2) + \boldsymbol{\delta}\boldsymbol{\delta}'G_{m+2}(\chi_m^2(\alpha); \Delta^2) - G_{m+4}(\chi_m^2(\alpha); \Delta^2) \\
E_3 & = -2E\left\{E\{T^{(3)}T^{(3)'}I^2(\mathcal{L}_n < \mathcal{L}_{n,\alpha}; \Delta^2)|T^{(3)}\}\right\} \\
& = -2E_2 + 2\boldsymbol{\delta}\boldsymbol{\delta}'G_{m+2}(\chi_m^2(\alpha); \Delta^2).
\end{aligned}$$

Hence,

$$\begin{aligned}
M_3(\hat{\boldsymbol{\theta}}^{PT}) & = \sigma^2[C^{-1} - AG_{m+2}(\chi_m^2(\alpha); \Delta^2)] + \\
& \quad \boldsymbol{\delta}\boldsymbol{\delta}'\{2G_{m+2}(\chi_m^2(\alpha); \Delta^2) - G_{m+4}(\chi_m^2(\alpha); \Delta^2)\}. \\
R_3(\hat{\boldsymbol{\theta}}^{PT}, W) & = \text{tr}(WM_3(\hat{\boldsymbol{\theta}}^{PT}))
\end{aligned}$$

$$\begin{aligned}
& tr(W(\sigma^2[C^{-1} - AG_{m+2}(\chi_m^2(\alpha); \Delta^2)] + \\
& \delta\delta\{2G_{m+2}(\chi_m^2(\alpha); \Delta^2) - G_{m+4}(\chi_m^2(\alpha); \Delta^2)\}) \\
& = \sigma^2 tr(WC^{-1}) - \sigma^2 tr(WA)G_{m+2}(\chi_m^2(\alpha); \Delta^2) + \\
& 2\delta W\delta\{G_{m+2}(\chi_m^2(\alpha); \Delta^2) - G_{m+4}(\chi_m^2(\alpha); \Delta^2)\}.
\end{aligned}$$

4. Also, note that

$$\begin{aligned}
n(\hat{\boldsymbol{\theta}}^S - \boldsymbol{\theta})(\hat{\boldsymbol{\theta}}^S - \boldsymbol{\theta})' &= n(\hat{\boldsymbol{\theta}}^U - (m-2)(\hat{\boldsymbol{\theta}}^U - \hat{\boldsymbol{\theta}}^R)\mathcal{L}_n^{-1} - \boldsymbol{\theta}) \\
& \quad (\hat{\boldsymbol{\theta}}^U - (m-2)(\hat{\boldsymbol{\theta}}^U - \hat{\boldsymbol{\theta}}^R)\mathcal{L}_n^{-1} - \boldsymbol{\theta})' \\
&= n(\hat{\boldsymbol{\theta}}^U - \boldsymbol{\theta})(\hat{\boldsymbol{\theta}}^U - \boldsymbol{\theta})' + n(m-2)^2(\hat{\boldsymbol{\theta}}^U - \hat{\boldsymbol{\theta}}^R)(\hat{\boldsymbol{\theta}}^U \\
& \quad - \hat{\boldsymbol{\theta}}^R)'\mathcal{L}_n^{-2} - 2n(m-2)(\hat{\boldsymbol{\theta}}^U - \hat{\boldsymbol{\theta}}^R)(\hat{\boldsymbol{\theta}}^U - \hat{\boldsymbol{\theta}}^R)'\mathcal{L}_n^{-1} \\
&= T_n^{(1)}T_n^{(1)'} + (m-2)^2T_n^{(3)}T_n^{(3)'}\mathcal{L}_n^{-2} - 2(m-2)T_n^{(1)} \\
& \quad T_n^{(3)'}\mathcal{L}_n^{-2}.
\end{aligned}$$

Therefore, as  $n \rightarrow \infty$ ,  $M_4(\hat{\boldsymbol{\theta}}^S) = E_1 + E_2 + E_3$ ,

where

$$\begin{aligned}
E_1 &= E(T^{(1)}T^{(1)'}) = \sigma^2 C^{-1} \\
E_2 &= (m-2)^2 E(T^{(3)}T^{(3)'}\mathcal{L}_n^{-2}) \\
&= (m-2)^2 \sigma^2 A E(\chi_{m+2}^{-4}(\Delta^2)) + (m-2)^2 \delta\delta E(\chi_{m+4}^{-4}(\Delta^2)) \\
E_3 &= -2(m-2) E\{T^{(1)}T^{(3)'}\mathcal{L}_n^{-1}\}
\end{aligned}$$

$$\begin{aligned}
&= -2(m-2)E\{T^{(1)}T^{(3)'}\mathcal{L}_n^{-1}|T_n^{(3)}\} \\
&= -2(m-2)\{E(T^{(1)}T^{(3)'}\mathcal{L}_n^{-1}) - \boldsymbol{\delta}E(T_n^{(3)'}\mathcal{L}_n^{-1})\} \\
&= -2(m-2)\sigma^2AE(\chi_{m+2}^{-2}(\Delta^2)) - 2(m-2)\boldsymbol{\delta}\boldsymbol{\delta}'\{E(\chi_{m+4}^{-2}(\Delta^2)) - \\
&\quad E(\chi_{m+2}^{-2}(\Delta^2))\}.
\end{aligned}$$

Then,

$$\begin{aligned}
M_4(\hat{\boldsymbol{\theta}}^S) &= \sigma^2C^{-1} - (m-2)\sigma^2A\{2E[\chi_{m+4}^{-4}(\Delta^2)] - (m-2)E[\chi_{m+2}^{-4}(\Delta^2)]\} \\
&\quad + (m-2)(m+2)\boldsymbol{\delta}\boldsymbol{\delta}'E[\chi_{m+4}^{-4}(\Delta^2)].
\end{aligned}$$

$$\begin{aligned}
R_4(\hat{\boldsymbol{\theta}}^S, W) &= \text{tr}(M_4(\hat{\boldsymbol{\theta}}^S)) \\
&= \sigma^2\text{tr}(WC^{-1}) - \sigma^2(m-2)\text{tr}(WA) \times \{2E[\chi_{m+4}^{-4}(\Delta^2)] - (m \\
&\quad - 2)E[\chi_{m+2}^{-4}(\Delta^2)]\} + (m-2)(m+2)\boldsymbol{\delta}W\boldsymbol{\delta}'E[\chi_{m+4}^{-4}(\Delta^2)].
\end{aligned}$$

5. Note that

$$\begin{aligned}
n(\hat{\boldsymbol{\theta}}^{S+} - \boldsymbol{\theta})(\hat{\boldsymbol{\theta}}^{S+} - \boldsymbol{\theta})' &= n[\hat{\boldsymbol{\theta}}^S - (1 - (m-2)\mathcal{L}_n^{-1})I\mathcal{L}_n < (m-2) \\
&\quad (\hat{\boldsymbol{\theta}}^U - \hat{\boldsymbol{\theta}}^R) - \boldsymbol{\theta}][\hat{\boldsymbol{\theta}}^S - (1 - (m-2)\mathcal{L}_n^{-1})I\mathcal{L}_n \\
&\quad < (m-2)(\hat{\boldsymbol{\theta}}^U - \hat{\boldsymbol{\theta}}^R) - \boldsymbol{\theta}]' \\
&= n(\hat{\boldsymbol{\theta}}^S - \boldsymbol{\theta})(\hat{\boldsymbol{\theta}}^S - \boldsymbol{\theta})' + n(\hat{\boldsymbol{\theta}}^U - \hat{\boldsymbol{\theta}}^R)(\hat{\boldsymbol{\theta}}^U - \hat{\boldsymbol{\theta}}^R)' \\
&\quad (1 - (m-2)\mathcal{L}_n^{-1})^2I(\mathcal{L}_n < (m-2)) - 2n(\hat{\boldsymbol{\theta}}^S - \boldsymbol{\theta}) \\
&\quad (\hat{\boldsymbol{\theta}}^S - \boldsymbol{\theta})'(1 - (m-2)\mathcal{L}_n^{-1})I(\mathcal{L}_n < (m-2)) \\
&= -2T_n^{(2)}T_n^{(3)'}(1 - (m-2)\mathcal{L}_n^{-1})I(\mathcal{L}_n < (m-2)) -
\end{aligned}$$

$$2T_n^{(3)}T_n^{(3)'}(1 - (m - 2)\mathcal{L}_n^{-1})^2I(\mathcal{L}_n < (m - 2)).$$

$$\text{Therefore, as } n \longrightarrow \infty, \quad M_5(\hat{\boldsymbol{\theta}}^{S+}) = E_1 + E_2 + E_3,$$

where

$$\begin{aligned} E_1 &= M_4(\hat{\boldsymbol{\theta}}^S) \\ E_2 &= E\{T^{(3)}T^{(3)'}(1 - (m - 2)\mathcal{L}^{-1})I(\mathcal{L} < (m - 2))\} \\ &= \sigma^2AE\{(1 - (m - 2)\chi_{m+2}^{-2}(\Delta^2))^2I(\chi_{m+2}^2(\Delta^2) < (m - 2))\} \\ &\quad + \delta\delta E\{(1 - (m - 2)\chi_{m+4}^{-2}(\Delta^2))^2I(\chi_{m+4}^2(\Delta^2) < (m - 2))\} \\ E_3 &= -2E(T^{(2)})E(T^{(3)'}(1 - (m - 2)\mathcal{L}^{-1})I(\mathcal{L} < (m - 2))) \\ &\quad - 2E(T^{(3)}T^{(3)'}(1 - (m - 2)\mathcal{L}^{-1})I(\mathcal{L} < (m - 2))) \\ &= 2\delta\delta E\{(1 - (m - 2)\chi_{m+2}^{-2}(\Delta^2))I(\chi_{m+2}^2(\Delta^2) < (m - 2))\} \\ &\quad 2\sigma^2AE\{(1 - (m - 2)\chi_{m+2}^{-2}(\Delta^2))I(\chi_{m+2}^2(\Delta^2) < (m - 2))\} \\ &\quad - 2\delta\delta E\{(1 - (m - 2)\chi_{m+4}^{-2}(\Delta^2))I(\chi_{m+4}^2(\Delta^2) < (m - 2))\}. \end{aligned}$$

$$\begin{aligned} M_5(\hat{\boldsymbol{\theta}}^{S+}) &= M_4(\hat{\boldsymbol{\theta}}^S) - \sigma^2AE[(1 - (m - 2)\chi_{(m+2)}^2(\Delta^2))^2I(\chi_{(m+2)}^2(\Delta^2) < \\ &\quad (m - 2))] + \delta\delta' \left\{ 2E[(1 - (m - 2)\chi_{m+2}^{-2}(\Delta^2))I(\chi_{m+2}^{-2}(\Delta^2) < \right. \\ &\quad (m - 2)) - E[(1 - (m - 2)\chi_{m+4}^{-2}(\Delta^2))^2(\chi_{m+4}^2(\Delta^2) \\ &\quad \left. < (m - 2))] \right\}. \end{aligned}$$

$$R_5(\hat{\boldsymbol{\theta}}^{S+}, W) = \text{tr}(M_5(\hat{\boldsymbol{\theta}}^{S+}))$$

$$\begin{aligned}
&= R_4(\hat{\boldsymbol{\theta}}^S, W) - \sigma^2(C^{-1} - A)E[(1 - (m - 2)\chi_{m+2}^{-2}(\Delta^2))^2 \\
&\quad I(\chi_{m+2}^{-2}(\Delta^2) < (m - 2)) + \boldsymbol{\delta}W\boldsymbol{\delta}'\left\{2E[(1 - (m - 2) \right. \\
&\quad \chi_{m+4}^2(\Delta^2))I(\chi_{m+4}^2(\Delta^2) < (m - 2))] - E[(1 - (m - 2) \\
&\quad \left. \chi_{m+4}^{-2}(\Delta^2))^2I(\chi_{m+4}^2(\Delta^2) < (m - 2))]\right\}.
\end{aligned}$$

## 2.7 Risk Analysis of the Estimators

In this subsection we will discuss and investigate the asymptotic weighted risk of the estimators using the loss function defined in (2.34).

### 2.7.1 Comparison of $\hat{\boldsymbol{\theta}}^U$ and $\hat{\boldsymbol{\theta}}^R$

It is clear that the risk of  $\hat{\boldsymbol{\theta}}^U$  is constant, whereas the risk of  $\hat{\boldsymbol{\theta}}^R$  depends on  $\boldsymbol{\delta}'W\boldsymbol{\delta}$ , hence the difference in their risks is

$$\begin{aligned}
R_1(\hat{\boldsymbol{\theta}}^U, W) - R_2(\hat{\boldsymbol{\theta}}^R, W) &= \sigma^2 \text{tr}(WC^{-1}) - \sigma^2 \text{tr}[WC^{-1}R'[RC^{-1}R']^{-1}RC^{-1}] \\
&\quad + \boldsymbol{\delta}'W\boldsymbol{\delta}.
\end{aligned}$$

Note that  $C^{-1/2}R'[RC^{-1}R']^{-1}RC^{-1/2}$  is a symmetric idempotent matrix with rank  $m(\leq q)$ . Therefore, by Courant's Theorem; see Theorem A.1, there exists an orthogonal matrix  $\Gamma$  such that

$$\Gamma C^{-1/2}R'[RC^{-1}R']^{-1}RC^{-1/2}\Gamma' = \begin{pmatrix} I_m & 0 \\ 0 & 0 \end{pmatrix},$$

and

$$\Gamma C^{-1/2} W C^{-1/2} \Gamma' = \begin{pmatrix} A_{11} & A_{12} \\ A'_{12} & A_{22} \end{pmatrix}.$$

Then

$$\begin{aligned} \text{tr} \left[ W \{ C^{-1} R' [RC^{-1} R']^{-1} RC^{-1} \} \right] &= \text{tr} \left[ \{ \Gamma C^{-1/2} W C^{-1/2} \Gamma' \} \{ \Gamma C^{-1/2} \right. \\ &\quad \left. R' [RC^{-1} R']^{-1} RC^{-1/2} \Gamma' \} \right] \\ &= \text{tr} \left\{ \begin{bmatrix} A_{11} & A_{12} \\ A_{21} & A_{22} \end{bmatrix} \begin{bmatrix} I_m & 0 \\ 0 & 0 \end{bmatrix} \right\} \\ &= \text{tr}(A_{11}). \end{aligned} \tag{2.38}$$

$$\begin{aligned} \delta' W \delta &= (R\boldsymbol{\theta} - r)' [RC^{-1} R']^{-1} RC^{-1} W C^{-1} R' [RC^{-1} R']^{-1} \\ &\quad (R\boldsymbol{\theta} - r) \\ &= [\Gamma C^{1/2} \boldsymbol{\theta} - \Gamma C^{-1/2} R' [RC^{-1} R']^{-1} r]^{-1} \\ &\quad \times [\Gamma C^{-1/2} R' [RC^{-1} R']^{-1} RC^{-1/2} \Gamma'] \\ &\quad [\Gamma C^{-1/2} W C^{-1/2} \Gamma'] \\ &\quad \times [\Gamma C^{-1/2} R' [RC^{-1} R']^{-1} RC^{-1/2} \Gamma'] \\ &\quad \times [\Gamma C^{1/2} \boldsymbol{\theta} - \Gamma C^{-1/2} R' [RC^{-1} R']^{-1} r] \\ &= \eta' \begin{pmatrix} I_m & 0 \\ 0 & 0 \end{pmatrix} \begin{pmatrix} A_{11} & A_{12} \\ A_{21} & A_{22} \end{pmatrix} \begin{pmatrix} I_m & 0 \\ 0 & 0 \end{pmatrix} \eta \\ &= \eta'_1 A_{11} \eta_1, \end{aligned} \tag{2.39}$$



where

$$\eta = \Gamma C^{1/2} \boldsymbol{\theta} - \Gamma C^{-1/2} R' [RC^{-1}R']^{-1} r = \begin{pmatrix} \eta_1 \\ \eta_2 \end{pmatrix}.$$

Thus, using (2.38) and (2.39) we obtain

$$R_2(\hat{\boldsymbol{\theta}}^R, W) = \sigma^2 \text{tr}(WC^{-1}) - \sigma^2 \text{tr}(A_{11}) + \eta'_1 A_{11} \eta_1.$$

By Courant's Theorem, we say

$$Ch_{\min}(A_{11}) \leq \frac{\eta'_1 A_{11} \eta_1}{\eta'_1 \eta_1} \leq Ch_{\max}(A_{11}),$$

or

$$\sigma^2 \Delta^2 Ch_{\min}(A_{11}) \leq \eta'_1 A_{11} \eta_1 \leq \sigma^2 \Delta^2 Ch_{\max}(A_{11}),$$

where  $Ch_{\min}(A_{11}), Ch_{\max}(A_{11})$  are respectively the minimum and the maximum characteristic roots of  $A_{11}$ , and  $\Delta^2 = \eta'_1 \eta_1 / \sigma^2$ , so,

$$\begin{aligned} R_1(\hat{\boldsymbol{\theta}}^U; W) - \sigma^2 \text{tr}(A_{11}) + Ch_{\max}(A_{11}) &\leq R_2(\hat{\boldsymbol{\theta}}^R, W) \leq R_1(\hat{\boldsymbol{\theta}}^U, W) - \\ &\sigma^2 \text{tr}(A_{11}) + Ch_{\min}(A_{11}), \end{aligned} \quad (2.40)$$

where  $\Delta^2 = 0$ , the bounds are equal. Therefore, the previous inequality indicates that  $\hat{\boldsymbol{\theta}}^R$  performs better than  $\hat{\boldsymbol{\theta}}^U$  where

$$\Delta^2 \leq \frac{\text{tr}(A_{11})}{Ch_{\max}(A_{11})},$$

whereas  $\hat{\theta}^U$  performs better than  $\hat{\theta}^R$  whenever

$$\Delta^2 \geq \frac{tr(A_{11})}{Ch_{min}(A_{11})}.$$

For  $W = C$ , we see  $\hat{\theta}^R$  performs better than  $\hat{\theta}^U$  in the interval  $[0, m]$  and outside this interval  $\hat{\theta}^U$  performs better than  $\hat{\theta}^R$ .

### 2.7.2 Comparison of $\hat{\theta}^{PT}$ and $\hat{\theta}^U$

The risk difference is given by:

$$\begin{aligned} R_1(\hat{\theta}^U, W) - R_3(\hat{\theta}^{PT}, W) &= \sigma^2 tr(A_{11}) G_{m+2}(\chi_m^2(\alpha); \Delta^2) - \\ &\quad 2(\eta_1' A_{11} \eta_1) \left\{ G_{m+2}(\chi_m^2(\alpha); \Delta^2) \right. \\ &\quad \left. - G_{m+4}(\chi_m^2(\alpha); \Delta^2) \right\}. \end{aligned} \quad (2.41)$$

The right hand side of (2.41) is non-negative whenever

$$\Delta^2 \leq \frac{tr(A_{11})}{Ch_{min}(A_{11})} \frac{G_{m+2}(\chi_m^2(\alpha); \Delta^2)}{\{2G_{m+2}(\chi_m^2(\alpha); \Delta^2) - G_{m+4}(\chi_m^2(\alpha); \Delta^2)\}},$$

in this range  $\hat{\theta}^{PT}$  performs better than  $\hat{\theta}^U$ , whereas,  $\hat{\theta}^U$  performs better than  $\hat{\theta}^{PT}$  whenever

$$\Delta^2 \geq \frac{tr(A_{11})}{Ch_{min}(A_{11})} \frac{G_{m+2}(\chi_m^2(\alpha); \Delta^2)}{\{2G_{m+2}(\chi_m^2(\alpha); \Delta^2) - G_{m+4}(\chi_m^2(\alpha); \Delta^2)\}}.$$

Under the hypothesis (1.2),  $\hat{\theta}^{PT}$  is superior to  $\hat{\theta}^U$ .

### 2.7.3 Comparison of $\hat{\theta}^S$ and $\hat{\theta}^U$

The risk difference is given by

$$R_1(\hat{\theta}^U, W) - R_4(\hat{\theta}^S, W) = \sigma^2(m-2)(m+2)\text{tr}(A_{11})\{(m-2)E(\chi_{(m+2)}^{-4}(\Delta^2))\} + \left[1 - \frac{(m+2)(\eta_1' A_{11} \eta_1)}{2\sigma^2 \Delta^2 \text{tr}(A_{11})}\right] (2\Delta^2) E[\chi_{m+4}^{-4}(\Delta^2)].$$

the risk difference is positive whenever

$$\frac{\text{tr}(A_{11})}{Ch_{max}(A_{11})} \geq \frac{m+2}{2}.$$

Note that  $A_{11}$  involves the matrix  $W$ , hence,  $\hat{\theta}^S$  dominates  $\hat{\theta}^U$ . As  $\Delta^2 \rightarrow \infty$ , the risk difference approaches to 0 from below.

### 2.7.4 Comparison of $\hat{\theta}^S$ and $\hat{\theta}^{S+}$

The risk difference is given by:

$$R_4(\hat{\theta}^S, W) - R_5(\hat{\theta}^{S+}, W) = \sigma^2(C^{-1} - A)E[(1 - (m-2)\chi_{m+2}^{-2}(\Delta^2))^2 I(\chi_{m+2}^{-2}(\Delta^2) < (m-2))] + \delta W \delta' \left\{ 2E[(1 - (m-2)\chi_{m+4}^2(\Delta^2))I(\chi_{m+4}^2(\Delta^2) < (m-2))] - E[(1 - (m-2)\chi_{m+4}^{-2}(\Delta^2))^2 I(\chi_{m+4}^2(\Delta^2) < (m-2))] \right\}.$$

The right hand side of the previous equation is positive semidefinite, since the expected value of the non-negative random variable is non-negative by the indicator function

$$[0 < \chi_{m+2}^{-2}(\Delta^2) < (m-2)] \longleftrightarrow [(m-2)\chi_{m+2}^{-2}(\Delta^2) - 1] \geq 0,$$

see (Saleh, 2006, p.360). Hence, we get

$$E[((m-2)\chi_{m+2}^{-2}(\Delta^2) - 1)I(\chi_{m+2}^{-2}(\Delta^2) < (m-2))] \geq 0,$$

and for all  $\Delta^2$ ,

$$R_5(\hat{\boldsymbol{\theta}}^{S+}, W) \leq R_4(\hat{\boldsymbol{\theta}}^S, W),$$

and  $\hat{\boldsymbol{\theta}}^{S+}$  not only assures inadmissibility of  $\hat{\boldsymbol{\theta}}^S$  but also provides a simple superior estimator.

As a result we can conclude that

$$R_5(\hat{\boldsymbol{\theta}}^{S+}, W) \leq R_4(\hat{\boldsymbol{\theta}}^S, W) \leq R_1(\hat{\boldsymbol{\theta}}^U, W).$$

which means that  $\hat{\boldsymbol{\theta}}^{S+}$  is uniformly dominates the unrestricted estimate.

## 2.8 MSE-Matrix Analysis of the Estimator

In this section we compare the array of estimators with respect to the unrestricted estimator in term of their mean squared error. Comparisons are given below in

the rest of the subsections.

### 2.8.1 Comparison of $\hat{\boldsymbol{\theta}}^R$ and $\hat{\boldsymbol{\theta}}^U$

$$M_1(\hat{\boldsymbol{\theta}}^U) - M_2(\hat{\boldsymbol{\theta}}^R) = \sigma^2 C^{-1} - \sigma^2 C^{-1} + \sigma^2 A - \boldsymbol{\delta}'\boldsymbol{\delta}.$$

The MSE difference matrix is positive semidefinite whenever for a nonzero vector  $\boldsymbol{\ell} = (\ell_1, \dots, \ell_q)'$  of length  $q$ , we have

$$\boldsymbol{\ell}'[M_1(\hat{\boldsymbol{\theta}}^U) - M_2(\hat{\boldsymbol{\theta}}^R)]\boldsymbol{\ell} \geq 0.$$

That is,

$$\sigma^2 \boldsymbol{\ell}'[C^{-1}R'[RC^{-1}R']^{-1}R'C^{-1}]\boldsymbol{\ell} \geq \boldsymbol{\ell}'\boldsymbol{\delta}\boldsymbol{\delta}'\boldsymbol{\ell}.$$

Therefore, we have

$$\frac{\boldsymbol{\ell}'\boldsymbol{\delta}\boldsymbol{\delta}'\boldsymbol{\ell}}{\sigma^2 \boldsymbol{\ell}'C^{-1}\boldsymbol{\ell}} \leq \frac{\sigma^2 \boldsymbol{\ell}'[C^{-1}R'[RC^{-1}R']^{-1}R'C^{-1}]\boldsymbol{\ell}}{\sigma^2 \boldsymbol{\ell}'C^{-1}\boldsymbol{\ell}}.$$

Hence,

$$\begin{aligned} \Delta^2 &= \text{Max}_{\boldsymbol{\ell}} \frac{\boldsymbol{\ell}'\boldsymbol{\delta}\boldsymbol{\delta}'\boldsymbol{\ell}}{\sigma^2 \boldsymbol{\ell}'C^{-1}\boldsymbol{\ell}} \leq \text{Max}[\boldsymbol{\ell}'[C^{-1}R'[RC^{-1}R']^{-1}R'C^{-1}]\boldsymbol{\ell}] \\ \Delta^2 &\leq Ch_{\text{Max}} \frac{\boldsymbol{\ell}'[R'[RC^{-1}R']^{-1}R'C^{-1}]\boldsymbol{\ell}}{\boldsymbol{\ell}'C^{-1}\boldsymbol{\ell}} = 1. \end{aligned}$$

Since  $C^{-1/2}R'[RC^{-1}R']^{-1}R'C^{-1/2}$  is an idempotent matrix with maximum characteristic value or eigenvalue equals to 1. Thus,  $M_1(\hat{\boldsymbol{\theta}}^U) - M_2(\hat{\boldsymbol{\theta}}^R)$  is positive semidefinite matrix if and only if  $\Delta^2 \leq 1$ . Therefore,  $\hat{\boldsymbol{\theta}}^R$  performs better than  $\hat{\boldsymbol{\theta}}^U$  when  $\Delta^2 \leq 1$ ; otherwise,  $\hat{\boldsymbol{\theta}}^U$  performs better than  $\hat{\boldsymbol{\theta}}^R$ . The range of the domination of  $\hat{\boldsymbol{\theta}}^R$  over  $\hat{\boldsymbol{\theta}}^U$  is bigger in term of risks.

If  $W = C$ , the range of the domination is  $[0, m]$  and  $m \geq 0$ . The MSE-based relative efficiency (MRE) of  $\hat{\boldsymbol{\theta}}^R$  with respect to  $\hat{\boldsymbol{\theta}}^U$  is meaningless, since

$$MRE(\hat{\boldsymbol{\theta}}^R, \hat{\boldsymbol{\theta}}^U) = |I_q - R'[RC^{-1}R']^{-1}R'C^{-1} - \sigma^{-2}C\boldsymbol{\delta}\boldsymbol{\delta}'|^{-1/q} = \mathbf{0}.$$

while the relative risk efficiency (RRE) is different from  $\mathbf{0}$  and given by

$$RRE(\hat{\boldsymbol{\theta}}^R, \hat{\boldsymbol{\theta}}^U) = \left[ 1 - \frac{A_{11}}{tr(WC^{-1})} + \frac{\eta_1' A_{11} \eta_1}{tr(WC^{-1})} \right]^{-1}.$$

### 2.8.2 Comparison of $\hat{\boldsymbol{\theta}}^{PT}$ and $\hat{\boldsymbol{\theta}}^U$

$$\begin{aligned} M_1(\hat{\boldsymbol{\theta}}^U) - M_3(\hat{\boldsymbol{\theta}}^{PT}) &= \sigma^2 \left( C^{-1}R'[RC^{-1}R']^{-1}RC^{-1} \right)^{-1} G_{m+2}(\chi_m^2(\alpha); \Delta^2) \\ &= \boldsymbol{\delta}\boldsymbol{\delta}' \left\{ 2G_{m+2}(\chi_m^2(\alpha); \Delta^2) - G_{m+4}(\chi_m^2(\alpha); \Delta^2) \right\} \end{aligned} \quad (2.42)$$

The MSE in (2.42) is p.s.d. if for any non-zero vector  $\ell$  we have

$$\begin{aligned} &\sigma^2 \ell' \left( C^{-1}R'[RC^{-1}R']^{-1}RC^{-1} \right)^{-1} \ell G_{m+2}(\chi_m^2(\alpha); \Delta^2) \\ &- (\ell' \boldsymbol{\delta}\boldsymbol{\delta}' \ell) \left\{ 2G_{m+2}(\chi_m^2(\alpha); \Delta^2) - G_{m+4}(\chi_m^2(\alpha); \Delta^2) \right\} \geq 0. \end{aligned}$$

Therefore, we can write the previous inequality as

$$(\ell' \boldsymbol{\delta} \boldsymbol{\delta}' \ell) \left\{ 2G_{m+2}(\chi_m^2(\alpha); \Delta^2) - G_{m+4}(\chi_m^2(\alpha); \Delta^2) \right\} \leq \sigma^2 \ell' \left[ C^{-1} R' [RC^{-1} R']^{-1} \right. \\ \left. RC^{-1} \right]^{-1} \ell G_{m+2}(\chi_m^2(\alpha); \Delta^2)$$

$$\ell' \boldsymbol{\delta} \boldsymbol{\delta}' \ell \left\{ 2G_{m+2}(\chi_m^2(\alpha); \Delta^2) \sigma^2 \ell' \left\{ C^{-1} R' [RC^{-1} R']^{-1} RC^{-1} \right\} \ell \right\} \leq \left\{ 2G_{m+2}(\chi_m^2(\alpha); \Delta^2) - G_{m+4}(\chi_m^2(\alpha); \Delta^2) \right\}$$

$$\ell' \boldsymbol{\delta} \boldsymbol{\delta}' \ell \leq \frac{\sigma^2 \ell' \left\{ C^{-1} R' [RC^{-1} R']^{-1} RC^{-1} \right\} \ell 2G_{m+2}(\chi_m^2(\alpha); \Delta^2)}{\left\{ 2G_{m+2}(\chi_m^2(\alpha); \Delta^2) - G_{m+4}(\chi_m^2(\alpha); \Delta^2) \right\} \ell' C^{-1} \ell}$$

By taking the maximum overall non-zero vectors  $\ell$  we obtain

$$\begin{aligned} \Delta^2 &= \underset{\ell}{Max} \ell' \boldsymbol{\delta} \boldsymbol{\delta}' \ell \\ \Delta^2 &\leq \underset{\ell}{Max} \frac{\sigma^2 \ell' \left\{ C^{-1} R' [RC^{-1} R']^{-1} RC^{-1} \right\} \ell 2G_{m+2}(\chi_m^2(\alpha); \Delta^2)}{\left\{ 2G_{m+2}(\chi_m^2(\alpha); \Delta^2) - G_{m+4}(\chi_m^2(\alpha); \Delta^2) \right\} \ell' C^{-1} \ell} \quad (2.43) \\ \Delta^2 &\leq \frac{2G_{m+2}(\chi_m^2(\alpha); \Delta^2)}{\left\{ 2G_{m+2}(\chi_m^2(\alpha); \Delta^2) - G_{m+4}(\chi_m^2(\alpha); \Delta^2) \right\}} \leq 0. \end{aligned}$$

This mean  $\hat{\boldsymbol{\theta}}^{PT}$  performs better than  $\hat{\boldsymbol{\theta}}^U$  in the range of  $\Delta^2$  that is given by

(2.43), otherwise  $\hat{\boldsymbol{\theta}}^U$  is superior to  $\hat{\boldsymbol{\theta}}^{PT}$ . The range of domination of  $\hat{\boldsymbol{\theta}}^{PT}$  over  $\hat{\boldsymbol{\theta}}^U$  is bigger in case of risk analysis. If  $W = C$ , the range of  $\Delta^2$  is  $\leq m$ . The risk-based efficiency of  $\hat{\boldsymbol{\theta}}^{PT}$  relative to  $\hat{\boldsymbol{\theta}}^U$  is given by

$$RER(\hat{\boldsymbol{\theta}}^{PT}, \hat{\boldsymbol{\theta}}^U) = \left[ 1 - \frac{tr(A_{11})}{tr(WC^{-1})} G_{m+2}(\chi_m^2(\alpha); \Delta^2) + \frac{\boldsymbol{\delta}'_1 A_{11} \boldsymbol{\delta}_1}{tr(WC^{-1})} \right. \\ \left. \times \left\{ 2G_{m+2}(\chi_m^2(\alpha); \Delta^2) - G_{m+4}(\chi_m^2(\alpha); \Delta^2) \right\} \right]^{-1}. \quad (2.44)$$

If  $W = C$ , then (2.44) reduces to

$$m \left[ m - 2mG_{m+2}(\chi_m^2(\alpha); \Delta^2) + \Delta^2 \left\{ 2G_{m+2}(\chi_m^2(\alpha); \Delta^2) - G_{m+4}(\chi_m^2(\alpha); \Delta^2) \right\} \right]^{-1}.$$

Thus, the risk efficiency of  $\hat{\boldsymbol{\theta}}^{PT}$  is bigger than  $\hat{\boldsymbol{\theta}}^U$  whenever,

$$\Delta^2 \leq \frac{mG_{m+2}(\chi_m^2(\alpha); \Delta^2)}{\left\{ 2G_{m+2}(\chi_m^2(\alpha); \Delta^2) - G_{m+4}(\chi_m^2(\alpha); \Delta^2) \right\}}.$$

The MSE-based efficiency of  $\hat{\boldsymbol{\theta}}^{PT}$  relative to  $\hat{\boldsymbol{\theta}}^U$  is given by

$$MRE(\hat{\boldsymbol{\theta}}^{PT}, \hat{\boldsymbol{\theta}}^U) = \left| I_q - \{R'[RC^{-1}R']^{-1}RC^{-1}\}mG_{m+2}(\chi_m^2(\alpha); \Delta^2) + \right. \\ \left. \sigma^{-2}C\boldsymbol{\delta}\boldsymbol{\delta}' \left\{ 2G_{m+2}(\chi_m^2(\alpha); \Delta^2) - G_{m+4}(\chi_m^2(\alpha); \Delta^2) \right\} \right|^{-1/q} \\ = \left[ 1 - G_{m+2}(\chi_m^2(\alpha); \Delta^2) + \Delta^2 \left\{ 2G_{m+2}(\chi_m^2(\alpha); \Delta^2) - \right. \right. \\ \left. \left. G_{m+4}(\chi_m^2(\alpha); \Delta^2) \right\} \right]^{-1} \times \left\{ 1 - G_{m+2}(\chi_m^2(\alpha); \Delta^2) \right\}^{q-1/q}.$$



Thus, MRE of  $\hat{\theta}^{PT}$  is bigger than  $\hat{\theta}^U$  whenever,

$$\Delta^2 \leq \frac{\{1 - mG_{m+2}(\chi_m^2(\alpha); \Delta^2)\}^{\frac{q-1}{q}} - \{1 - mG_{m+2}(\chi_m^2(\alpha); \Delta^2)\}}{\left\{2G_{m+2}(\chi_m^2(\alpha); \Delta^2) - G_{m+4}(\chi_m^2(\alpha); \Delta^2)\right\}}.$$

### 2.8.3 Comparison of $\hat{\theta}^S$ and $\hat{\theta}^U$

We compare  $\hat{\theta}^S$  and  $\hat{\theta}^U$ . The MSE difference in this case is

$$\begin{aligned} M_1(\hat{\theta}^U) - M_4(\hat{\theta}^R) &= (m-2)(m+2)\sigma^2 \left\{ C^{-1}R'[RC^{-1}R']^{-1}RC^{-1} \right\} \\ &\quad \times \left\{ (m-2)E(\chi_{m+2}^{-4}(\Delta^2)) + 2\Delta^2 E(\chi_{m+4}^{-4}(\Delta^2)) \right\} \\ &\quad - (m-2)(m+2)^2 \boldsymbol{\delta}\boldsymbol{\delta}' E(\chi_{m+4}^{-4}(\Delta^2)). \end{aligned}$$

The difference is p.s.d. For a given nonzero vector  $\ell$  we have

$$\begin{aligned} &m(m-2)\sigma^2 \left\{ \ell' C^{-1}R'[RC^{-1}R']^{-1}RC^{-1}\ell \right\} \times \left\{ (m-2)E(\chi_{m+2}^{-4}(\Delta^2)) + \right. \\ &\left. 2\Delta^2 E(\chi_{m+4}^{-4}(\Delta^2)) \right\} - (m-2)(m+2)^2 (\ell'\boldsymbol{\delta}\boldsymbol{\delta}'\ell) E(\chi_{m+4}^{-4}(\Delta^2)) \geq 0. \end{aligned}$$

which implies

$$m\Delta^2 E(\chi_{m+4}^{-4}(\Delta^2)) \leq (m-2)E(\chi_{m+2}^{-4}(\Delta^2)),$$

but it does not hold for all  $\Delta^2$ . Thus, the performance of  $\hat{\theta}^S$  compared with  $\hat{\theta}^U$  varies.

In this case, the  $MSE(\hat{\boldsymbol{\theta}}^S, \hat{\boldsymbol{\theta}}^U)$  is given by:

$$\begin{aligned}
MSE(\hat{\boldsymbol{\theta}}^S, \hat{\boldsymbol{\theta}}^U) &= \left| I_q - m(m-2)R'[RC^{-1}R']^{-1}RC^{-1} \left\{ (m-2)E(\chi_{m+2}^{-4}(\Delta^2)) + \right. \right. \\
&\quad \left. \left. 2\Delta^2 E(\chi_{m+4}^{-4}(\Delta^2)) \right\} - m(m-2)(m+2)C\boldsymbol{\delta}\boldsymbol{\delta}'E(\chi_{m+4}^{-4}(\Delta^2)) \right|^{-1/q} \\
&= \left( 1 - m(m-2) \left\{ (m-2)E(\chi_{m+2}^{-4}(\Delta^2)) + 2\Delta^2 E(\chi_{m+2}^{-4}(\Delta^2)) \right\} \right. \\
&\quad \left. + m(m-2)(m+2)2\Delta^2 E(\chi_{m+4}^{-4}(\Delta^2)) \right)^{-1} \times \left( 1 - m(m-2) \right. \\
&\quad \left. \left\{ (m-2) \times E(\chi_{m+2}^{-4}(\Delta^2)) + 2\Delta^2 E(\chi_{m+2}^{-4}(\Delta^2)) \right\} \right)^{q-1/q}.
\end{aligned}$$

#### 2.8.4 Comparison of $\hat{\boldsymbol{\theta}}^S$ and $\hat{\boldsymbol{\theta}}^{S+}$

The comparison between  $\hat{\boldsymbol{\theta}}^S$  and  $\hat{\boldsymbol{\theta}}^{S+}$  with respect to their MSE starts by taking their difference as follows

$$\begin{aligned}
M_4(\hat{\boldsymbol{\theta}}^S) - M_5(\hat{\boldsymbol{\theta}}^{S+}) &= \sigma^2 AE[(1 - (m-2)\chi_{(m+2)}^2(\Delta^2))^2 I(\chi_{(m+2)}^2(\Delta^2) < (m-2))] \\
&\quad + \boldsymbol{\delta}\boldsymbol{\delta}' \left\{ 2E[(1 - (m-2)\chi_{m+2}^{-2}(\Delta^2)) I(\chi_{m+2}^{-2}(\Delta^2) < (m-2)) \right. \\
&\quad \left. - E[(1 - (m-2)\chi_{m+4}^{-2}(\Delta^2))^2 I(\chi_{m+4}^2(\Delta^2) < (m-2))] \right\}.
\end{aligned}$$

The MSE difference is positive semidefinite for all  $\Delta^2$ , and hence,  $\hat{\boldsymbol{\theta}}^{S+}$  dominates  $\hat{\boldsymbol{\theta}}^S$  uniformly.

## 2.9 Numerical Studies

In this section we will carry out numerical study to investigate the performance of the proposed estimators. In the first subsection we aim to examine the relative performance of the restricted, pretest and shrinkage estimators, while appointing the unrestricted estimator as a benchmark for comparison using Monte Carlo simulation. A real dataset from S&P500 stock market will be used to compare the performance of the estimators to confirm the analytical results obtained in the previous section.

### 2.9.1 Monte Carlo simulation experiments

The Monte Carlo simulation experiments will be conducted to compare the restricted, pretest and shrinkage estimators with respect to the unrestricted estimator. The following algorithm is used for the Monte Carlo simulation

1. We consider the model in Equation (2.9), we partition  $\boldsymbol{\theta}$  as  $\boldsymbol{\theta} = (\boldsymbol{\theta}_1, \boldsymbol{\theta}_2)$ , where  $\boldsymbol{\theta}_1$  is a  $(q - m + 1) \times 1$  of non-zeros and  $\boldsymbol{\theta}_2$  is  $m \times 1$  vector of zeros. We define the parameter  $\Delta^2 = \|\boldsymbol{\theta} - \boldsymbol{\theta}_0\|$ , where  $\boldsymbol{\theta}_0 = (\boldsymbol{\theta}_1, \mathbf{0})$ ,  $\boldsymbol{\theta} = (\boldsymbol{\theta}_1, \mathbf{0} + \boldsymbol{\delta})$  and  $\|\cdot\|$  denotes the Euclidian norm. In addition,  $\Delta^2 = \|\boldsymbol{\delta}\|$ , where this vector of alternative values was chosen to vary from 0 to .55 and  $m = 3, 4, 5, 9, 12$  and 15.
2. Generate an error term  $(\eta_t)$  from standard normal distribution.
3. Generate  $\mathbf{X}$  matrix of size  $n \times (q + 1)$  with initial values simulated from

standard normal distribution with  $n = 30, 50, 75, 100$  and  $150$ .

4. Estimate a matrix  $\mathbf{U}_{nx1} = (\boldsymbol{\eta}^2 - 1) * X\boldsymbol{\theta}_0$ .
5. Estimate the Vector  $Y = X\boldsymbol{\theta}_0 + \mathbf{U}$
6. Estimate the unrestricted, restricted, pretest, shrinkage and positive shrinkage estimators using the formulas in (2.11), (2.21), (2.24), (2.25) and (2.26) respectively.
7. Compute the simulated mean squared errors (SMSE) for each estimator by using the following formula

$$SMSE(\hat{\boldsymbol{\theta}}^*) = \sum_{i=1}^{q+1} (\hat{\boldsymbol{\theta}}^* - \boldsymbol{\theta})^2, \quad (2.45)$$

where  $\hat{\boldsymbol{\theta}}^*$  denotes any one of  $\{\hat{\boldsymbol{\theta}}^U, \hat{\boldsymbol{\theta}}^R, \hat{\boldsymbol{\theta}}^{PT}, \hat{\boldsymbol{\theta}}^S, \hat{\boldsymbol{\theta}}^{S+}\}$ .

8. Repeat the steps (2) - (7) for  $K$ -times, we see  $K = 3000$  is suitable to obtain stable results.
9. Compute the simulated relative efficiency (SRE) as follows

$$SRE(\hat{\boldsymbol{\theta}}^U, \hat{\boldsymbol{\theta}}^*) = \frac{SMSE(\hat{\boldsymbol{\theta}}^U)}{SMSE(\hat{\boldsymbol{\theta}}^*)}, \quad (2.46)$$

where  $\hat{\boldsymbol{\theta}}^U$  is appointed as benchmark. A value greater than one of the  $SRE(\hat{\boldsymbol{\theta}}^U, \hat{\boldsymbol{\theta}}^*)$  indicates that  $\hat{\boldsymbol{\theta}}^*$  performs better than  $\hat{\boldsymbol{\theta}}^U$  and vice versa.

The results of these simulations are reported in Figures 2.1 to 2.5 and Tables

2.1 to 2.30. The numerical results effectively assured our analytical results that positive shrinkage estimator plays as a safeguard against the high risks associated with the reduced model that we get under the set of local alternatives.  $\hat{\theta}^R$  shows the best performance under the null space and it degrades towards zero as the value of  $\Delta^2$  goes way from the null space.

As the value of  $\Delta^2$  increases, the superiority changes from  $\hat{\theta}^R$  to  $\hat{\theta}^{PT}$ ,  $\hat{\theta}^S$  and  $\hat{\theta}^{S+}$ .  $\hat{\theta}^{S+}$  dominantly superior others as it works as a safeguard against the high risks associated with the reduced model as we go away from the null space.

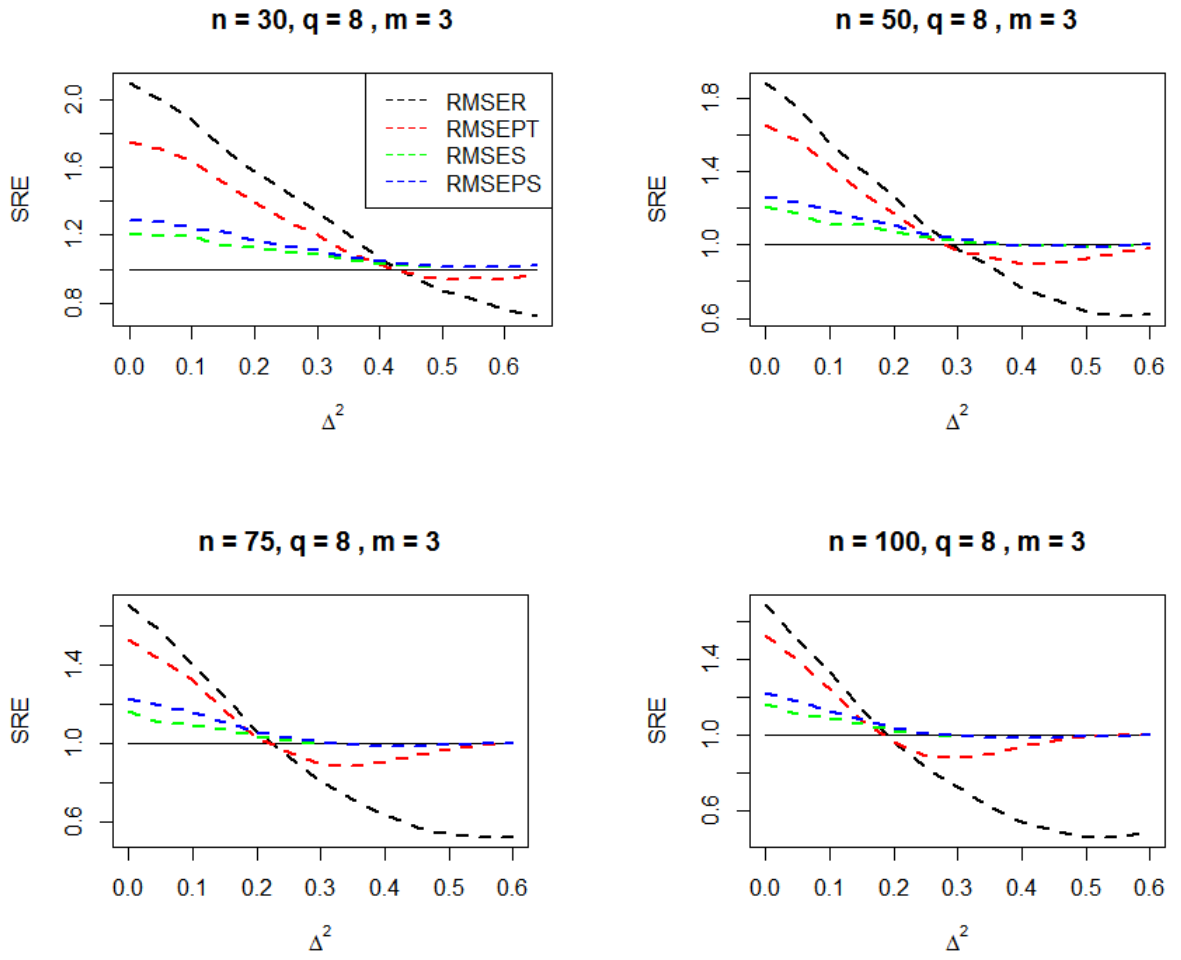


Figure 2.1: Simulated relative efficiency of the restricted, pretest and shrinkage estimators with respect to  $\hat{\theta}^U$  when  $m = 3$  and  $q = 8$  and different sample sizes.

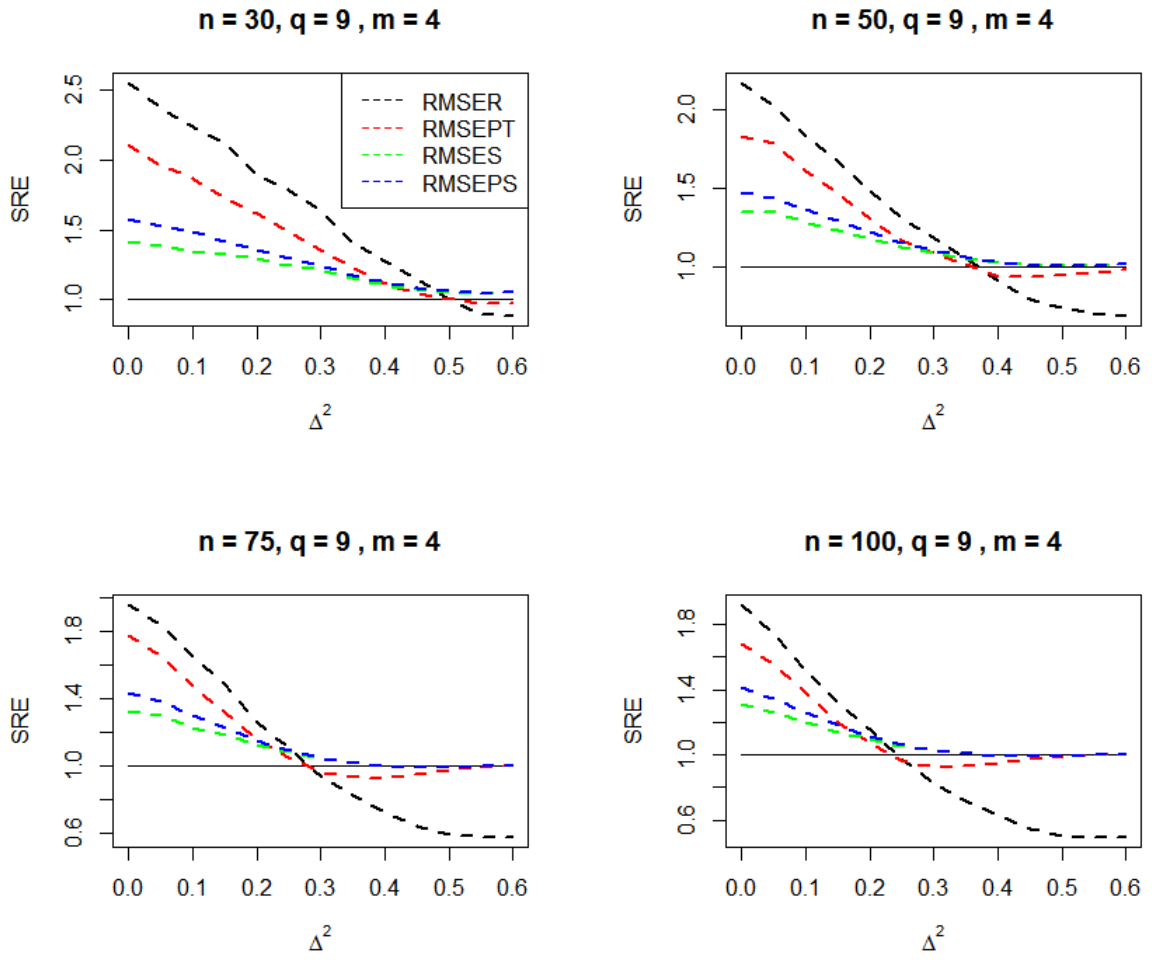


Figure 2.2: Simulated relative efficiency of the restricted, pretest and shrinkage estimators with respect to  $\hat{\theta}^U$  when  $m = 4$  and  $q = 9$  and different sample sizes.

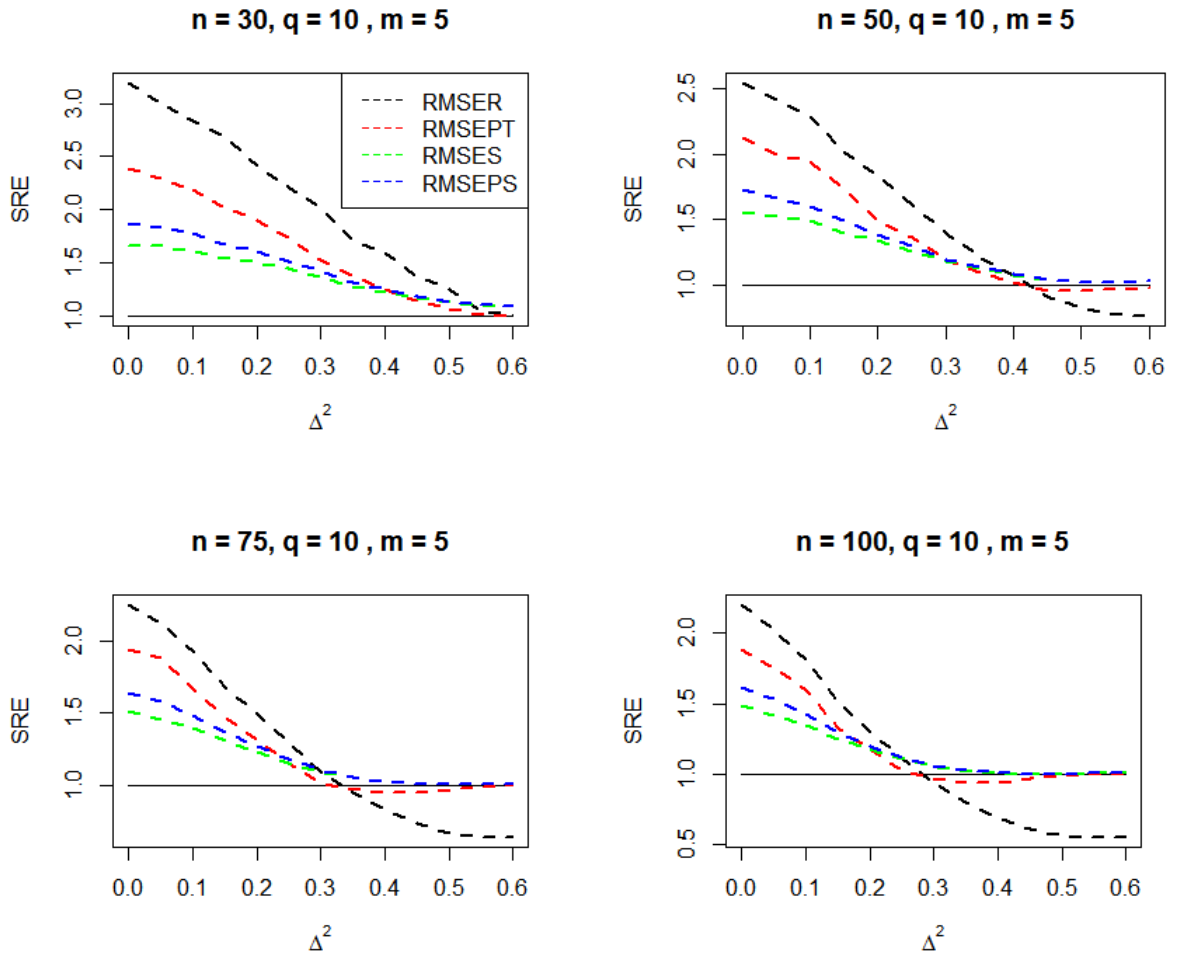


Figure 2.3: Simulated relative efficiency of the restricted, pretest and shrinkage estimators with respect to  $\hat{\theta}^U$  when  $m = 5$  and  $q = 10$  and different sample sizes.



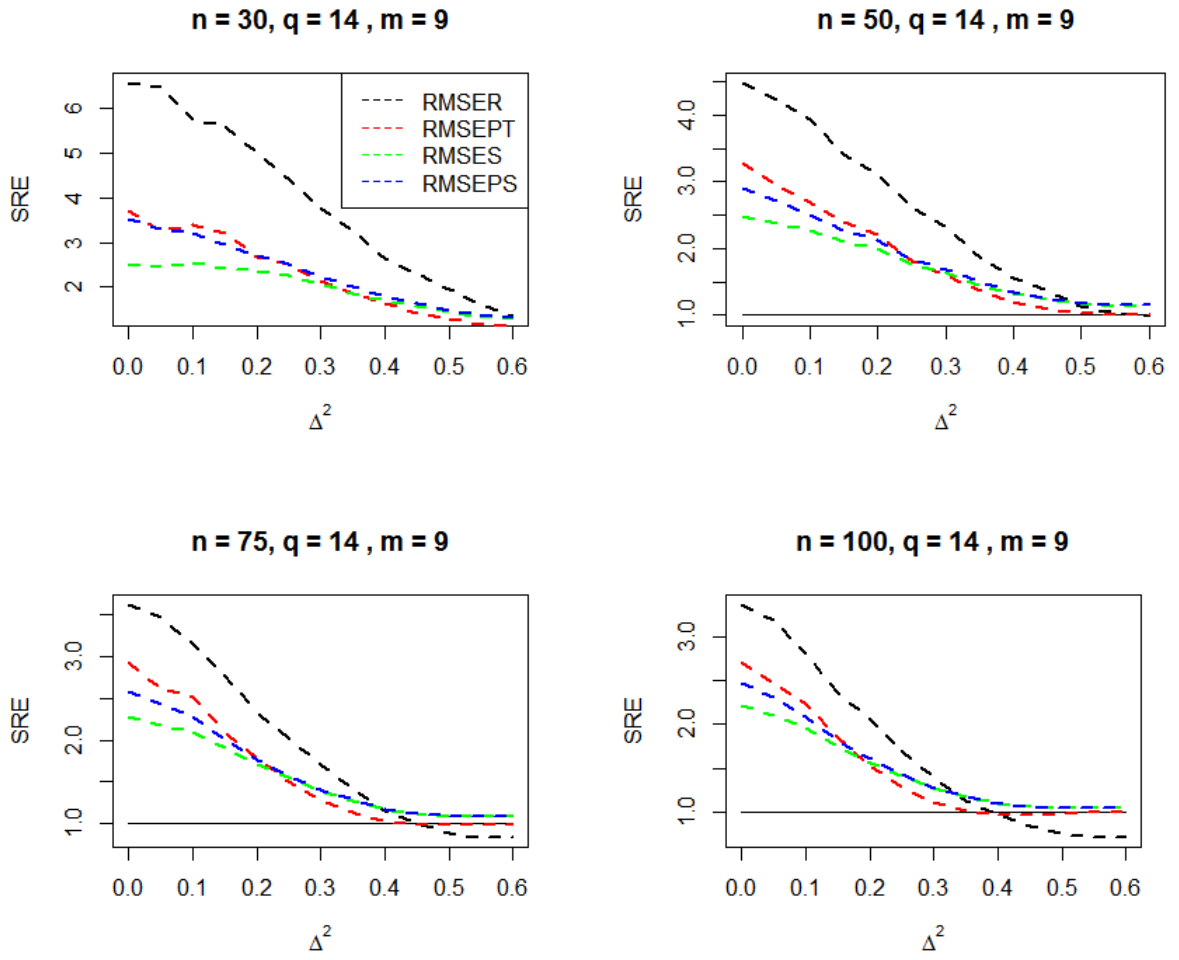


Figure 2.4: Simulated relative efficiency of the restricted, pretest and shrinkage estimators with respect to  $\hat{\theta}^U$  when  $m = 9$  and  $q = 14$  and different sample sizes.

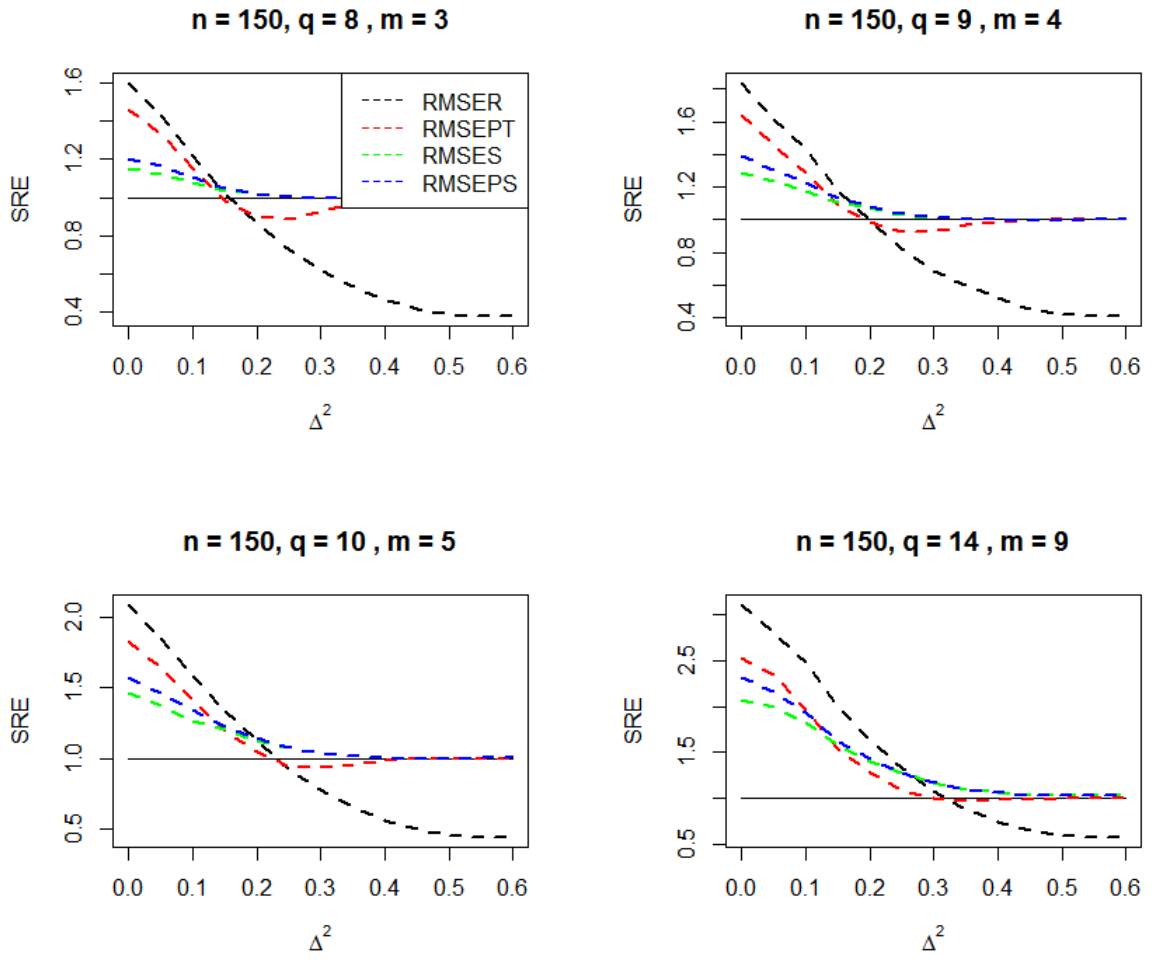


Figure 2.5: Simulated relative efficiency of the restricted, pretest and shrinkage estimators with respect to  $\hat{\theta}^U$  when the sample size is  $n = 150$  and different values of  $q$  and  $m$ .

Table 2.1: Simulated relative efficiency of the restricted, pretest and shrinkage estimators with respect to  $\hat{\theta}^U$  when  $n = 30$ ,  $q = 8$ ;  $m = 3$ .

$\Delta^2$	$\hat{\theta}^R$	$\hat{\theta}^{PT}$	$\hat{\theta}^S$	$\hat{\theta}^{S+}$
0	2.104136	1.75143	1.212327	1.290395
0.05	2.000851	1.713064	1.199043	1.276196
0.1	1.887176	1.645324	1.197501	1.248848
0.15	1.715757	1.512479	1.137894	1.218756
0.2	1.576797	1.392189	1.126848	1.169788
0.25	1.462254	1.287964	1.105508	1.139124
0.3	1.333649	1.203817	1.08871	1.11034
0.35	1.20728	1.09457	1.058294	1.074054
0.4	1.064451	1.028872	1.026928	1.044556
0.45	0.9659671	0.9713615	1.022277	1.029468
0.5	0.8726239	0.9399235	1.009984	1.01308
0.55	0.8173684	0.9431094	1.009244	1.011075

Table 2.2: Simulated relative efficiency of the restricted, pretest and shrinkage estimators with respect to  $\hat{\theta}^U$  when  $n = 30$ ;  $q = 9$ ,  $m = 4$ .

$\Delta^2$	$\hat{\theta}^R$	$\hat{\theta}^{PT}$	$\hat{\theta}^S$	$\hat{\theta}^{S+}$
0	2.552432	2.10818	1.417582	1.576352
0.05	2.37206	1.963409	1.381515	1.524656
0.1	2.240254	1.864241	1.348298	1.483403
0.15	2.121926	1.727952	1.325107	1.418309
0.2	1.891001	1.612841	1.295939	1.359839
0.25	1.792557	1.491379	1.250461	1.296639
0.3	1.641709	1.358783	1.213037	1.245442
0.35	1.404039	1.231871	1.151993	1.174427
0.4	1.278358	1.113461	1.109727	1.121834
0.45	1.147132	1.040114	1.075861	1.083542
0.5	1.004951	1.001396	1.05717	1.060852
0.55	0.8955249	0.9746145	1.041071	1.044665

Table 2.3: Simulated relative efficiency of the restricted, pretest and shrinkage estimators with respect to  $\hat{\theta}^U$  when  $n = 30$ ;  $q = 10$ ,  $m = 5$ .

$\Delta^2$	$\hat{\theta}^R$	$\hat{\theta}^{PT}$	$\hat{\theta}^S$	$\hat{\theta}^{S+}$
0	3.19693	2.386291	1.664032	1.872871
0.05	3.008924	2.297271	1.659515	1.836073
0.1	2.83329	2.182789	1.605118	1.781506
0.15	2.689897	2.01671	1.543177	1.676339
0.2	2.406686	1.900087	1.493938	1.602759
0.25	2.218949	1.737851	1.449061	1.510199
0.3	2.015128	1.520739	1.366071	1.413886
0.35	1.715963	1.380165	1.275106	1.31308
0.4	1.588221	1.243347	1.219897	1.24266
0.45	1.36578	1.146735	1.161197	1.17826
0.5	1.242981	1.066013	1.122433	1.133555
0.55	1.043152	1.010785	1.090618	1.09904

Table 2.4: Simulated relative efficiency of the restricted, pretest and shrinkage estimators with respect to  $\hat{\theta}^U$  when  $n = 30$ ;  $q = 14$ ,  $m = 9$ .

$\Delta^2$	$\hat{\theta}^R$	$\hat{\theta}^{PT}$	$\hat{\theta}^S$	$\hat{\theta}^{S+}$
0	6.570444	3.714694	2.52844	3.524378
0.05	6.479066	3.276733	2.457829	3.315546
0.1	5.758203	3.400918	2.533253	3.195185
0.15	5.578326	3.198912	2.427677	2.943745
0.2	4.983793	2.666512	2.360153	2.717917
0.25	4.416597	2.527606	2.252278	2.522882
0.3	3.774371	2.138715	2.066209	2.23338
0.35	3.26916	1.849453	1.868957	2.003584
0.4	2.648351	1.651983	1.710846	1.802083
0.45	2.307191	1.432443	1.562174	1.629432
0.5	1.956187	1.278753	1.44684	1.489495
0.55	1.618764	1.16775	1.338616	1.371167

Table 2.5: Simulated relative efficiency of the restricted, pretest and shrinkage estimators with respect to  $\hat{\theta}^U$  when  $n = 30$ ;  $q = 17$ ,  $m = 12$ .

$\Delta^2$	$\hat{\theta}^R$	$\hat{\theta}^{PT}$	$\hat{\theta}^S$	$\hat{\theta}^{S+}$
0	11.56614	4.579641	2.780781	5.183608
0.05	11.23318	4.364053	2.836567	4.902555
0.1	10.12542	4.055135	2.865431	4.658327
0.15	9.014248	3.672961	2.77225	4.282353
0.2	8.273367	3.120334	2.596316	3.7534
0.25	7.064858	3.006406	2.707284	3.50152
0.3	5.793548	2.563277	2.530572	3.01126
0.35	5.094857	2.079782	2.244242	2.581886
0.4	4.294406	1.902884	2.112954	2.3792
0.45	3.420984	1.686259	1.904184	2.092347
0.5	2.883215	1.50193	1.771854	1.889444
0.55	2.296521	1.398146	1.641466	1.731688

Table 2.6: Simulated relative efficiency of the restricted, pretest and shrinkage estimators with respect to  $\hat{\theta}^U$  when  $n = 30$ ;  $q = 20$ ,  $m = 15$ .

$\Delta^2$	$\hat{\theta}^R$	$\hat{\theta}^{PT}$	$\hat{\theta}^S$	$\hat{\theta}^{S+}$
0	22.39156	4.719919	2.456481	6.82472
0.05	21.40142	4.71492	2.584493	6.725844
0.1	20.8785	3.926422	2.483605	5.712119
0.15	17.84861	3.920784	2.68171	5.828242
0.2	15.02462	3.627244	2.776626	5.244147
0.25	12.874	3.190111	2.772309	4.622105
0.3	10.33621	2.756811	2.658384	4.021372
0.35	8.607472	2.785741	2.655128	3.73402
0.4	6.769556	2.320744	2.445546	3.230603
0.45	5.897395	1.90544	2.286864	2.791506
0.5	4.504014	1.893761	2.155251	2.567587
0.55	3.292715	1.699549	1.929789	2.251823



Table 2.7: Simulated relative efficiency of the restricted, pretest and shrinkage estimators with respect to  $\hat{\theta}^U$  when  $n = 50$ ;  $q = 8$ ,  $m = 3$ .

$\Delta^2$	$\hat{\theta}^R$	$\hat{\theta}^{PT}$	$\hat{\theta}^S$	$\hat{\theta}^{S+}$
0	1.882182	1.653836	1.206535	1.260334
0.05	1.749729	1.565952	1.167519	1.229073
0.1	1.553288	1.432243	1.105353	1.188944
0.15	1.409113	1.28453	1.10962	1.140861
0.2	1.261267	1.170865	1.066763	1.104972
0.25	1.099433	1.044018	1.041126	1.05896
0.3	0.9776256	0.9732809	1.024985	1.032685
0.35	0.8877122	0.9322131	1.003082	1.010527
0.4	0.7678225	0.8920633	0.9928294	0.9943561
0.45	0.7071472	0.9034118	0.990522	0.9914094
0.5	0.6344332	0.9265624	0.9874288	0.9895817
0.55	0.6120487	0.9571493	0.9942591	0.9941987

Table 2.8: Simulated relative efficiency of the restricted, pretest and shrinkage estimators with respect to  $\hat{\theta}^U$  when  $n = 50$ ;  $q = 9$ ,  $m = 4$ .

$\Delta^2$	$\hat{\theta}^R$	$\hat{\theta}^{PT}$	$\hat{\theta}^S$	$\hat{\theta}^{S+}$
0	2.171119	1.834962	1.349146	1.472984
0.05	2.026735	1.789136	1.352465	1.439959
0.1	1.827369	1.607491	1.288889	1.365121
0.15	1.669108	1.460511	1.230362	1.297549
0.2	1.481711	1.306889	1.178118	1.222372
0.25	1.311158	1.169433	1.126586	1.149812
0.3	1.185095	1.086448	1.093197	1.107856
0.35	1.058446	1.015057	1.05734	1.064759
0.4	0.9138158	0.9427188	1.024243	1.029423
0.45	0.7927976	0.9352463	1.007685	1.008829
0.5	0.7439466	0.9500719	1.006205	1.00702
0.55	0.7058621	0.9661377	1.009567	1.009567

Table 2.9: Simulated relative efficiency of the restricted, pretest and shrinkage estimators with respect to  $\hat{\theta}^U$  when  $n = 50$ ;  $q = 10$ ,  $m = 5$ .

$\Delta^2$	$\hat{\theta}^R$	$\hat{\theta}^{PT}$	$\hat{\theta}^S$	$\hat{\theta}^{S+}$
0	2.541064	2.12368	1.553523	1.727573
0.05	2.40837	1.990078	1.526387	1.662402
0.1	2.278273	1.936847	1.497703	1.598629
0.15	2.011187	1.73772	1.398808	1.49352
0.2	1.830201	1.491114	1.343199	1.382542
0.25	1.605171	1.367598	1.256944	1.296355
0.3	1.396491	1.198939	1.179778	1.196838
0.35	1.211252	1.099238	1.129024	1.140911
0.4	1.075062	1.019603	1.080762	1.085827
0.45	0.9138245	0.9612503	1.039274	1.044057
0.5	0.8349521	0.9552649	1.027019	1.028082
0.55	0.781798	0.9683618	1.026952	1.027879

Table 2.10: Simulated relative efficiency of the restricted, pretest and shrinkage estimators with respect to  $\hat{\theta}^U$  when  $n = 50$ ;  $q = 14$ ,  $m = 9$ .

$\Delta^2$	$\hat{\theta}^R$	$\hat{\theta}^{PT}$	$\hat{\theta}^S$	$\hat{\theta}^{S+}$
0	4.486833	3.290393	2.477851	2.912986
0.05	4.226516	2.938553	2.369133	2.714898
0.1	3.931467	2.686199	2.281303	2.50434
0.15	3.419301	2.399681	2.097122	2.276157
0.2	3.1057	2.210063	2.007958	2.118729
0.25	2.612945	1.805309	1.774699	1.836494
0.3	2.31034	1.597015	1.637872	1.677474
0.35	1.873885	1.367114	1.456707	1.482842
0.4	1.56022	1.198444	1.327181	1.341412
0.45	1.367787	1.083035	1.241605	1.248497
0.5	1.135317	1.02707	1.179943	1.182288
0.55	1.021177	1.000179	1.144313	1.146352

Table 2.11: Simulated relative efficiency of the restricted, pretest and shrinkage estimators with respect to  $\hat{\theta}^U$  when  $n = 50$ ;  $q = 17$ ,  $m = 12$ .

$\Delta^2$	$\hat{\theta}^R$	$\hat{\theta}^{PT}$	$\hat{\theta}^S$	$\hat{\theta}^{S+}$
0	6.208332	4.078501	3.04343	4.001418
0.05	5.915682	3.965545	3.106717	3.821898
0.1	5.28637	3.772884	2.973924	3.5125
0.15	4.950642	3.283239	2.888126	3.216175
0.2	4.300543	2.817087	2.671101	2.863527
0.25	3.592303	2.219502	2.271017	2.397794
0.3	2.938706	1.862945	2.019143	2.096186
0.35	2.479259	1.610415	1.800123	1.838457
0.4	1.963996	1.398207	1.595079	1.619561
0.45	1.669845	1.21235	1.429908	1.450006
0.5	1.412281	1.105109	1.331624	1.344331
0.55	1.266492	1.047176	1.283201	1.288707

Table 2.12: Simulated relative efficiency of the restricted, pretest and shrinkage estimators with respect to  $\hat{\theta}^U$  when  $n = 50$ ;  $q = 20$ ,  $m = 15$ .

$\Delta^2$	$\hat{\theta}^R$	$\hat{\theta}^{PT}$	$\hat{\theta}^S$	$\hat{\theta}^{S+}$
0	9.32338	4.783295	3.909768	5.516804
0.05	8.699592	4.496532	3.823275	5.13735
0.1	7.711028	4.198651	3.572021	4.611336
0.15	6.698563	3.812773	3.490226	4.118101
0.2	5.927034	3.085762	3.202275	3.612886
0.25	4.684158	2.845323	2.849568	3.112489
0.3	3.962361	2.262005	2.527749	2.655628
0.35	3.351782	1.847312	2.198956	2.28267
0.4	2.668381	1.487449	1.873695	1.92832
0.45	2.052024	1.353243	1.66426	1.69221
0.5	1.753301	1.201978	1.523656	1.542565
0.55	1.432978	1.104897	1.409367	1.417963

Table 2.13: Simulated relative efficiency of the restricted, pretest and shrinkage estimators with respect to  $\hat{\theta}^U$  when  $n = 75$ ;  $q = 8$ ,  $m = 3$ .

$\Delta^2$	$\hat{\theta}^R$	$\hat{\theta}^{PT}$	$\hat{\theta}^S$	$\hat{\theta}^{S+}$
0	1.708045	1.528128	1.166605	1.225358
0.05	1.572873	1.428245	1.109689	1.194354
0.1	1.402505	1.323098	1.089511	1.154417
0.15	1.238036	1.161954	1.071315	1.10389
0.2	1.058511	1.028451	1.033583	1.055637
0.25	0.9317579	0.9529123	1.015174	1.026648
0.3	0.8095086	0.895206	1.000675	1.005337
0.35	0.7121585	0.8838709	0.9900654	0.9910169
0.4	0.6334416	0.9071845	0.9876936	0.9876393
0.45	0.5718482	0.940628	0.9869446	0.9870273
0.5	0.5364263	0.9714434	0.9894097	0.9891165
0.55	0.5203594	0.990723	0.9959126	0.9959157

Table 2.14: Simulated relative efficiency of the restricted, pretest and shrinkage estimators with respect to  $\hat{\theta}^U$  when  $n = 75$ ;  $q = 9$ ,  $m = 4$ .

$\Delta^2$	$\hat{\theta}^R$	$\hat{\theta}^{PT}$	$\hat{\theta}^S$	$\hat{\theta}^{S+}$
0	1.959433	1.771842	1.324188	1.433697
0.05	1.837986	1.660852	1.298758	1.38039
0.1	1.648833	1.474169	1.229679	1.301567
0.15	1.484233	1.319725	1.187219	1.228621
0.2	1.259127	1.163186	1.127985	1.152469
0.25	1.108219	1.050436	1.083793	1.095984
0.3	0.9441927	0.9673276	1.041267	1.047841
0.35	0.8298637	0.9324421	1.017409	1.019823
0.4	0.7248615	0.9260339	0.9996599	1.000393
0.45	0.6464553	0.9541238	0.9928472	0.9931473
0.5	0.5911707	0.9743389	0.9919731	0.9919799
0.55	0.577166	0.9916975	1.001956	1.001959



Table 2.15: Simulated relative efficiency of the restricted, pretest and shrinkage estimators with respect to  $\hat{\theta}^U$  when  $n = 75$ ;  $q = 10$ ,  $m = 5$ .

$\Delta^2$	$\hat{\theta}^R$	$\hat{\theta}^{PT}$	$\hat{\theta}^S$	$\hat{\theta}^{S+}$
0	2.253583	1.940645	1.50847	1.641068
0.05	2.128641	1.878727	1.452945	1.581418
0.1	1.928781	1.671173	1.396331	1.478343
0.15	1.675827	1.472372	1.307822	1.363313
0.2	1.490223	1.30604	1.227463	1.264964
0.25	1.294344	1.149628	1.153976	1.175831
0.3	1.093737	1.018715	1.08728	1.098143
0.35	0.9470151	0.9686145	1.049705	1.054391
0.4	0.8284425	0.9426387	1.022143	1.023528
0.45	0.7326094	0.9491431	1.007023	1.007535
0.5	0.6615012	0.9697087	1.002835	1.003109
0.55	0.6355173	0.9886514	1.009129	1.009131

Table 2.16: Simulated relative efficiency of the restricted, pretest and shrinkage estimators with respect to  $\hat{\theta}^U$  when  $n = 75$ ;  $q = 14$ ,  $m = 9$ .

$\Delta^2$	$\hat{\theta}^R$	$\hat{\theta}^{PT}$	$\hat{\theta}^S$	$\hat{\theta}^{S+}$
0	3.625941	2.941088	2.277902	2.58721
0.05	3.471273	2.613353	2.185218	2.422271
0.1	3.14895	2.513692	2.100793	2.274217
0.15	2.761006	2.095308	1.908082	2.002396
0.2	2.322751	1.772961	1.709852	1.762402
0.25	2.026751	1.500568	1.556204	1.580846
0.3	1.704233	1.280528	1.392081	1.40563
0.35	1.419944	1.128169	1.27306	1.282751
0.4	1.157549	1.01849	1.172188	1.175079
0.45	0.9953561	0.9807035	1.113279	1.114822
0.5	0.8771407	0.9824674	1.090304	1.090609
0.55	0.8347648	0.9887283	1.083265	1.083325

Table 2.17: Simulated relative efficiency of the restricted, pretest and shrinkage estimators with respect to  $\hat{\theta}^U$  when  $n = 75$ ;  $q = 17$ ,  $m = 12$ .

$\Delta^2$	$\hat{\theta}^R$	$\hat{\theta}^{PT}$	$\hat{\theta}^S$	$\hat{\theta}^{S+}$
0	4.933363	3.551064	2.872862	3.439751
0.05	4.522742	3.408877	2.802273	3.229221
0.1	4.222907	3.066553	2.734878	2.972459
0.15	3.59337	2.650341	2.458894	2.595418
0.2	3.125018	2.141906	2.18718	2.262111
0.25	2.558208	1.743795	1.874911	1.91622
0.3	2.145908	1.425394	1.648214	1.671107
0.35	1.772969	1.244623	1.468698	1.481734
0.4	1.433532	1.098156	1.319206	1.325151
0.45	1.172748	1.0241	1.215544	1.218476
0.5	1.058164	0.9945946	1.174938	1.175692
0.55	0.9679932	0.9970074	1.162675	1.162767

Table 2.18: Simulated relative efficiency of the restricted, pretest and shrinkage estimators with respect to  $\hat{\theta}^U$  when  $n = 75$ ;  $q = 20$ ,  $m = 15$ .

$\Delta^2$	$\hat{\theta}^R$	$\hat{\theta}^{PT}$	$\hat{\theta}^S$	$\hat{\theta}^{S+}$
0	6.715262	4.284339	3.600641	4.45134
0.05	6.191224	4.107053	3.476219	4.172438
0.1	5.503218	3.495781	3.286069	3.694906
0.15	4.884118	3.129364	3.033851	3.285467
0.2	3.901818	2.657661	2.64774	2.784566
0.25	3.310599	2.086963	2.315774	2.381371
0.3	2.637253	1.64394	1.932123	1.974214
0.35	2.093146	1.396842	1.682464	1.70472
0.4	1.734586	1.194101	1.509476	1.515363
0.45	1.375824	1.060782	1.329813	1.334842
0.5	1.17665	1.016126	1.272354	1.273967
0.55	1.108257	1.005829	1.25249	1.253168

Table 2.19: Simulated relative efficiency of the restricted, pretest and shrinkage estimators with respect to  $\hat{\theta}^U$  when  $n = 100$ ;  $q = 8$ ,  $m = 3$ .

$\Delta^2$	$\hat{\theta}^R$	$\hat{\theta}^{PT}$	$\hat{\theta}^S$	$\hat{\theta}^{S+}$
0	1.689623	1.522832	1.165546	1.221807
0.05	1.502754	1.389101	1.111834	1.178527
0.1	1.330774	1.246462	1.087371	1.130186
0.15	1.131937	1.071715	1.056249	1.079169
0.2	0.9642133	0.9621126	1.021533	1.036476
0.25	0.8293624	0.8914788	1.005864	1.01149
0.3	0.7283002	0.8792115	0.9932157	0.9974269
0.35	0.6220229	0.898049	0.9865939	0.9874183
0.4	0.5441814	0.9385519	0.986167	0.986666
0.45	0.4955462	0.9721512	0.9884045	0.9884188
0.5	0.461804	0.9935837	0.9910515	0.9910655
0.55	0.4613039	0.9987832	0.9968983	0.9968983

Table 2.20: Simulated relative efficiency of the restricted, pretest and shrinkage estimators with respect to  $\hat{\theta}^U$  when  $n = 100$ ;  $q = 9$ ,  $m = 4$ .

$\Delta^2$	$\hat{\theta}^R$	$\hat{\theta}^{PT}$	$\hat{\theta}^S$	$\hat{\theta}^{S+}$
0	1.921002	1.680018	1.307754	1.41131
0.05	1.738347	1.562874	1.261516	1.344955
0.1	1.520288	1.382005	1.198846	1.258695
0.15	1.320435	1.20125	1.142059	1.178929
0.2	1.155533	1.074014	1.095872	1.116503
0.25	0.9759147	0.9644159	1.052604	1.059665
0.3	0.8276594	0.9249392	1.023633	1.026309
0.35	0.718031	0.9326677	1.006739	1.007242
0.4	0.6287244	0.9504103	0.9967858	0.9969687
0.45	0.5458691	0.9762056	0.9901502	0.9901625
0.5	0.506812	0.9919778	0.9938089	0.9938089
0.55	0.4955322	0.9991259	1.000486	1.000486

Table 2.21: Simulated relative efficiency of the restricted, pretest and shrinkage estimators with respect to  $\hat{\theta}^U$  when  $n = 100$ ;  $q = 10$ ,  $m = 5$ .

$\Delta^2$	$\hat{\theta}^R$	$\hat{\theta}^{PT}$	$\hat{\theta}^S$	$\hat{\theta}^{S+}$
0	2.201394	1.879692	1.490101	1.613406
0.05	2.016624	1.755261	1.419729	1.535381
0.1	1.814858	1.593274	1.348454	1.429631
0.15	1.51229	1.331728	1.248739	1.293509
0.2	1.301205	1.176845	1.175817	1.199959
0.25	1.115804	1.026795	1.104911	1.116647
0.3	0.9397393	0.9667597	1.059998	1.064146
0.35	0.8052039	0.9371567	1.024378	1.025436
0.4	0.695397	0.9444294	1.00562	1.006224
0.45	0.6134931	0.9683479	0.995822	0.996081
0.5	0.568228	0.9907401	1.000558	1.000698
0.55	0.5539776	0.9984419	1.006116	1.006116

Table 2.22: Simulated relative efficiency of the restricted, pretest and shrinkage estimators with respect to  $\hat{\theta}^U$  when  $n = 100$ ;  $q = 14$ ,  $m = 9$ .

$\Delta^2$	$\hat{\theta}^R$	$\hat{\theta}^{PT}$	$\hat{\theta}^S$	$\hat{\theta}^{S+}$
0	3.362558	2.715125	2.207016	2.469648
0.05	3.180076	2.470276	2.103871	2.313258
0.1	2.805073	2.222492	1.955457	2.082409
0.15	2.355347	1.851086	1.752095	1.820634
0.2	2.050234	1.526583	1.562336	1.600541
0.25	1.697006	1.294622	1.415253	1.43038
0.3	1.395405	1.116006	1.268908	1.278939
0.35	1.13287	1.011956	1.169818	1.171569
0.4	0.9668882	0.976799	1.104245	1.105343
0.45	0.8356316	0.9747509	1.069331	1.069667
0.5	0.7467799	0.9881934	1.054973	1.055167
0.55	0.7166567	0.9971307	1.058156	1.058156



Table 2.23: Simulated relative efficiency of the restricted, pretest and shrinkage estimators with respect to  $\hat{\theta}^U$  when  $n = 100$ ;  $q = 17$ ,  $m = 12$ .

$\Delta^2$	$\hat{\theta}^R$	$\hat{\theta}^{PT}$	$\hat{\theta}^S$	$\hat{\theta}^{S+}$
0	4.43088	3.27463	2.766701	3.207631
0.05	4.11634	3.109288	2.663808	2.977821
0.1	3.720197	2.62855	2.461541	2.655149
0.15	3.095008	2.204722	2.193741	2.286788
0.2	2.531603	1.821711	1.917159	1.958865
0.25	2.165444	1.483952	1.676365	1.702791
0.3	1.812373	1.267352	1.49423	1.503122
0.35	1.391551	1.08783	1.305243	1.309878
0.4	1.175262	1.008068	1.212269	1.213557
0.45	0.9646022	0.9851524	1.138375	1.138277
0.5	0.8830812	0.9912316	1.118158	1.118197
0.55	0.842786	0.9966471	1.115186	1.115186

Table 2.24: Simulated relative efficiency of the restricted, pretest and shrinkage estimators with respect to  $\hat{\theta}^U$  when  $n = 100$ ;  $q = 20$ ,  $m = 15$ .

$\Delta^2$	$\hat{\theta}^R$	$\hat{\theta}^{PT}$	$\hat{\theta}^S$	$\hat{\theta}^{S+}$
0	5.491058	4.03833	3.302268	3.999251
0.05	5.406529	3.850217	3.342387	3.854964
0.1	4.642768	3.263637	3.021934	3.331345
0.15	3.940119	2.677068	2.668403	2.823668
0.2	3.267766	2.158094	2.315572	2.392805
0.25	2.617454	1.692915	1.963917	1.994736
0.3	2.096242	1.38874	1.678962	1.695164
0.35	1.686941	1.18703	1.474871	1.480418
0.4	1.344196	1.046984	1.315158	1.317441
0.45	1.111987	1.000457	1.228497	1.229518
0.5	0.9826225	0.9884691	1.177656	1.177767
0.55	0.9676562	0.9989364	1.192927	1.192981

Table 2.25: Simulated relative efficiency of the restricted, pretest and shrinkage estimators with respect to  $\hat{\theta}^U$  when  $n = 150$ ;  $q = 8$ ,  $m = 3$ .

$\Delta^2$	$\hat{\theta}^R$	$\hat{\theta}^{PT}$	$\hat{\theta}^S$	$\hat{\theta}^{S+}$
0	1.60248	1.460381	1.152673	1.20594
0.05	1.434098	1.33347	1.120526	1.165833
0.1	1.217712	1.155216	1.078434	1.110463
0.15	1.01674	0.9837865	1.036749	1.049975
0.2	0.8643125	0.9029896	1.016373	1.021822
0.25	0.734031	0.8868909	1.003648	1.007231
0.3	0.6200795	0.9199448	0.9998953	1.000348
0.35	0.5312845	0.9641733	0.9964615	0.996488
0.4	0.4672182	0.9850532	0.9944729	0.9944729
0.45	0.4121031	0.9971681	0.9953903	0.9953903
0.5	0.3844723	0.9997288	0.9966524	0.9966524
0.55	0.3778178	1	0.9993655	0.9993655

Table 2.26: Simulated relative efficiency of the restricted, pretest and shrinkage estimators with respect to  $\hat{\theta}^U$  when  $n = 150$ ;  $q = 9$ ,  $m = 4$ .

$\Delta^2$	$\hat{\theta}^R$	$\hat{\theta}^{PT}$	$\hat{\theta}^S$	$\hat{\theta}^{S+}$
0	1.8392	1.642166	1.286065	1.389952
0.05	1.611729	1.460241	1.233019	1.303376
0.1	1.433187	1.289656	1.173058	1.225483
0.15	1.176647	1.089676	1.110051	1.132783
0.2	0.99477	0.9828568	1.072444	1.081058
0.25	0.8195542	0.9270918	1.032682	1.033914
0.3	0.6892106	0.9230542	1.014586	1.015016
0.35	0.5990257	0.9654686	1.007061	1.007195
0.4	0.525813	0.9858188	0.9998248	0.9998266
0.45	0.4554265	0.9980538	0.9970104	0.9970104
0.5	0.4205218	0.9998923	0.9984857	0.9984857
0.55	0.4102188	1	1.002351	1.002351

Table 2.27: Simulated relative efficiency of the restricted, pretest and shrinkage estimators with respect to  $\hat{\theta}^U$  when  $n = 150$ ;  $q = 10$ ,  $m = 5$ .

$\Delta^2$	$\hat{\theta}^R$	$\hat{\theta}^{PT}$	$\hat{\theta}^S$	$\hat{\theta}^{S+}$
0	2.085569	1.826796	1.461794	1.574239
0.05	1.845638	1.642225	1.367814	1.464578
0.1	1.584206	1.410293	1.265932	1.342726
0.15	1.330872	1.192565	1.202448	1.226626
0.2	1.127554	1.042165	1.129781	1.140541
0.25	0.9251077	0.9504701	1.071915	1.076595
0.3	0.7762226	0.933986	1.034519	1.036174
0.35	0.662528	0.9598565	1.016503	1.016701
0.4	0.5640421	0.9831989	1.005443	1.005449
0.45	0.4982335	0.9957216	0.9992659	0.9992659
0.5	0.4530251	0.9994732	1.000064	1.000064
0.55	0.4443944	0.9999005	1.004121	1.004121

Table 2.28: Simulated relative efficiency of the restricted, pretest and shrinkage estimators with respect to  $\hat{\theta}^U$  when  $n = 150$ ;  $q = 14$ ,  $m = 9$ .

$\Delta^2$	$\hat{\theta}^R$	$\hat{\theta}^{PT}$	$\hat{\theta}^S$	$\hat{\theta}^{S+}$
0	3.112598	2.533301	2.074431	2.317666
0.05	2.807332	2.347496	1.999747	2.165119
0.1	2.481315	1.970791	1.825715	1.926868
0.15	1.990209	1.540452	1.576878	1.62194
0.2	1.62588	1.274571	1.405946	1.427307
0.25	1.335971	1.093076	1.276201	1.28233
0.3	1.072017	0.9991179	1.167321	1.168787
0.35	0.8862027	0.9760577	1.09938	1.099379
0.4	0.7428506	0.982382	1.056417	1.056449
0.45	0.6560518	0.9933149	1.035235	1.035235
0.5	0.5822771	0.9985969	1.029191	1.029191
0.55	0.574454	0.9999541	1.038207	1.038207

Table 2.29: Simulated relative efficiency of the restricted, pretest and shrinkage estimators with respect to  $\hat{\theta}^U$  when  $n = 150$ ;  $q = 17$ ,  $m = 12$ .

$\Delta^2$	$\hat{\theta}^R$	$\hat{\theta}^{PT}$	$\hat{\theta}^S$	$\hat{\theta}^{S+}$
0	3.912052	2.935993	2.588664	2.916345
0.05	3.548694	2.787348	2.463699	2.713697
0.1	3.041092	2.363813	2.2386	2.357956
0.15	2.545059	1.837276	1.917341	1.983205
0.2	2.057217	1.494066	1.665647	1.695456
0.25	1.656286	1.220775	1.455748	1.464451
0.3	1.351405	1.073701	1.308394	1.311866
0.35	1.081617	0.9964053	1.191725	1.192198
0.4	0.8872752	0.9878561	1.11908	1.119096
0.45	0.7408562	0.9921211	1.0756	1.0756
0.5	0.6908329	0.9984562	1.070453	1.070453
0.55	0.6653772	0.9999684	1.070942	1.070942

Table 2.30: Simulated relative efficiency of the restricted, pretest and shrinkage estimators with respect to  $\hat{\theta}^U$  when  $n = 150$ ;  $q = 20$ ,  $m = 15$ .

$\Delta^2$	$\hat{\theta}^R$	$\hat{\theta}^{PT}$	$\hat{\theta}^S$	$\hat{\theta}^{S+}$
0	4.757122	3.458535	3.11706	3.599373
0.05	4.510583	3.278694	3.004409	3.369066
0.1	3.710512	2.684621	2.670762	2.846881
0.15	3.160508	2.175446	2.310845	2.397222
0.2	2.510573	1.720939	1.970721	2.005301
0.25	2.011936	1.354044	1.666108	1.677449
0.3	1.601107	1.13138	1.445671	1.45126
0.35	1.28998	1.025637	1.294568	1.295846
0.4	1.007923	0.9939973	1.18677	1.186926
0.45	0.8478734	0.9891063	1.125042	1.125062
0.5	0.756721	0.9976797	1.106322	1.106322
0.55	0.7663377	0.9998741	1.120029	1.120029

## 2.9.2 Application on Standard & Poor 500 (SP500) stock market

The "sp500dgc" dataset contains daily closing prices of the Standard & Poor 500 (SP500) stock market; that has been used by Ding et al. (1993). The dataset is also available in **fGarch/R-package** produced by Wuertz et al. (2008).

Following the illustrative example of Ding et al. (1993), we took the most recent



returns as our targeted subset from December 3, 1988 to August 30, 1991. It contains 1000 daily returns (i.e, the official work days in the financial market is 252).

To fit ARCH model, at first we conduct Lagrange-Multiplier (LM) test to check the effect of ARCH, for more details about this test, the reader is referred to Tsay (2006). Then, we fit ARCH model with an adequate order considering that all the coefficients should be significant at that order. We found that order  $q = 12$  is an adequate selection for our data, it represents the full model that given by the formula (2.47). Therefore, from fitting the full model we obtain the unrestricted estimator  $(\hat{\theta}^U)$ .

$$\sqrt{y_t} = \sigma_t \epsilon_t, \epsilon_t \sim N(0, 1), \quad \sigma_t^2 = \omega + \alpha_1 y_{t-1} + \dots + \alpha_q y_{t-q}. \quad (2.47)$$

In order to get the UPI from the data; we use AIC and BIC selection criteria to pick the significant order under the forward selection strategy, the selected order under the auxiliary information of AIC and BIC represents the reduced model that given by formula (2.48). Consequently, from the reduced model we compute the restricted estimator  $(\hat{\theta}^R)$ .

$$\sqrt{y_t} = \sigma_t \epsilon_t, \epsilon_t \sim N(0, 1), \quad \sigma_t^2 = \omega + \alpha_1 y_{t-1} + \dots + \alpha_{q-m+1} y_{t-q-m+1}. \quad (2.48)$$

Later on, we compute the pretest, Shrinkage and positive Shrinkage estimator.

To assess the performance of the estimators, we use the relative efficiency of the mean squared error (RMSE) with respect to the true parameters  $\boldsymbol{\theta}$ , that will be estimated by  $\hat{\boldsymbol{\theta}}^*$ . The approach is based on bootstrapping method similar to that been introduced by Freedman et al. (1981)

After fitting the full model on the original data, the procedure is conducted in two steps. First,

1. Select a sample of size  $n$  from the residuals of the full model, say  $R_1, \dots, R_n$  with replacement.
2. Compute the observations  $Y_1^*, \dots, Y_n^*$  as follow

$$Y_i^* = \hat{Y}_i + R_i, \quad i = 1, \dots, n, \quad (2.49)$$

where  $\hat{Y}_i$  is the  $i^{th}$  fitted observation from the full model applied on the original data, and  $R_i$  is the  $i^{th}$  residual in (1).

3. Fit ARCH model on  $Y_i^*$  to obtain  $\hat{\boldsymbol{\theta}}_{boot}^U(1)$ .
4. Repeat steps (1) - (3)  $K$  times, where  $K$  is chosen arbitrary to get stable results. We found that  $K = 3000$  worked well.
5. Take the average of the  $K$  iterations, that will represent the true parameter  $\boldsymbol{\theta}$ .

After the true parameters' vector has been estimated in the previous step, the second step is conducted as follows

1. Select a sample of size  $n$  from the residuals of the full model, say  $R_1, \dots, R_n$  with replacement.
2. Compute  $Y_1^*, \dots, Y_n^*$  as follow

$$Y_i^* = \hat{Y}_i + R_i, \quad i = 1, \dots, n, \quad (2.50)$$

where  $\hat{Y}_i$  is the  $i^{th}$  fitted observation from the full model applied on the original data, and  $R_i$  is the  $i^{th}$  residual in (1).

3. Fit both full and reduced models, and compute  $\hat{\boldsymbol{\theta}}_{boot}^U(1)$  and  $\hat{\boldsymbol{\theta}}_{boot}^R(1)$ , then, obtain  $\hat{\boldsymbol{\theta}}_{boot}^{PT}(1)$ ,  $\hat{\boldsymbol{\theta}}_{boot}^S(1)$  and  $\hat{\boldsymbol{\theta}}_{boot}^{S+}(1)$ .
4. Compute the predicted values  $\hat{Y}_i^*$  using the estimated parameters of all estimators

$$\hat{Y}_i^*(1) = X\hat{\boldsymbol{\theta}}_{boot}(1),$$

where  $\hat{\boldsymbol{\theta}}_{boot}^*(1) \in \{\hat{\boldsymbol{\theta}}_{boot}^U(1), \hat{\boldsymbol{\theta}}_{boot}^R(1), \hat{\boldsymbol{\theta}}_{boot}^{PT}(1), \hat{\boldsymbol{\theta}}_{boot}^S(1), \hat{\boldsymbol{\theta}}_{boot}^{S+}(1)\}$ .

5. Compute the mean squared error of Bootstrapping (MSEB) based on the true  $\boldsymbol{\theta}$  as follow

$$MSEB\hat{\boldsymbol{\theta}}_{boot}^*(1) = \sum_{i=1}^n (\hat{\boldsymbol{\theta}}_{boot}^*(1) - \hat{\boldsymbol{\theta}}^*)^2. \quad (2.51)$$

6. Repeat steps (1) - (5) a number of times, say  $K$  until obtains stable results.

We found  $K = 3000$  is reasonable number of iterations.

7. Compute the relative efficiency of the mean squared error (RMSE) as follows,

$$RMSE(\boldsymbol{\theta}^*) = \frac{\text{Average of MSEB for } \hat{\boldsymbol{\theta}}^U}{\text{Average of MSEB for } \hat{\boldsymbol{\theta}}^*}. \quad (2.52)$$

Results of the RMSEs for our data are reported in Table 2.31.

Table 2.31: Relative MSE with respect to  $\hat{\boldsymbol{\theta}}^U$  for S&P500 stock market daily closing prices.

Estimator	$\hat{\boldsymbol{\theta}}^R$	$\hat{\boldsymbol{\theta}}^{PT}$	$\hat{\boldsymbol{\theta}}^S$	$\hat{\boldsymbol{\theta}}^{S+}$
RMSE	1.1236	1.0010	1.0236	1.0382

It is clear that  $\hat{\boldsymbol{\theta}}^R$  outperforms all other estimators, which indicates that it is optimum if the null hypothesis is correct.  $\hat{\boldsymbol{\theta}}^{S+}$  comes the second, then  $\hat{\boldsymbol{\theta}}^S$ .  $\hat{\boldsymbol{\theta}}^{PT}$  performs better than  $\hat{\boldsymbol{\theta}}^U$ , even though it was the worst among the other estimators.

This may be an indication that the AIC/BIC selection criteria worked quite well on this data set.

## 2.10 Conclusion

In this chapter, we proposed the pretest and James-Stein shrinkage estimators for the parameter's vector  $\boldsymbol{\theta}$  for the ARCH model. These estimators were compared analytically via the asymptotic quadratic risk and asymptotic mean square error matrices, and numerically using simulated and real datasets to confirm our analytical results.

Our analytical and numerical results showed that, in general, the class of the proposed estimators safeguard against the high risks associated with the reduced model that we get under the set of local alternatives, where the reduced model in some cases may not be the right choice.

Our findings indicate that, it is better to use the positive James-Stein estimator as it outperforms all other estimators. To get a UPI, we used AIC, BIC selection criteria to select the reduced model.

**CHAPTER 3**

**ON EFFICIENT ESTIMATION  
STRATEGIES IN  
MONITORING OF LINEAR  
PROFILES**

**3.1 Introduction**

In many industries, variable of interest can be modeled by a relation between a response variable and one or more predictor variables. The functional form of this relationship is denoted as profile and is addressed by different authors with fixed and random predictor variables.

We consider control charts for the parameters of the simple linear regression model is known as linear profiling. Control charts mainly are classified based on their

sensitivity to the shifts: memory less control charts, such as Shewhart chart, it is effective in monitoring of large shifts as it makes the use of the current sample information. In contrast, memory control charts, such as Exponentially Weighted Moving Average (EWMA) and Cumulative Sum (CUSUM) charts are both use the past and present information about the process which makes them effective in the detection of small and moderate shifts. From practical perspective, monitoring a process using control charts consists of two parts: Phase I (retrospective phase) and Phase II (monitoring phase). In phase I, a dataset is collected from the targeted process under stable conditions that represents the in-control state of the process to construct the control limits and investigate their reliability to monitor the process in the future. Phase II employs the control limits from phase I to monitor the process.

In many manufacturing situations practitioners are interested in characterizing the quality of a process by a relationship between the response variable (Y) and one or more explanatory variables (X) instead of a single quality characteristic, this state is known as a profile or a function. Profile monitoring mainly aims at checking the stability of this relationship.

$$y_{ij} = \beta_0 + \beta_1 x_i + e_{ij}, \quad (3.1)$$

where  $e_{ij}$  is the error component associated with the response variable. Errors are independently and identically distributed as normal random variables with mean

zero and variance  $\sigma^2$ . Considering phase II state, where the process is in-control, the parameters  $\beta_0, \beta_1, \sigma^2$  are assumed to be known.

Gupta et al. (2006) compared the performance of two control charts for linear profiling in phase II. Their first control charting scheme was proposed by Crowder and Hamilton (1992) that is known as the classical calibration method to monitor the deviation from the regression line. The second one is known as the individual monitoring of linear profile parameters of Kim et al. (2003). Results showed that Crowder & Hamilton's method performed poorly compared to Kim's scheme.

Noorossana et al. (2010) proposed the use of three control chart schemes for Phase II monitoring of multivariate simple linear profiles. The results revealed that their schemes were effective in detecting the shifts in the process parameters.

Recently, Ding et al. (2017) proposed a novel control chart for jointly monitoring the linear profile, location shifts in the latent continuous distribution, and the random explanatory variables. Their simulated results revealed that the proposed chart was efficient in detecting abnormalities and was robust to various latent distributions. For more details about linear profiling, the reader is referred to Stover and Brill (1998); Aggarwal et al. (1999); Kang and Albin (2000); Ding et al. (2017); Riaz et al. (2017).

The purpose of this study is to introduce more efficient estimation strategies to



estimate the linear profile coefficients that will lead to detect the shifts quickly. We employ the estimation strategies introduced by Khan and Hoque (2002); Khan et al. (2005); Al-Momani et al. (2016). Our results are compared with the results of Kim et al. (2003).

The rest of the chapter is organized as follows: Section 3.2 contains some conceptual terminologies and assumptions of the simple linear regression. Section 3.3 is dedicated to introduce the concept of restricted and pretest estimations of simple linear regression model. We construct the limits of our control charts in Section 3.4. Then, in Section 3.5, we propose the strategy of performance evaluation of the different control charting structures. We conduct extensive simulation study and discuss the results of our proposed estimators in Section 3.6. Section 3.7 represents a real world example that assures our simulated results. The chapter will be rapped up by summary and conclusion in Section 3.8.

## **3.2 Simple Linear regression model**

The estimation of the unknown parameters in statistical inference has seen much concern from statisticians. Before the involvement of Bayesian statistics widely as an estimation strategy, the slope and intercept parameters of linear regression model were estimated by using the *maximum likelihood estimator* (MLE) or *least square estimator* (LSE), as they are very common in the literature. Such estimates are completely relay on sample information and disregard any other kind of non-sample prior information in their definition as in Bayesian context.

Consider a linear regression model with intercept and slope parameters  $\beta_0$  and  $\beta_1$  respectively. Assume that we have a set of samples that has been collected each of size  $n$ , the observations were given in a form of explanatory variable  $x$  and response variable  $y$  as  $(x_{ij}, y_{ij}), i = 1, \dots, n$  and  $j = 1, \dots, N$ , where  $N$  is the number of samples. The model for the  $j^{th}$  sample is given by the following regression equation

$$y_{ij} = \beta_0 + \beta_1 x_{ij} + e_{ij}, \quad (3.2)$$

where  $e$  is the error component associated with the response variable. Errors are independently and identically distributed as normal random variables with mean zero and variance  $\sigma^2$ . Considering phase II state, where the process is in-control, the parameters  $\beta_0, \beta_1, \sigma^2$  are assumed to be known.

For the  $j^{th}$  sample, the MLE estimator of  $\beta_0$  and  $\beta_1$  are given as follow

$$\beta_{0j}^U = \bar{y}_j - \beta_{1j}^U \bar{x}_j \quad (3.3)$$

$$\beta_{1j}^U = \frac{\sum_{i=1}^n (x_{ij} - \bar{x}_j) y_{ij}}{\sum_{i=1}^n (x_{ij} - \bar{x}_j)^2}, \quad (3.4)$$

where  $\bar{x}_j = \frac{\sum_{i=1}^n x_{ij}}{n}$  and  $\bar{y}_j = \frac{\sum_{i=1}^n y_{ij}}{n}$ ,

$\beta_{0j}^U$  and  $\beta_{1j}^U$  have a bivariate normal distribution with the mean and variance-covariance given as follow

$$\boldsymbol{\mu} = \begin{bmatrix} \beta_0 \\ \beta_1 \end{bmatrix}, \quad \boldsymbol{\Sigma} = \frac{\sigma^2}{n} \begin{bmatrix} 1 + \frac{n\bar{x}_j^2}{Q} & -\frac{n\bar{x}_j}{Q} \\ -\frac{n\bar{x}_j}{Q} & \frac{n}{Q} \end{bmatrix},$$

where  $Q = \mathbf{x}'_j \mathbf{x}_j - \frac{1}{n}(\mathbf{1}'_n \mathbf{x}_j)^2$ .

The LSE of  $\sigma^2$  of the model in (3.2) is estimated by  $S^2$ , that is given as follows

$$S^2 = \frac{(y - \hat{y})'(y - \hat{y})}{n - 2}, \quad (3.5)$$

where  $\hat{y}_j = \beta_{0j}^U + \beta_{1j}^U x_j$ .

This unbiased estimator of  $\sigma^2$  follows the  $\chi^2$  distribution with  $(n-2)$  degrees of freedom.

Assuming that the UPI of the parameters is available, either from previous studies or from practical experience of the researchers or experts. The UPI may be expressed in the form of a null hypothesis. First we obtain the MLE  $\boldsymbol{\beta}_j^U = (\beta_{0j}^U, \beta_{1j}^U)$  of the unknown parameter  $\boldsymbol{\beta} = (\beta_0, \beta_1)$ . Then, we estimate the parameters under the null hypothesis which is called the *restricted estimator*  $\boldsymbol{\beta}_j^R = (\beta_{0j}^R, \beta_{1j}^R)$ . Based on the *unrestricted* and the *restricted* estimator, the preliminary test estimator of the unknown parameters denoted by  $\boldsymbol{\beta}_j^{PT} = (\beta_{0j}^{PT}, \beta_{1j}^{PT})$  is obtained. Details about these estimators are given in the following section.

### 3.3 Efficient estimation strategies

By considering the simple linear regression model of the  $j^{th}$  sample defined in (3.2), the model can be represent in a matrix form as

$$\mathbf{Y} = \mathbf{X}\boldsymbol{\beta} + \mathbf{e}, \quad (3.6)$$

$$\text{where } \boldsymbol{\beta} = \begin{bmatrix} \beta_{0j} & \beta_{1j} \end{bmatrix}_{1 \times 2}, \mathbf{X} = \begin{bmatrix} 1 & x_{1j} \\ \vdots & \vdots \\ 1 & x_{nj} \end{bmatrix}_{n \times 2} \quad \text{and} \quad \mathbf{e} = \begin{bmatrix} e_{1j} \\ \vdots \\ e_{nj} \end{bmatrix}_{n \times 1},$$

$E(\mathbf{e}) = \mathbf{0}$  and  $E(\mathbf{e}\mathbf{e}') = \sigma^2 \mathbf{I}_n$ , where  $\mathbf{I}_n$  is the identity matrix of order  $n$ .

Based on sample information only, the *unrestricted estimators* of the slope and the intercept are the usual MLE. For more details about the MLE estimates of the slope and intercept, the reader is referred to Khan and Hoque (2002); Kim et al. (2003); Khan et al. (2005); ?. The proposed estimators are given the forthcoming subsections.

### 3.3.1 Slope parameter

Assuming the UPI of the slope parameter is given by the following null hypothesis

$$H_0 : \beta_1 = \beta_{10}. \quad (3.7)$$

Our target is to incorporate both the sample information and the UPI to estimate the slope.

The LRT test statistics for testing the hypothesis using the  $j^{\text{th}}$  sample in (3.7) is given by

$$\mathcal{L}_j = \frac{S_{xx_j}(\beta_{1j}^U - \beta_{10})^2}{S_j^2}. \quad (3.8)$$

The statistic follows central F-distribution with degree of freedom  $(1, n - 2)$  under the null hypotheses (3.7), whereas under the alternative hypothesis  $H_1 : \beta_1 \neq \beta_{10}$

it follows non-central F-distribution with  $(1, n - 2)$  degrees of freedom with non-centrality parameter  $\frac{1}{2}\Delta^2$ , where

$$\Delta^2 = \frac{S_{xx_j}(\beta_1 - \beta_{10})^2}{\sigma^2}. \quad (3.9)$$

Usually  $\Delta^2$  is the departure constant from the null-hypothesis.

Following Khan and Hoque (2002); Saleh (2006), we found the proposed estimators to estimate the slope parameter  $(\beta_1)$  as follow

### Restricted estimator of the slope

It is a simple linear combination of  $\beta_{1j}^U$  and  $\beta_{10}$  and given as

$$\beta_{1j}^R(d) = d\beta_{1j}^U + (1 - d)\beta_{10}. \quad 0 \leq d \leq 1, \quad (3.10)$$

where  $d$  is the degree of distrust in the hypothesis (3.7). Here,  $d = 0$ , means there is no distrust in  $H_0$  or  $\beta_{1j}^R(d = 0) = \beta_{10}$ , while  $d = 1$  means there is a complete distrust in the  $H_0$  and we get  $\beta_{1j}^R(d = 1) = \beta_{1j}^U$ .

$\beta_{1j}^R(d)$  is normally distributed with mean  $(\mu)$  and variance  $(\sigma_{1j}^{2R})$  given as

$$\mu = d\beta_1 + (1 - d)\beta_{10} \quad (3.11)$$

$$\sigma_{1j}^{2R} = \frac{\sigma^2}{S_{xx_j}}[d^2 + (1 - d)^2\Delta^2] + \left[\frac{\sigma}{\sqrt{S_{xx_j}}}(1 - d)\Delta\right]^2. \quad (3.12)$$

As a result, the biasness (B) and *mean square error* (MSE) based on the  $j^{th}$

sample are given as follow

$$B(\beta_{1j}^R) = -\frac{\sigma}{\sqrt{S_{xx_j}}}(1-d)\Delta \quad (3.13)$$

$$MSE(\beta_{1j}^R) = \frac{\sigma^2}{S_{xx_j}}[d^2 + (1-d)^2\Delta^2] \quad (3.14)$$

### Preliminary test estimation of the slope

The preliminary test uses the test statistics defined in (3.8) and the pretest estimate of the slope parameter  $\beta_1$ , denoted by  $\beta_{1j}^{PT}$  using the  $j^{th}$  sample, and defined as

$$\beta_{1j}^{PT}(d) = \beta_{1j}^U - (1-d)(\beta_{1j}^U - \beta_{10})I(\mathcal{L}_j < F_\alpha), \quad (3.15)$$

where  $F_\alpha$  is a one-sided  $(1-\alpha)$ -level critical value from  $F$ -distribution with  $(1, n-2)$  degrees of freedom.

The mean, the biasness (B) and *mean square error* (MSE) of  $\beta_{1j}^{PT}(d)$  are given by

$$\begin{aligned} E(\beta_{1j}^{PT}(d)) &= E(\beta_{1j}^U) - (1-d)E\left[(\beta_{1j}^U - \beta_{10})I(\mathcal{L}_j < F_\alpha)\right] \\ &= \beta_1 - (1-d)\frac{\sigma}{\sqrt{S_{xx_j}}}E\left(\frac{\sqrt{S_{xx_j}}(\beta_{1j}^U - \beta_{10})}{\sigma}I\left(\frac{S_{xx_j}(\beta_{1j}^U - \beta_{10})^2}{S_{nj}^2} < F_\alpha\right)\right) \end{aligned} \quad (3.16)$$

$$B(\beta_{1j}^{PT}(d)) = -(1-d)(\beta_1 - \beta_{10})G_{3,n-2}\left(\frac{1}{3}F_\alpha; \Delta^2\right) \quad (3.17)$$

$$\begin{aligned} MSE(\beta_{1j}^{PT}(d)) &= \frac{\sigma^2}{S_{xx_j}}\left[1 - (1-d)^2G_{3,n-2}\left(\frac{1}{3}F_\alpha; \Delta^2\right) + (1-d)\Delta^2\left\{2G_{3,n-2}\left(\frac{1}{3}F_\alpha; \Delta^2\right) - 5G_{5,n-2}\left(\frac{1}{5}F_\alpha; \Delta^2\right)\right\}\right] \end{aligned} \quad (3.18)$$

where  $G_{m_1, m_2}(\cdot; \Delta^2)$  is the non-central F-distribution with  $(m_1, m_2)$  degrees of freedom and non-centrality parameter  $\Delta^2$ .

For the proofs about these formulas the reader is referred to Khan and Hoque (2002); Saleh (2006).

### 3.3.2 Intercept parameter

For estimating the intercept parameter, we use the UPI provided in (3.7) with the same test statistics.

Following Khan et al. (2005); Saleh (2006), in the forthcoming two subsections, efficient estimators of the intercept will be discussed.

#### Restricted estimator of the intercept

Consider the MLE estimate of the intercept  $\beta_{1j}^U = \bar{y}_j - \beta_{1j}^U \bar{x}_j$ , and the UPI given in (3.7). The *restricted estimator* of the slope is given by

$$\beta_{0j}^R(d) = d\beta_{0j}^U + (1-d)(\bar{y}_j - \beta_{1j}^U \bar{x}_j), \quad 0 \leq d \leq 1. \quad (3.19)$$

The restricted estimator  $\beta_{0j}^R(d)$  is normally distributed with mean  $(\mu_0^R)$  and variance  $(\sigma_{0j}^{2R})$  given as

$$\mu_0^R = \beta_0 + (1-d)\beta_1 \bar{x}_j. \quad (3.20)$$

$$\begin{aligned} \sigma_{0j}^{2R} &= \sigma^2 \left\{ d^2 \left\{ \frac{1}{n} + \frac{\bar{x}_j^2}{S_{xx_j}} \right\} + (1-d)^2 \frac{\bar{x}_j \Delta^2}{S_{xx_j}} \right\} \\ &\quad - \left[ \frac{\bar{x}_j \sigma}{\sqrt{S_{xx_j}}} (1-d) \Delta \right]^2. \end{aligned} \quad (3.21)$$

As a result, the biasness and MSE are given as

$$B(\beta_{0j}^R(d)) = \frac{\bar{x}_j \sigma}{\sqrt{S_{xx_j}}} (1-d) \Delta. \quad (3.22)$$

$$MSE(\beta_{0j}^R(d)) = \sigma^2 \left\{ d^2 \left\{ \frac{1}{n} + \frac{\bar{x}_j^2}{S_{xx_j}} \right\} + (1-d)^2 \frac{\bar{x}_j \Delta^2}{S_{xx_j}} \right\}. \quad (3.23)$$

### Preliminary test estimator of the intercept

By using the combination of the unrestricted and the restricted estimators of the intercept parameter, besides employing the UPI given in (3.7), the preliminary test estimate is defined as follows

$$\beta_{0j}^R(d) = \beta_{0j}^U + \beta_{1j}^U \bar{x}_j (1-d) I(\mathcal{L}_j < F_\alpha) \quad (3.24)$$

$F_\alpha$  is the  $(1 - \alpha)\%$  quantile of a central  $F$ -distribution with  $(1, n - 2)$  degrees of freedom.

The mean, the biasness and the mean squared error (MSE) for the pretest estimator of the intercept parameter are given below:

$$E(\beta_{0j}^{PT}(d)) = \beta_0 + (1-d) \bar{x}_j \frac{\sigma}{\sqrt{S_{xx_j}}} E \left[ \frac{\sqrt{S_{xx_j}} \beta_{1j}^U}{\sigma} I \left( \frac{\sqrt{S_{xx_j}} \beta_{1j}^U}{S_{n_j}^2} < F_\alpha \right) \right]. \quad (3.25)$$

$$B(\beta_{0j}^{PT}(d)) = (1-d) \bar{x}_j \beta_1 G_{3, n-2} \left( \frac{1}{3} F_\alpha, \Delta^2 \right). \quad (3.26)$$

$$MSE(\beta_{0j}^{PT}(d)) = \sigma^2 \left\{ \frac{1}{n} + \frac{\bar{x}_j^2}{S_{xx_j}} \right\} + (1-d)^2 \bar{x}_j^2 E(\beta_{1j}^U)^2 I(\mathcal{L}_j < F_\alpha) + 2\bar{x}_j (1-d) E(\beta_{1j}^U (\beta_{0j}^U - \beta_0) I(\mathcal{L}_j < F_\alpha)) \quad (3.27)$$



Proofs of the results are available in Khan et al. (2005); Saleh (2006).

### 3.3.3 Residuals

Following Kang and Albin (2000); Kim et al. (2003), to extract the residuals of a simple linear regression model at the  $j^{th}$  sample can be achieved by the following formula

$$e_{ij} = y_{ij} - \beta_{0j}^* - \beta_{1j}^* x_i, i = 1, \dots, n \quad (3.28)$$

where  $\beta_{0j}^* \in \{\beta_{0j}^U, \beta_{0j}^R, \beta_{0j}^{PT}\}$  and  $\beta_{1j}^* \in \{\beta_{1j}^U, \beta_{1j}^R, \beta_{1j}^{PT}\}$ .

The average of the residuals at the  $j^{th}$  sample can be formulated as follows

$$\bar{e}_j = \frac{\sum_{i=1}^n e_{ij}}{n}, \quad (3.29)$$

Residuals are independent and normally distributed random variables with mean equal zero and variance  $\sigma^2$ , where  $\sigma^2$  is estimated by

$$MSE_j = \frac{\sum_{i=1}^n e_{ij}^2}{n-2}. \quad (3.30)$$

$MSE_j$  is unbiased estimator for  $\sigma^2$ . In literature, the natural log of  $MSE_j$  is used more than  $MSE_j$ , hence we will use  $\ln(MSE_j)$  as a measure of error variance. An approximation of the variance of  $\ln(MSE_j)$  due to Crowder and Hamilton (1992) is given by

$$Var(\ln(MSE_j)) \approx \frac{2}{n-2} + \frac{2}{(n-2)^2} + \frac{4}{3(n-2)^3} - \frac{16}{15(n-2)^5}. \quad (3.31)$$

For more details about the error variance, the reader is referred to Crowder and Hamilton (1992); Kang and Albin (2000); Kim et al. (2003); Maravelakis and Castagliola (2009); Huwang et al. (2010).

### **3.4 Monitoring linear profile coefficients in phase**

#### **II**

In this section we will discuss the structures of control charts that can be used in the monitoring of the linear profile parameters. The Slope and the intercept will be monitored with addition to the residuals.

As the slope and the intercept are correlated, it will be complex to study their performance simultaneously. The out-of-control signal might come from a shift in the intercept or slope or both of them together. Therefore, initially we should make them uncorrelated, then monitor the parameters simultaneously. Following Kim et al. (2003), we eliminate the correlation between the slope and the intercept before constructing the control charts for linear profiles, that can be achieved by replacing  $X$  by  $X' = (X - \bar{X})$ . So that the mean of the adjusted- $X$  is zero. After the adjustment, the model in (3.3) will be as

$$\mathbf{Y} = \mathbf{X}'\boldsymbol{\beta} + \mathbf{e}, \tag{3.32}$$

$$\text{where } \mathbf{X} = \begin{bmatrix} 1 & x'_1 \\ \vdots & \vdots \\ 1 & x'_n \end{bmatrix}_{n \times 2}, \quad \boldsymbol{\beta} = \begin{bmatrix} \beta_0 + \beta_1 \bar{x} & \beta_1 \end{bmatrix}_{1 \times 2}, \quad \mathbf{e} = \begin{bmatrix} e_1 \\ \vdots \\ e_n \end{bmatrix}_{n \times 1},$$

and the value of each term is similar to the model in (3.3). Hence, we can conduct separate control chart to monitor each parameter without any problem that might result if the estimators were correlated.

To construct the EWMA structure for monitoring the intercept ( $\beta_0$ ), we use the estimate of  $\beta_0$  at sample  $j$ ;  $\beta_{0j}^*$ , then compute the EWMA statistics as follows

$$EWMA[j] = \lambda \beta_{0j}^* + (1 - \lambda)EWMA[j - 1], \quad j = 1, 2, \dots \quad (3.33)$$

where  $0 < \lambda \leq 1$  is a smoothing constant and  $EWMA[0] = \beta_0$ .

The out-of-control signal of monitoring the parameter is given when  $EWMA[j] < LCL$  or  $EWMA[j] > UCL$ , where LCL and UCL are the lower control limit and the upper control limit respectively. The value of LCL and UCL are relying on the MSE of the estimator, and are given by

$$LCL = \beta_0 - L \sqrt{\frac{MSE(\beta_{0j}^*)\lambda}{(2 - \lambda)n}}, \text{ and } UCL = \beta_0 + L \sqrt{\frac{MSE(\beta_{0j}^*)\lambda}{(2 - \lambda)n}}, \quad (3.34)$$

where  $MSE(\beta_{0j}^*) \in \{MSE(\beta_{0j}^U), MSE(\beta_{0j}^R), MSE(\beta_{0j}^{PT})\}$  and  $L$  is chosen arbitrary to give specified in-control average run length (ARL).

Similarly, to construct the EWMA structure for monitoring the slope ( $\beta_1$ ), we use the estimate of  $\beta_1$  at sample  $j$ ;  $\beta_{1j}^* \in \{\beta_{1j}^U, \beta_{1j}^R, \beta_{1j}^{PT}\}$ , then compute the EWMA

statistics as follows

$$EWMA[j] = \lambda\beta_{1j}^* + (1 - \lambda)EWMA[j - 1], \quad (3.35)$$

where  $EWMA[0] = \beta_1$ .

The LCL and UCL are given as follow

$$LCL = \beta_1 - L\sqrt{\frac{MSE(\beta_{1j}^*)\lambda}{(2 - \lambda)n}}, \text{ and } UCL = \beta_1 + L\sqrt{\frac{MSE(\beta_{1j}^*)\lambda}{(2 - \lambda)n}}. \quad (3.36)$$

Finally, to construct the EWMA structure for monitoring the error variance ( $\sigma^2$ ), we use the estimate of  $\sigma^2$  at sample  $j$ ;  $MSE_j$ , then compute the EWMA statistics as follows

$$EWMA[j] = \max\{\lambda \ln(MSE_j) + (1 - \lambda)EWMA[j - 1], \ln(\sigma_0^2)\}, \quad (3.37)$$

where  $EWMA[0] = \ln(\sigma_0^2)$ .

It is more significant to detect the increases in the error variance, therefore we well focus on UCL; see Lawless (2002); Kim et al. (2003). UCL uses the estimated MSE of  $\ln(MSE_j)$  as defined in (3.31) that is given by

$$UCL = L\sqrt{\frac{Var(\ln(MSE_j))\lambda}{(2 - \lambda)n}}, \quad (3.38)$$

As we adopted the EWMA control chart structure, we will come up with two proposed control charts that are by

1.  $EWMA_R$  : this control chart will use the EWMA structure with the restricted estimators.
2.  $EWMA_{PT}$  : this control chart will use the EWMA structure with the pretest estimators.

### 3.5 Performance evaluation of charts in phase II

In this section we compare and contrast the efficiency of our proposed control charts in Phase II against the control charts that proposed by Kim et al. (2003), we compare the performance of the ARL. We adopted the same example used in their simulation study.

We used the underlying in-control linear profile model used by Kim et al. (2003); Kang and Albin (2000). The model is given by

$$Y_{ij} = 3 + 2X_i + e_{ij}, \quad (3.39)$$

where  $\beta_0 = 3, \beta_1 = 2$  and  $e_{ij}$  are i.i.d. normally distributed random variables with mean zero and variance one.  $X_i$  where taken arbitrary for the purpose of comparison with the previous proposed methods, hence  $X_i = \{2, 4, 6, 8\}$ .

As we mentioned in the previous section, we start by adjusting the values of the explanatory variable. So,  $X'_i = \{-3, -1, 1, 3\}$  with  $\bar{x} = 0$ , the model is represented as

$$Y_{ij} = 13 + 2X'_i + e_{ij}, \quad (3.40)$$

Table 3.1: Control chart multiplier  $L$  to fix  $ARL_0 = 200$  for  $EWMA_R$  and  $EWMA_{PT}$  control charts with different values of  $d$ .

Chart	Estimator	$d$				
		0.1	0.25	0.5	0.75	0.95
$EWMA_R$	$\beta_0^R$	3.8552	4.137	3.084	3.82	3.16
	$\beta_1^R$	3.498	3.283	3.1	3.039	3.028
	MSE	1.624	1.504	1.407	1.374	1.368
$EWMA_{PT}$	$\beta_0^{PT}$	3.8552	3.25	3.086	3.016	3.005
	$\beta_1^{PT}$	3.498	4.75	3.625	3.139	3.028
	MSE	1.624	1.492	1.407	1.373	1.368

As our proposed estimators are biased estimators, following Montgomery (2009), the biasness should be removed. To setup of the control limits for the unrestricted estimator we followed Kim et al. (2003), as they chose  $L$  for each control chart separately in order to get the in-control  $ARL(ARL_0) = 584$ . As a result, they got the joint  $ARL_0 = 200$  for the simultaneous monitoring for all the parameters. The values of  $L$  as reported by Kim et al. (2003) are given as: intercept ( $\beta_0^U$ ),  $L = 3.0156$ , the Slope ( $\beta_1^U$ ),  $L = 3.0109$ , and for the error variance (MSE),  $L = 1.3723$ .

Following the same methodology with the new estimation strategies, we choose  $L$  that will give  $ARL_0 = 200$  under the simultaneous monitoring. Some values of the constant  $L$  for some cases are given in Table 3.1.

A 10,000 replications has been used in our simulation study to estimate each ARL that will assure for getting stable results. In our simulation, we considered four different types of shifts. We started by introducing shifts into the intercept ( $\beta_0$ ), slope ( $\beta_1$ ) and the error variance, besides that, we introduced negative shifts into

the slope. Similarly to Kim et al. (2003), the description of these shifts is given as follows:

1. Shifts for the intercept  $\delta = (0.2, 0.4, 0.6, 0.8, 1.0, 1.2, 1.4, 1.6, 1.8, 2)$  in model (3.40),
2. Shifts for the slope  $\delta = (0.025, 0.050, 0.075, 0.100, 0.125, 0.150, 0.175, 0.200, 0.225, 0.250)$  in model (3.39),
3. Shifts for error variance  $\gamma = (1.2, 1.4, 1.6, 1.8, 2.0, 2.2, 2.4, 2.6, 2.8, \text{and } 3.0)$  in model (3.39),
4. Negative shifts for the slope  $\delta = (-1, -0.9, -0.8, -0.7, -0.6, -0.5, -0.4, -0.3, -0.2)$  in model (3.40).

All our results in tables and figures are based on  $ARL = 200$ .

## 3.6 Discussion and comparative analysis

In this section we are trying to investigate the performance of our proposed methods and compare the results under different shifts with the results reported by Kim et al. (2003). All the control charts under the in-control state (the null hypothesis) have the same ARL, which is modified regarding to the value of  $\mathbf{L}$ .

To study the performance of the control charts under the shifts of the intercept ( $\beta_0$ ), the results are reported in Tables 3.2-3.6 and Figures 3.1-3.3. The different values of shifts have introduced into the intercept in term of  $\sigma$  as  $\beta_0 + \delta\sigma$ . From the results, it is clear that the performance of our proposed methods did not excel

Table 3.2: ARL, MDRL and SDRL comparisons for  $d = 0.95$  under intercept shifts from  $\beta_0$  to  $\beta_0 + \delta\sigma$

$\delta$	EWMA_3			$EWMA_R$			$EWMA_{PT}$		
	ARL	MDRL	SDRL	ARL	MDRL	SDRL	ARL	MDRL	SDRL
0.2	59.1	43	53.84	58.13	43	53.15	58.02	42	52.97
0.4	16.2	13	11.53	16.05	13	11.43	16.13	13	11.52
0.6	7.9	7	4.18	7.88	7	4.10	7.86	7	4.08
0.8	5.1	5	2.14	5.15	5	2.16	5.14	5	2.16
1	3.8	4	1.36	3.9	4	1.34	3.79	4	1.33
1.2	3.1	3	0.95	3.058	3	0.96	3.07	3	0.96
1.4	2.6	2	0.73	2.59	2	0.72	2.58	2	0.72
1.6	2.3	2	0.57	2.27	2	0.57	2.27	2	0.57
1.8	2.1	2	0.47	2.04	2	0.46	2.05	2	0.46
2	1.9	2	0.43	1.89	2	0.43	1.89	2	0.44

the performance of EWMA\_3, this is due to the phenomena of adjusting our explanatory variable to have a zero mean to get rid of the autocorrelation between the intercept and the slope, where  $\beta_0^U = \beta^R = \beta_0^{PT} = \bar{Y}$ .

As we use an approximate control limits instead of the *exact* limits of the original EWMA control chart, they slightly delay in the detection of shifts occurring with the first samples, for more details, see Stefan (1999).

Tables 3.7-3.11 and Figures 3.4-3.6 depict the performance of our proposed methods compared to EWMA\_3 under the shifts introduced into the slope a function of  $\sigma$  as  $\beta_1 = \delta\sigma$ . The performance of our proposed methods significantly are relying on the value of the *distrust parameter* ( $d$ ). The large values of  $d$  means that we are more distrust in the null hypothesis and the performance approach towards EWMA\_3 which are typically equal when  $d = 1$ .



Table 3.3: ARL, MDRL and SDRL comparisons for  $d = 0.75$  under intercept shifts from  $\beta_0$  to  $\beta_0 + \delta\sigma$

$\delta$	EWMA <sub>3</sub>			$EWMA_R$			$EWMA_{PT}$		
	ARL	MDRL	SDRL	ARL	MDRL	SDRL	ARL	MDRL	SDRL
0.2	59.1	72	94.8	58.7	43	53.8	58.3	42	53.6
0.4	16.2	28	31.4	16.3	13	11.6	16.3	13	11.6
0.6	7.9	14	12	7.9	7	4.1	7.9	7	4.1
0.8	5.1	9	6	5.2	5	2.2	5.2	5	2.2
1	3.8	6	3.5	3.8	4	1.3	3.8	4	1.3
1.2	3.1	5	2.3	3.1	3	1	3.1	3	1
1.4	2.6	4	1.7	2.6	2	0.7	2.6	2	0.7
1.6	2.3	4	1.3	2.3	2	0.6	2.3	2	0.6
1.8	2.1	3	1	2.1	2	0.5	2.1	2	0.5
2	1.9	3	0.9	1.9	2	0.4	1.9	2	0.4

Table 3.4: ARL, MDRL and SDRL comparisons for  $d = 0.5$  under intercept shifts from  $\beta_0$  to  $\beta_0 + \delta\sigma$

$\delta$	EWMA <sub>3</sub>			$EWMA_R$			$EWMA_{PT}$		
	ARL	MDRL	SDRL	ARL	MDRL	SDRL	ARL	MDRL	SDRL
0.2	59.1	43	53.8	63.5	56	72.1	63.7	46	58.7
0.4	16.2	13	11.5	17.3	16	15.1	17.2	14	12.3
0.6	7.9	7	4.2	8.3	8	5	8.3	7	4.5
0.8	5.1	5	2.1	5.3	5	2.4	5.3	5	2.2
1	3.8	4	1.4	3.9	4	1.5	3.9	4	1.4
1.2	3.1	3	1	3.2	3	1	3.2	3	1
1.4	2.6	2	0.7	2.7	3	0.8	2.7	3	0.7
1.6	2.3	2	0.6	2.3	2	0.6	2.3	2	0.6
1.8	2.1	2	0.5	2.1	2	0.5	2.1	2	0.5
2	1.9	2	0.4	1.9	2	0.4	1.9	2	0.4

Table 3.5: ARL, MDRL and SDRL comparisons for  $d = 0.25$  under intercept shifts from  $\beta_0$  to  $\beta_0 + \delta\sigma$

$\delta$	EWMA <sub>3</sub>			$EWMA_R$			$EWMA_{PT}$		
	ARL	MDRL	SDRL	ARL	MDRL	SDRL	ARL	MDRL	SDRL
0.2	59.1	43	53.8	77.8	70	93.7	58.3	55	69.2
0.4	16.2	13	11.5	20.4	20	19	16.3	16	14.7
0.6	7.9	7	4.2	9.3	9	6	7.9	8	5
0.8	5.1	5	2.1	5.8	6	2.8	5.2	5	2.4
1	3.8	4	1.4	4.2	4	1.6	3.8	4	1.5
1.2	3.1	3	1	3.4	3	1.1	3.1	3	1
1.4	2.6	2	0.7	2.8	3	0.8	2.6	3	0.8
1.6	2.3	2	0.6	2.5	3	0.7	2.3	2	0.6
1.8	2.1	2	0.5	2.2	2	0.5	2.1	2	0.5
2	1.9	2	0.4	2	2	0.4	1.9	2	0.4

Table 3.6: ARL, MDRL and SDRL comparisons for  $d = 0.1$  under intercept shifts from  $\beta_0$  to  $\beta_0 + \delta\sigma$

$\delta$	EWMA <sub>3</sub>			$EWMA_R$			$EWMA_{PT}$		
	ARL	MDRL	SDRL	ARL	MDRL	SDRL	ARL	MDRL	SDRL
0.2	59.1	43	53.8	99.5	46	58.3	63.7	45.7	57.8
0.4	16.2	13	11.5	25.2	14	12.5	17.2	13.9	12.4
0.6	7.9	7	4.2	10.7	7	4.4	8.3	7	4.4
0.8	5.1	5	2.1	6.4	5	2.2	5.3	5	2.2
1	3.8	4	1.4	4.6	4	1.4	3.9	4	1.4
1.2	3.1	3	1	3.6	3	1	3.2	3	1
1.4	2.6	2	0.7	3	3	0.7	2.7	2.9	0.7
1.6	2.3	2	0.6	2.6	2	0.6	2.3	2	0.6
1.8	2.1	2	0.5	2.3	2	0.5	2.1	2	0.5
2	1.9	2	0.4	2.1	2	0.4	1.9	2	0.4

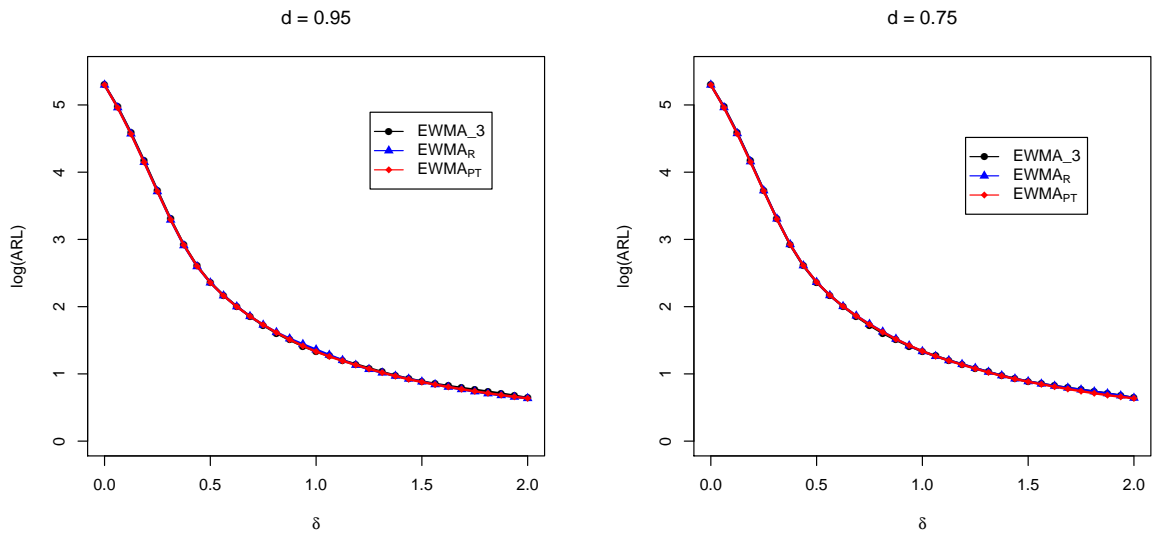


Figure 3.1: ARL comparisons under intercept shifts from  $\beta_0$  to  $\beta_0 + \delta\sigma$

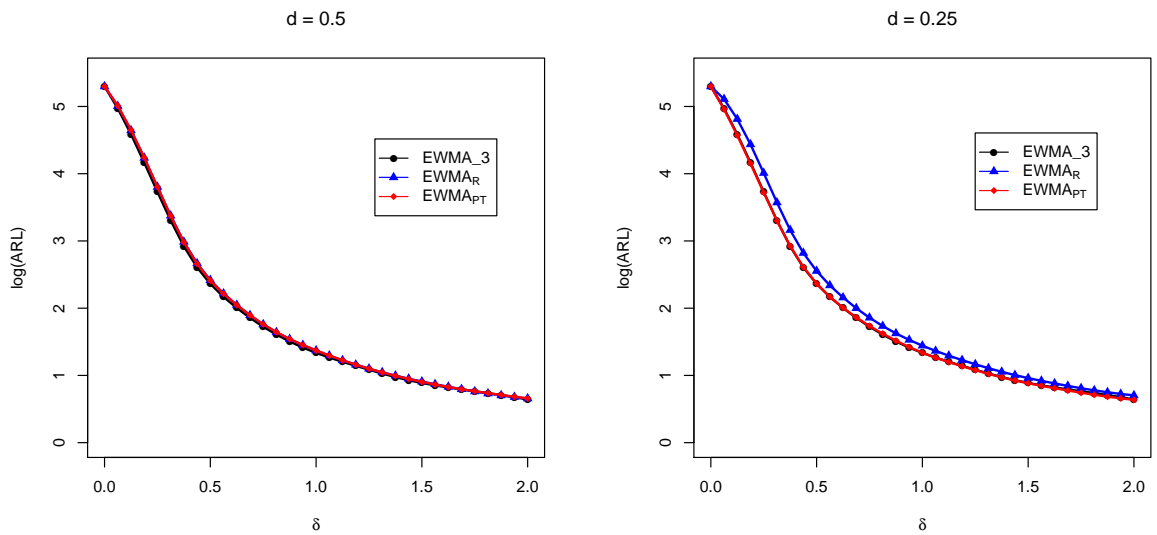


Figure 3.2: ARL comparisons under intercept Shifts from  $\beta_0$  to  $\beta_0 + \delta\sigma$

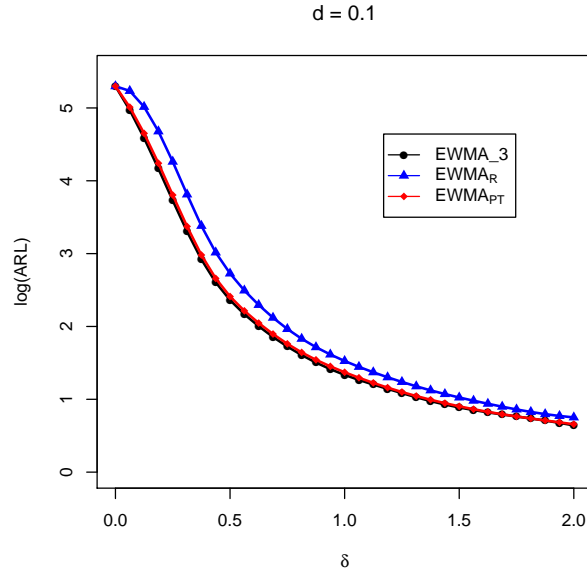


Figure 3.3: ARL comparisons under intercept Shifts from  $\beta_0$  to  $\beta_0 + \delta\sigma$

Our proposed methods uniformly excel EWMA\_3 with smaller values of  $d$ , where we are more trust in the null hypothesis over the entire range of shifts considered. The performance of the restricted estimator outperforms the other estimators under the small amount of shifts and its performance decays with moderate and big shifts.

Tables 3.12-3.16 and Figures 3.7-3.9 show the ARL performance of our proposed methods compared to EWMA\_3 chart for detecting out-control state in  $\sigma$  under a range of shifts that are expressed in terms of  $\sigma$  as  $\gamma\sigma$ . Our proposed methods outperform EWMA\_3 under smaller shifts, whereas under larger shifts all the methods approximately have the same performance. Addition to that, the degree of the distrust has a significant impact on the performance of the proposed methods as the methods with the smaller degree of the distrust excelled the methods with the larger degree of the distrust.

Table 3.7: ARL, MDRL and SDRL comparisons for  $d = 0.95$  under slope shifts from  $\beta_1$  to  $\beta_1 + \delta\sigma$

$\delta$	EWMA_3			$EWMA_R$			$EWMA_{PT}$		
	ARL	MDRL	SDRL	ARL	MDRL	SDRL	ARL	MDRL	SDRL
0.025	101.6	72	94.82	99.62	70.5	93.54	99.22	119	165.73
0.05	36.5	28	31.38	36.65	27	31.05	35.86	87	114.19
0.075	17	14	12.01	16.8	14	11.79	16.8	55	72.79
0.1	10.3	9	5.98	10.13	9	5.95	10.2	37	43.22
0.125	7.2	6	3.49	7.03	6	3.38	7.07	24	27.34
0.15	5.5	5	2.31	5.46	5	2.32	5.36	18	17.21
0.175	4.5	4	1.72	4.42	4	1.67	4.43	14	12.03
0.2	3.8	4	1.29	3.74	4	1.29	3.72	11	8.74
0.225	3.3	3	1.04	3.24	3	1.02	3.24	9	6.40
0.25	2.9	3	0.86	2.9	3	0.85	2.89	8	4.90

Table 3.8: ARL, MDRL and SDRL comparisons for  $d = 0.75$  under slope shifts from  $\beta_1$  to  $\beta_1 + \delta\sigma$

$\delta$	EWMA_3			$EWMA_R$			$EWMA_{PT}$		
	ARL	MDRL	SDRL	ARL	MDRL	SDRL	ARL	MDRL	SDRL
0.025	101.6	72	94.8	95.9	68	90.5	97.7	118	164.1
0.05	36.5	28	31.4	34.8	26	29.1	35.4	87	116.5
0.075	17	14	12.0	16.1	13	11.2	16.5	56	74.5
0.1	10.3	9	6.0	9.7	8	5.4	10.0	37	44.5
0.125	7.2	6	3.5	6.9	6	3.3	7.0	25	28.5
0.15	5.5	5	2.3	5.3	5	2.1	5.4	18	17.7
0.175	4.5	4	1.7	4.3	4	1.6	4.4	14	12.6
0.2	3.8	4	1.3	3.7	3	1.2	3.8	11	8.9
0.225	3.3	3	1.0	3.2	3	1.0	3.2	9	6.6
0.25	2.9	3	0.9	2.9	3	0.8	2.9	8	5.1

Table 3.9: ARL, MDRL and SDRL comparisons for  $d = 0.5$  under slope shifts from  $\beta_1$  to  $\beta_1 + \delta\sigma$

$\delta$	EWMA_3			$EWMA_R$			$EWMA_{PT}$		
	ARL	MDRL	SDRL	ARL	MDRL	SDRL	ARL	MDRL	SDRL
0.025	101.6	72	94.8	88.79	63	82.80	95.2	123	170.40
0.05	36.5	28	31.4	29.75	23	24.17	33.13	98	135.38
0.075	17	14	12.0	14.06	12	9.04	15.53	71	94.58
0.1	10.3	9	6.0	8.56	8	4.39	9.43	48	61.90
0.125	7.2	6	3.5	6.11	6	2.63	6.66	34	40.79
0.15	5.5	5	2.3	4.77	4	1.76	5.14	25	28.00
0.175	4.5	4	1.7	3.95	4	1.28	4.23	19	19.22
0.2	3.8	4	1.3	3.39	3	1.01	3.6	15	13.43
0.225	3.3	3	1.0	2.99	3	0.83	3.15	12	9.68
0.25	2.9	3	0.9	2.67	3	0.69	2.79	10	7.54

Table 3.10: ARL, MDRL and SDRL comparisons for  $d = 0.25$  under slope Shifts from  $\beta_1$  to  $\beta_1 + \delta\sigma$

$\delta$	EWMA_3			$EWMA_R$			$EWMA_{PT}$		
	ARL	MDRL	SDRL	ARL	MDRL	SDRL	ARL	MDRL	SDRL
0.025	101.6	72	94.8	58.64	42	53.40	69.38	121	170.6
0.05	36.5	28	31.4	14.8	12	9.54	20.23	107	145.2
0.075	17	14	12.0	7.2	6	3.38	9.65	82	112.4
0.1	10.3	9	6.0	4.76	4	1.75	6.15	61	79.2
0.125	7.2	6	3.5	3.59	3	1.11	4.49	45	58.8
0.15	5.5	5	2.3	2.9	3	0.79	3.55	35	42.5
0.175	4.5	4	1.7	2.48	2	0.62	2.99	27	32.2
0.2	3.8	4	1.3	2.19	2	0.47	2.59	22	24.3
0.225	3.3	3	1.0	2	2	0.38	2.33	19	20.1
0.25	2.9	3	0.9	1.9	2	0.39	2.15	16	16.2

Table 3.11: ARL, MDRL and SDRL comparisons for  $d = 0.1$  under slope Shifts from  $\beta_1$  to  $\beta_1 + \delta\sigma$

$\delta$	EWMA_3			$EWMA_R$			$EWMA_{PT}$		
	ARL	MDRL	SDRL	ARL	MDRL	SDRL	ARL	MDRL	SDRL
0.025	101.6	72	94.8	12.19	10	7.19	21.13	16.2	15.96
0.05	36.5	28	31.4	3.97	4	1.29	7.22	6.4	4.30
0.075	17	14	12.0	2.48	2	0.62	3.93	3.2	1.76
0.1	10.3	9	6.0	1.96	2	0.35	2.79	2.7	0.91
0.125	7.2	6	3.5	1.6	2	0.49	2.16	2.4	0.79
0.15	5.5	5	2.3	1.19	1	0.39	1.62	1.4	0.58
0.175	4.5	4	1.7	1.02	1	0.15	1.37	1.3	0.30
0.2	3.8	4	1.3	1	1	0.03	1.28	1.3	0.15
0.225	3.3	3	1.0	1	1	0.00	1.23	1.2	0.10
0.25	2.9	3	0.9	1	1	0.00	1.19	1.2	0.09

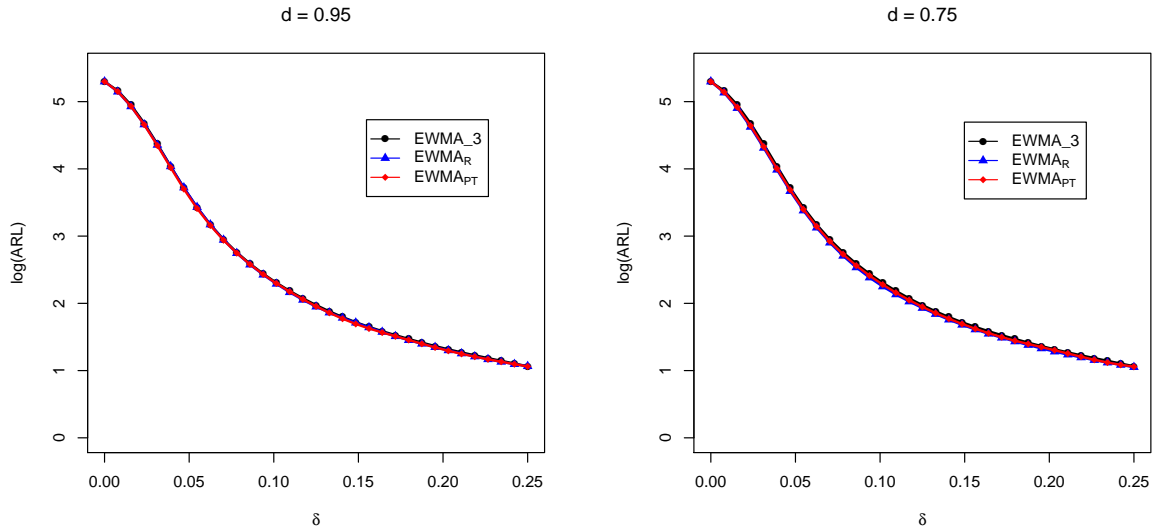


Figure 3.4: ARL comparisons under slope Shifts from  $\beta_1$  to  $\beta_1 + \delta\sigma$

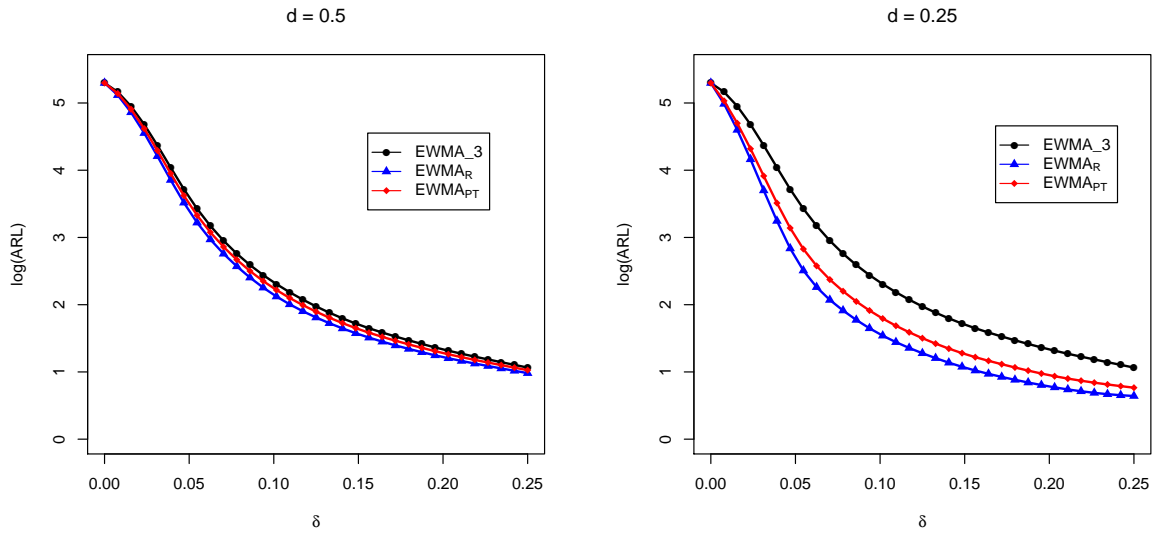


Figure 3.5: ARL comparisons under slope Shifts from  $\beta_1$  to  $\beta_1 + \delta\sigma$

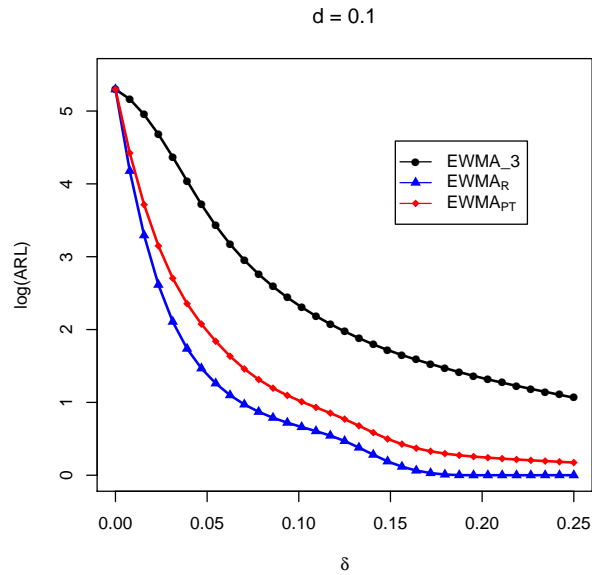


Figure 3.6: ARL comparisons under slope Shifts from  $\beta_1$  to  $\beta_1 + \delta\sigma$



Table 3.12: ARL, MDRL and SDRL comparisons for  $d = 0.95$  under standard deviation shifts from  $\sigma$  to  $\gamma\sigma$

$\gamma$	EWMA <sub>3</sub>			$EWMA_R$			$EWMA_{PT}$		
	ARL	MDRL	SDRL	ARL	MDRL	SDRL	ARL	MDRL	SDRL
1.2	33.5	24	30.36	33.21	24	30.27	33.09	24	30.07
1.4	12.7	10	10.10	12.7	10	10.12	12.72	10	10.06
1.6	7.2	6	5.16	7.28	6	5.11	7.3	6	5.08
1.8	5.1	4	3.21	5.1	4	3.17	5.09	4	3.16
2	3.9	3	2.20	3.92	3	2.19	3.94	3	2.19
2.2	3.2	3	1.69	3.27	3	1.72	3.26	3	1.67
2.4	2.8	3	1.42	2.85	3	1.43	2.83	2	1.41
2.6	2.5	2	1.20	2.5	2	1.21	2.52	2	1.25
2.8	2.3	2	1.08	2.25	2	1.08	2.24	2	1.05
3	2.1	2	0.96	2.08	2	0.95	2.06	2	0.96

Table 3.13: ARL, MDRL and SDRL comparisons for  $d = 0.75$  under standard deviation shifts from  $\sigma$  to  $\gamma\sigma$

$\gamma$	EWMA <sub>3</sub>			$EWMA_R$			$EWMA_{PT}$		
	ARL	MDRL	SDRL	ARL	MDRL	SDRL	ARL	MDRL	SDRL
1.2	33.5	24	30.36	31.98	23	28.87	32.32	23	29.16
1.4	12.7	10	10.10	12.27	9	9.59	12.37	9	9.77
1.6	7.2	6	5.16	7.04	6	4.76	7.06	6	4.82
1.8	5.1	4	3.21	4.95	4	3.01	4.98	4	3.04
2	3.9	3	2.20	3.88	3	2.10	3.89	3	2.15
2.2	3.2	3	1.69	3.2	3	1.62	3.19	3	1.63
2.4	2.8	3	1.42	2.8	2	1.33	2.81	3	1.34
2.6	2.5	2	1.20	2.49	2	1.16	2.49	2	1.16
2.8	2.3	2	1.08	2.23	2	1.03	2.25	2	1.04
3	2.1	2	0.96	2.04	2	0.92	2.04	2	0.91

Table 3.14: ARL, MDRL and SDRL comparisons for  $d = 0.5$  under standard deviation shifts from  $\sigma$  to  $\gamma\sigma$

	EWMA <sub>3</sub>			$EWMA_R$			$EWMA_{PT}$		
$\gamma$	ARL	MDRL	SDRL	ARL	MDRL	SDRL	ARL	MDRL	SDRL
1.2	33.5	24	30.36	28.53	21	24.74	29.59	22	26.01
1.4	12.7	10	10.10	10.87	9	7.94	11.34	9	8.63
1.6	7.2	6	5.16	6.4	5	4.06	6.54	5	4.30
1.8	5.1	4	3.21	4.65	4	2.57	4.74	4	2.75
2	3.9	3	2.20	3.68	3	1.87	3.75	3	2.02
2.2	3.2	3	1.69	3.11	3	1.45	3.13	3	1.51
2.4	2.8	3	1.42	2.7	2	1.20	2.74	2	1.26
2.6	2.5	2	1.20	2.42	2	1.04	2.47	2	1.06
2.8	2.3	2	1.08	2.2	2	0.93	2.25	2	0.96
3	2.1	2	0.96	2.04	2	0.85	2.09	2	0.89

Table 3.15: ARL, MDRL and SDRL comparisons for  $d = 0.25$  under standard deviation shifts from  $\sigma$  to  $\gamma\sigma$

	EWMA <sub>3</sub>			$EWMA_R$			$EWMA_{PT}$		
$\gamma$	ARL	MDRL	SDRL	ARL	MDRL	SDRL	ARL	MDRL	SDRL
1.2	33.5	24	30.36	23.91	18	19.84	33.09	19	21.96
1.4	12.7	10	10.10	9.51	8	6.46	12.72	8	7.09
1.6	7.2	6	5.16	5.99	5	3.40	7.3	5	3.62
1.8	5.1	4	3.21	4.38	4	2.20	5.09	4	2.43
2	3.9	3	2.20	3.58	3	1.65	3.94	3	1.82
2.2	3.2	3	1.69	3.07	3	1.31	3.26	3	1.40
2.4	2.8	3	1.42	2.7	2	1.09	2.83	2	1.18
2.6	2.5	2	1.20	2.46	2	0.97	2.52	2	1.02
2.8	2.3	2	1.08	2.24	2	0.85	2.24	2	0.88
3	2.1	2	0.96	2.09	2	0.80	2.06	2	0.82

Table 3.16: ARL, MDRL and SDRL comparisons for  $d = 0.1$  under standard deviation shifts from  $\sigma$  to  $\gamma\sigma$

$\gamma$	EWMA_3			$EWMA_R$			$EWMA_{PT}$		
	ARL	MDRL	SDRL	ARL	MDRL	SDRL	ARL	MDRL	SDRL
1.2	33.5	24	30.36	22.71	17	18.43	32.32	17.7	19.62
1.4	12.7	10	10.10	9.34	8	6.06	12.37	8.2	6.46
1.6	7.2	6	5.16	5.99	5	3.23	7.06	5.1	3.43
1.8	5.1	4	3.21	4.45	4	2.14	4.98	4	2.25
2	3.9	3	2.20	3.65	3	1.61	3.89	3	1.67
2.2	3.2	3	1.69	3.15	3	1.28	3.19	3	1.32
2.4	2.8	3	1.42	2.81	3	1.09	2.81	3	1.12
2.6	2.5	2	1.20	2.55	2	0.95	2.49	2	0.97
2.8	2.3	2	1.08	2.34	2	0.83	2.25	2	0.86
3	2.1	2	0.96	2.19	2	0.79	2.04	2	0.80

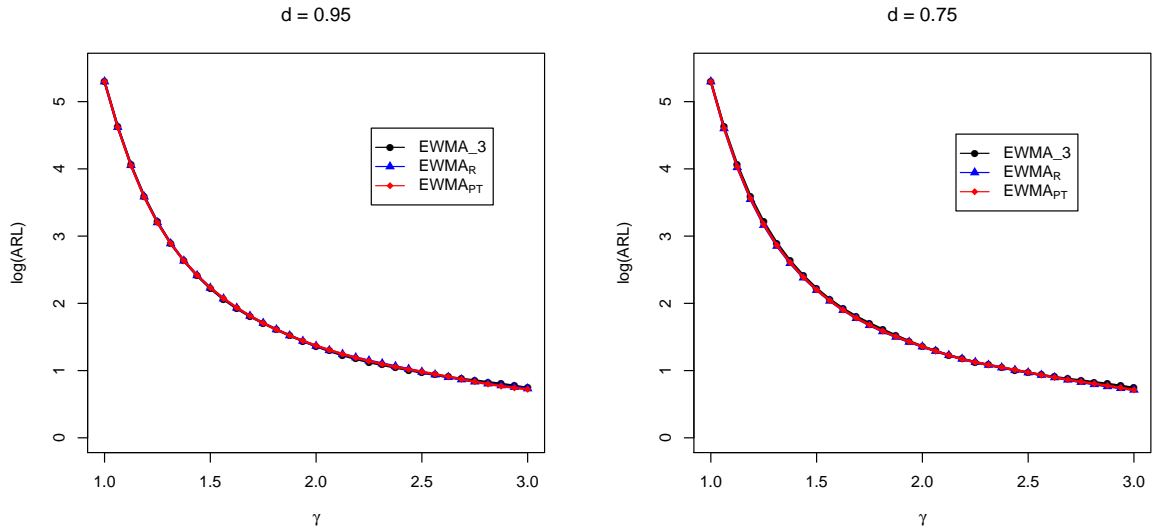


Figure 3.7: ARL comparisons under standard deviation shifts from  $\sigma$  to  $\gamma\sigma$ .

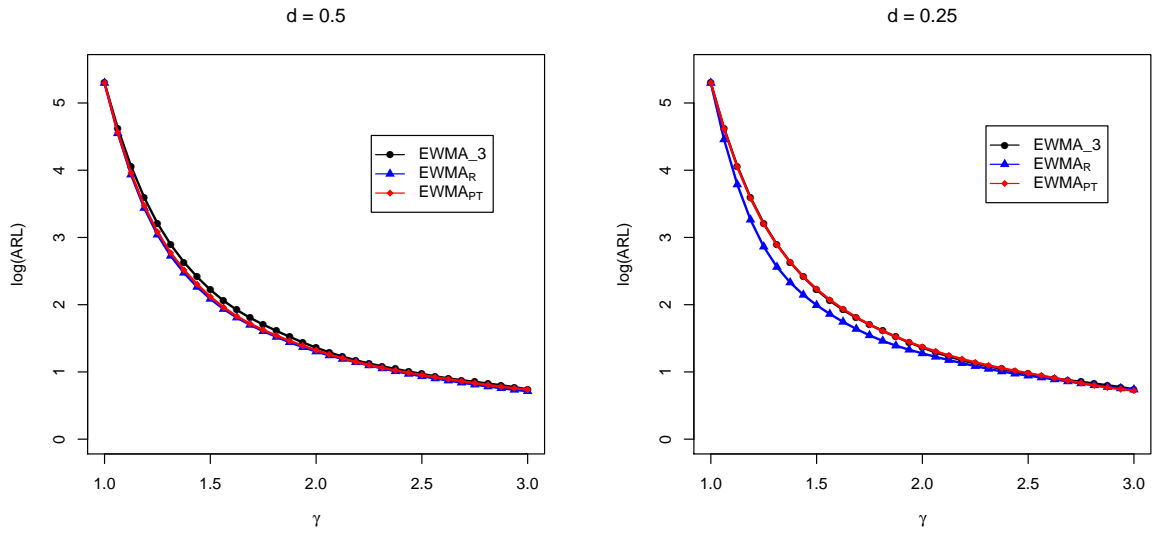


Figure 3.8: ARL comparisons under standard deviation shifts from  $\sigma$  to  $\gamma\sigma$ .

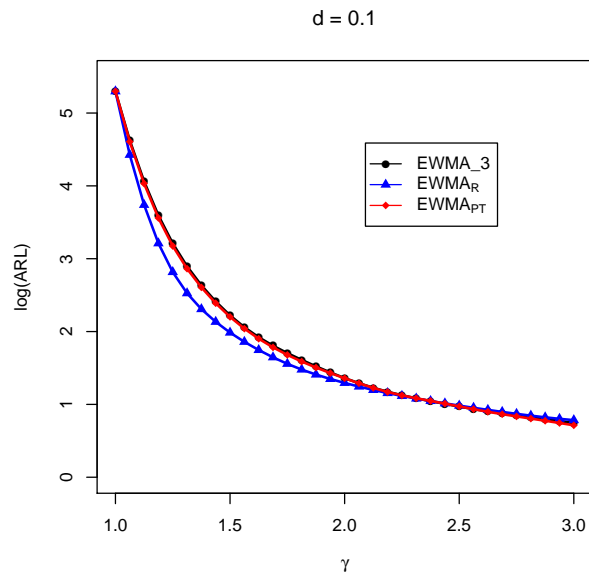


Figure 3.9: ARL comparisons under standard deviation shifts from  $\sigma$  to  $\gamma\sigma$ .

Table 3.17: ARL, MDRL and SDRL comparisons for  $d = 0.95$  under slope shifts from  $\beta_1$  to  $\beta_1 + \delta\sigma$

$\delta$	EWMA_3			$EWMA_R$			$EWMA_{PT}$		
	ARL	MDRL	SDRL	ARL	MDRL	SDRL	ARL	MDRL	SDRL
-0.2	13.1	11	8.58	12.17	4	1.28	12.58	11	8.62
-0.3	6.6	6	3.22	6.18	2	0.62	6.4	6	3.23
-0.4	4.4	4	1.72	4.16	2	0.43	4.28	4	1.68
-0.5	3.3	3	1.07	3.17	1	0.50	3.26	3	1.09
-0.6	2.7	3	0.77	2.58	1	0.36	2.65	3	0.78
-0.7	2.3	2	0.59	2.23	1	0.15	2.29	2	0.60
-0.8	2.1	2	0.46	1.99	1	0.04	2.05	2	0.47
-0.9	1.9	2	0.44	1.81	1	0	1.87	2	0.43
-1	1.7	2	0.47	1.63	1	0	1.7	2	0.47

Table 3.18: ARL, MDRL and SDRL comparisons for  $d = 0.75$  under slope shifts from  $\beta_1$  to  $\beta_1 + \delta\sigma$

$\delta$	EWMA_3			$EWMA_R$			$EWMA_{PT}$		
	ARL	MDRL	SDRL	ARL	MDRL	SDRL	ARL	MDRL	SDRL
-0.2	13.1	11	8.58	8.19	3	1.23	10.16	87	116.45
-0.3	6.6	6	3.22	4.46	2	0.60	5.34	56	74.50
-0.4	4.4	4	1.72	3.12	2	0.42	3.73	37	44.48
-0.5	3.3	3	1.07	2.46	2	0.50	2.91	25	28.53
-0.6	2.7	3	0.77	2.09	1	0.36	2.45	18	17.69
-0.7	2.3	2	0.59	1.84	1	0.14	2.17	14	12.62
-0.8	2.1	2	0.46	1.62	1	0.02	1.99	11	8.89
-0.9	1.9	2	0.44	1.38	1	0.00	1.84	9	6.55
-1	1.7	2	0.47	1.19	1	0.00	1.7	8	5.05

Table 3.19: ARL, MDRL and SDRL comparisons for  $d = 0.5$  under slope shifts from  $\beta_1$  to  $\beta_1 + \delta\sigma$

$\delta$	EWMA_3			$EWMA_R$			$EWMA_{PT}$		
	ARL	MDRL	SDRL	ARL	MDRL	SDRL	ARL	MDRL	SDRL
-0.2	13.1	11	8.58	4.57	3	1.01	8.94	98.00	135.38
-0.3	6.6	6	3.22	2.81	2	0.50	4.72	71.00	94.58
-0.4	4.4	4	1.72	2.11	2	0.39	3.4	48.00	61.90
-0.5	3.3	3	1.07	1.77	1	0.49	2.74	34.00	40.79
-0.6	2.7	3	0.77	1.41	1	0.27	2.34	25.00	28.00
-0.7	2.3	2	0.59	1.13	1	0.06	2.13	19.00	19.22
-0.8	2.1	2	0.46	1.02	1	0.01	2.02	15.00	13.43
-0.9	1.9	2	0.44	1	1	0.00	1.96	12.00	9.68
-1	1.7	2	0.47	1	1	0.00	1.91	10.00	7.54

Table 3.20: ARL, MDRL and SDRL comparisons for  $d = 0.25$  under slope shifts from  $\beta_1$  to  $\beta_1 + \delta\sigma$

$\delta$	EWMA_3			$EWMA_R$			$EWMA_{PT}$		
	ARL	MDRL	SDRL	ARL	MDRL	SDRL	ARL	MDRL	SDRL
-0.2	13.1	11	8.58	2.21	2	0.47	12.58	22.00	24.40
-0.3	6.6	6	3.22	1.54	2	0.50	6.4	12.00	11.59
-0.4	4.4	4	1.72	1.05	1	0.20	4.28	8.00	6.11
-0.5	3.3	3	1.07	1	1	0.01	3.26	6.00	3.24
-0.6	2.7	3	0.77	1	1	0	2.65	5.00	2.13
-0.7	2.3	2	0.59	1	1	0	2.29	4.00	1.57
-0.8	2.1	2	0.46	1	1	0	2.05	3.00	1.17
-0.9	1.9	2	0.44	1	1	0	1.87	3.00	0.93
-1	1.7	2	0.47	1	1	0	1.7	2.00	0.73

Table 3.21: ARL, MDRL and SDRL comparisons for  $d = 0.1$  under slope shifts from  $\beta_1$  to  $\beta_1 + \delta\sigma$

$\delta$	EWMA_3			$EWMA_R$			$EWMA_{PT}$		
	ARL	MDRL	SDRL	ARL	MDRL	SDRL	ARL	MDRL	SDRL
-0.2	13.1	11	8.58	1	1	0.022	10.16	2.00	0.88
-0.3	6.6	6	3.22	1	1	0	5.34	1.50	0.32
-0.4	4.4	4	1.72	1	1	0	3.73	1.30	0.17
-0.5	3.3	3	1.07	1	1	0	2.91	1.20	0.11
-0.6	2.7	3	0.77	1	1	0	2.45	1.20	0.08
-0.7	2.3	2	0.59	1	1	0	2.17	1.10	0.06
-0.8	2.1	2	0.46	1	1	0	1.99	1.10	0.05
-0.9	1.9	2	0.44	1	1	0	1.84	1.10	0.04
-1	1.7	2	0.47	1	1	0	1.7	1.10	0.05

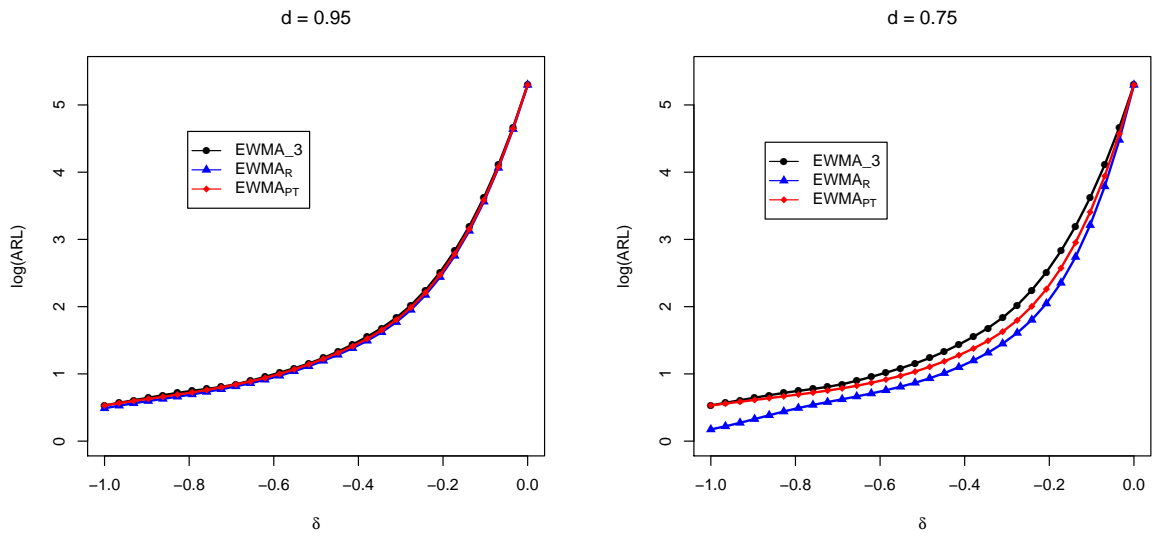


Figure 3.10: ARL comparisons under slope Shifts from  $\beta_1$  to  $\beta_1 + \delta\sigma$

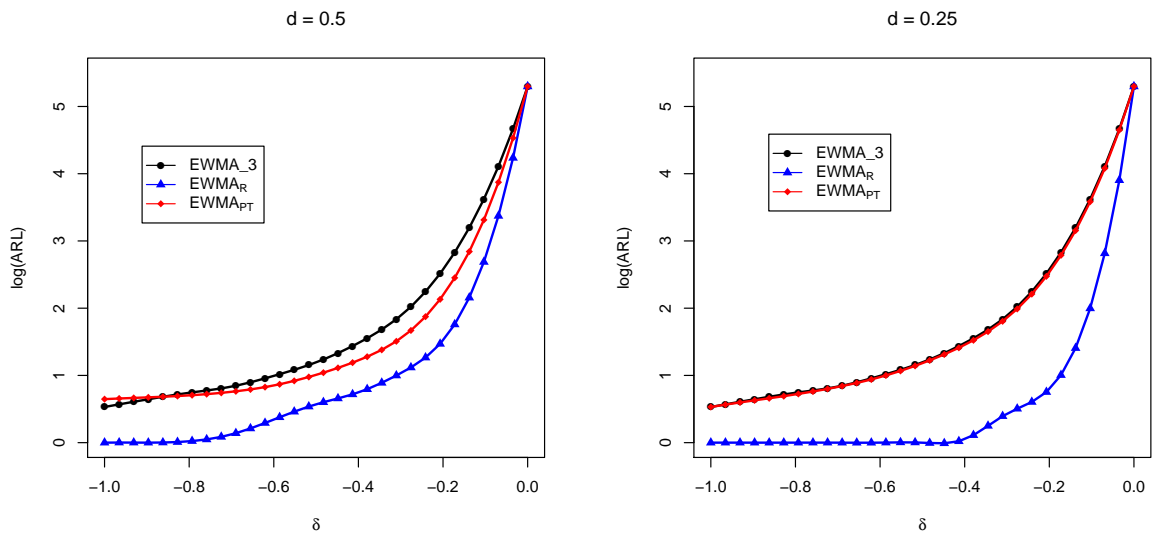


Figure 3.11: ARL comparisons under slope Shifts from  $\beta_1$  to  $\beta_1 + \delta\sigma$

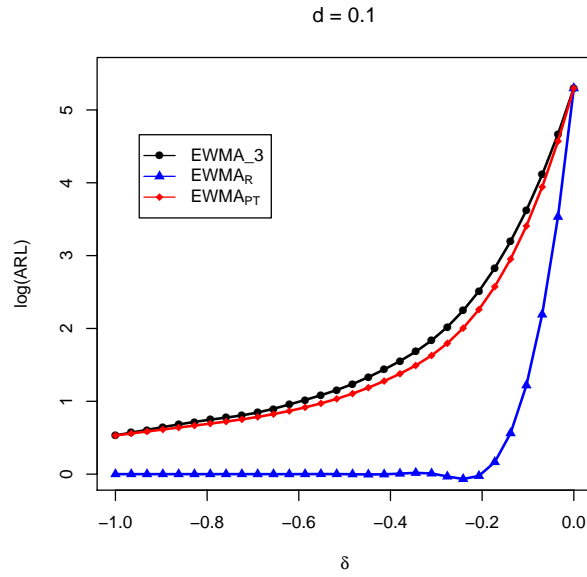


Figure 3.12: ARL comparisons under slope Shifts from  $\beta_1$  to  $\beta_1 + \delta\sigma$

## 3.7 Illustrative example

In this section, illustrations with the real-life example of linear profiles in the oil industry is discussed.

### 3.7.1 Darcy law of single-phase flow

Very early, Darcy (1856) investigated the flow of water (single-phase) through sand filter, and throughout his experiment he concluded the following points:

- The flow rate is directly proportional to the difference of water levels in the two manometers.
- The flow rate is directly proportional to the cross-sectional area of the sand pack.
- The flow rate is inversely proportional to the length of the pack.



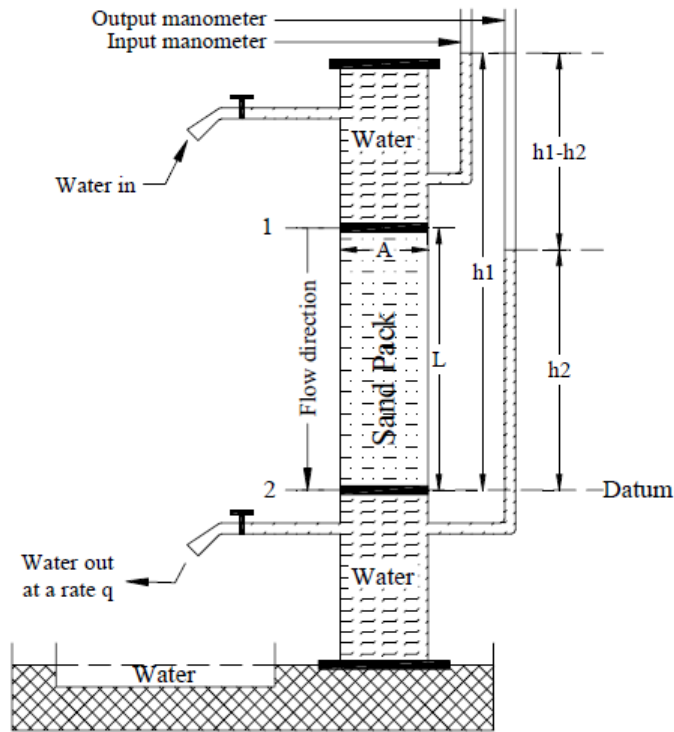


Figure 3.13: Darcy law of the flow of water through sand filter.

The water level in the manometer can be represented as the pressure head at that point, so the levels difference can be replaced by the pressure difference. The following figure shows the experimental setup of Darcy. The outcomes of Darcy experiment is summarized in the following formula:

$$q = C \frac{A}{L} (h_1 - h_2), \quad (3.41)$$

where  $q$  is the measured flow rate,  $A$  is the cross-sectional area,  $L$  is the Length,  $h$  is the Level of water and  $C$  is the proportionality constant.

### **3.7.2 multiphase flow**

The term of multiphase flow refers to flow of any fluid consists of more than one phase or component with different chemical properties through a pipe or channel simultaneously. This term was coined lately by Soo et al. (1969) and it comprises of fluid dynamics motion of multiple phases. Multiphase flow is commonly seen in industrial processes such as pipeline transportation, fluidized beds and power plants. Liquid-liquid flows have many important applications in a diverse range of process industries in the petroleum production particularly, where oil and water are often produced and transported together. A typical multiphase oil-water two-phase flow is often encountered in petroleum industries, and measuring their process parameters (especially individual flow rate of oil and water) is an important issue in oil exploitation and transportation. Analogously in multiphase flow, probably the key toward understanding the phenomena of pressure drop behavior in oil field industries in order to optimize between the huge costs of production and transportation. For more details, the reader refers to Elobeid et al. (2016).

### **3.7.3 Experimental setup and data description**

The experiment of two-phase flow has been conducted in the laboratories of Petroleum and Geological sciences college at KFUPM, Dhahran, Saudi Arabia. The experiment was designed to investigate the influence of some additives on the flow behavior of water, oil and air mixture. The loop contains two 200-liter barrels

for water and oil respectively, besides an air connection instrument to supply the air. The flow rate of the feed streams was measured and adjusted by regulating valves.

The feed pumps for the liquids (oil and water) are rotary pumps equipped with axial face sealing. Water, air and oil can be separated in the separator or using cyclone and separator which are connected to the outlet of the test section. The test section was made of stainless steel tube with an outer diameter of 0.5 inch and an inner diameter of 0.4 inch. Its total length is approximately 5 m divided into two straight horizontal sections separated by elbows (90 degree elbow). The horizontal sections are equipped with differential pressure transducer to measure the pressure drop inside the test section. At the end of the test section an acrylic section of 20 cm allows the visible inspection of the flow behavior. After having passed the test section, the fluid can be directed to the phase separator where water and oil can be separated by gravity or alternatively to the cyclone whose outlet is connected to the phase separator. The sketch layout of the experiment is given is the following figure.

The generated air-water two-phase flow is circulated through the flow loop using a vertical centrifugal pump that can provide a maximum flow rate of 40 liter/min of water. On the other hand, the air is introduced to the system using a pressure regulator connected at the inlet of the compressed air. The flow rate of the water is measured using an electromagnetic flow meter and an accurate pressure transducer is used to measure the differential pressure drop over 1.5 millibar long and

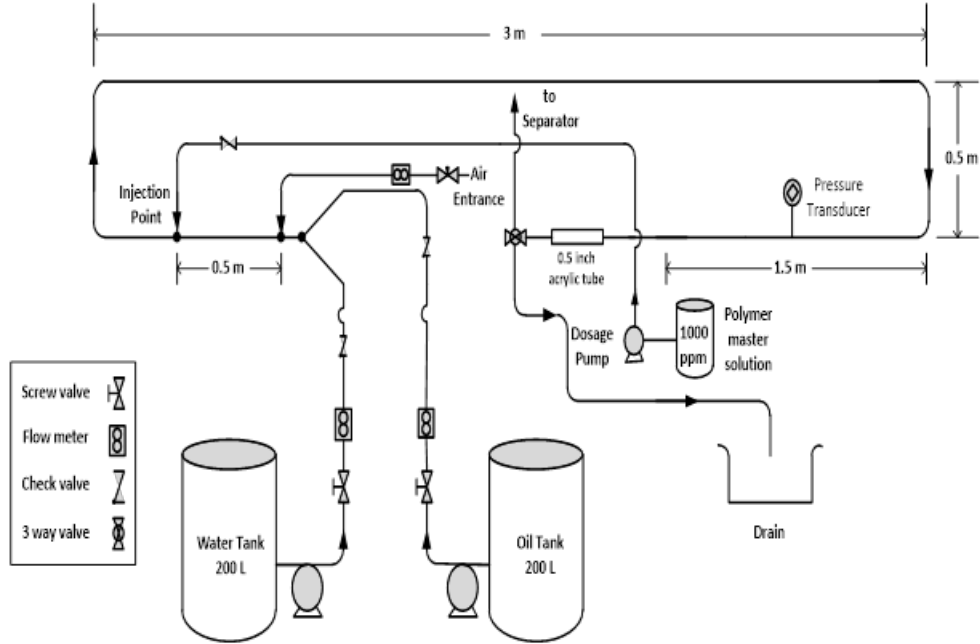


Figure 3.14: Two-phase experimental setup

mounted about 3.5 millibar downstream the mixing section.

The data acquisition procedure is carried out for better and more accurate data gathering. We targeted a group of the experimental observations at 25° Celsius, 54 different measurements of  $Q$  and  $\Delta P$  has been collected, preliminary investigations has been conducted on the gathered data to assure that it satisfies the regression model properties. There exist 18 levels of the volume flow rate (in liter/min) that equal 2.5, 3.8, 5.6, 7.2, 8.9, 10.6, 12.3, 13.9, 18.6, 20.3, 22.3, 24.0, 21.4, 22.2, 23.1, 24.3, 25.7 and 26.7. In the stated study, we consider the difference of pressure in two point ( $\Delta P$ ) as a dependent variable and the flow rate ( $Q$ ) as an independent variable. We used an approach based on bootstrapping method similar to that been introduced by Freedman et al. (1981), and repeated

Table 3.22: The values of the constant  $L$

	EWMA_3	$EWMA_R$	$EWMA_{PT}$
Intercept	2.997	3.137	3.009
slope	2.992	2.973	3.005
MSE	65.897	66.32	65.91

the scenario for 10000 iterations to extract the true parameters for our model.

The flow rate ( $Q$ ) is direct proportion to the difference of pressure in two points ( $\Delta P$ ) and the model mathematically is represented as

$$\Delta P = -43.46 + 25.37 * Q \quad (3.42)$$

The model in (3.42) is considered as a reference to the relationship between the flow rate ( $Q$ ) and the difference of pressure in two points ( $\Delta P$ ) with  $\sigma$  equals 48.9.

### 3.7.4 Implementation of $EWMA_R$ and $EWMA_{PT}$ charts

To monitor the flow rate ( $Q$ ) as it is a direct proportion to the difference of pressure in two points ( $\Delta P$ ), we estimated the model in (3.42), and then proceed with the following steps:

- From bootstrapping, we found the value of the distrust constant  $d = 0.0524$ .
- We transformed the flow rate ( $Q$ ) into  $Q' = (Q - \bar{Q})$ .
- Following Riaz et al. (2017) we fixed the value of  $\lambda = 0.2$ . We also fixed the value of  $ARL_0 = 200$  with the associated  $L$  given in Table 3.22.

Table 3.23: Control limits for each control chart

		EWMA <sub>.3</sub>	$EWMA_R$	$EWMA_{PT}$
Intercept	LCL	358.6052	358.6989	358.7782
	UCL	381.6548	381.5611	381.4818
slope	LCL	25.32463	25.32673	24.33698
	UCL	26.84755	25.47537	26.46302
MSE	UCL	8.01482	8.066268	8.0642

- For the diagnosis purpose, the plotting statistics were plotted against the control limits given in Table 3.23.

The findings of diagnose has been plotted in Figure 3.15-3.17. As it shown in the figures, the results assure our findings in the simulation part. For the intercept parameter, as we mentioned, there is no significant improvement in under the different estimation strategy as we standardized our explanatory variable. For the slope and the error variance, it is clear that  $EWMA_{PT}$  and  $EWMA_R$  excelled EWMA<sub>.3</sub> to detect the shift in the fluid's pressure difference ( $\Delta P$ ) regarding to the associate changes in the flow rate.

### 3.8 Summary and conclusions

In this chapter, we discussed different charts using restricted and pretest estimation methods and proposed new control charts based on the two estimators and we compared their performance with EWMA<sub>.3</sub> via ARL.

The results showed that, the  $EWMA_R$  control chart outperforms all the other control charts under the different values of shifts in the slope and the error variance of the considered linear profile. In contrast, the three control charts performed

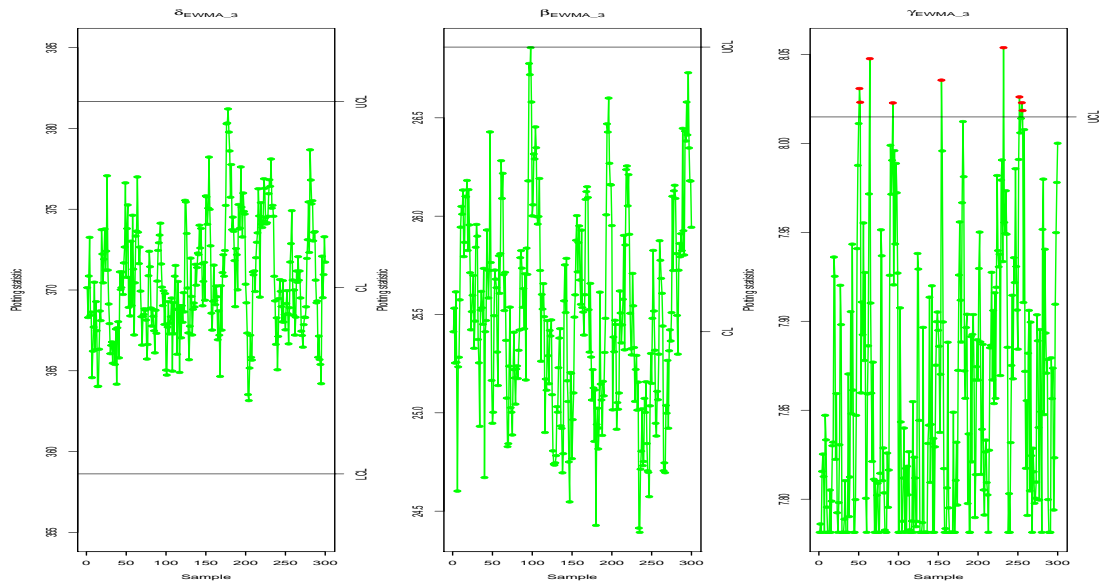


Figure 3.15: EWMA<sub>3</sub>

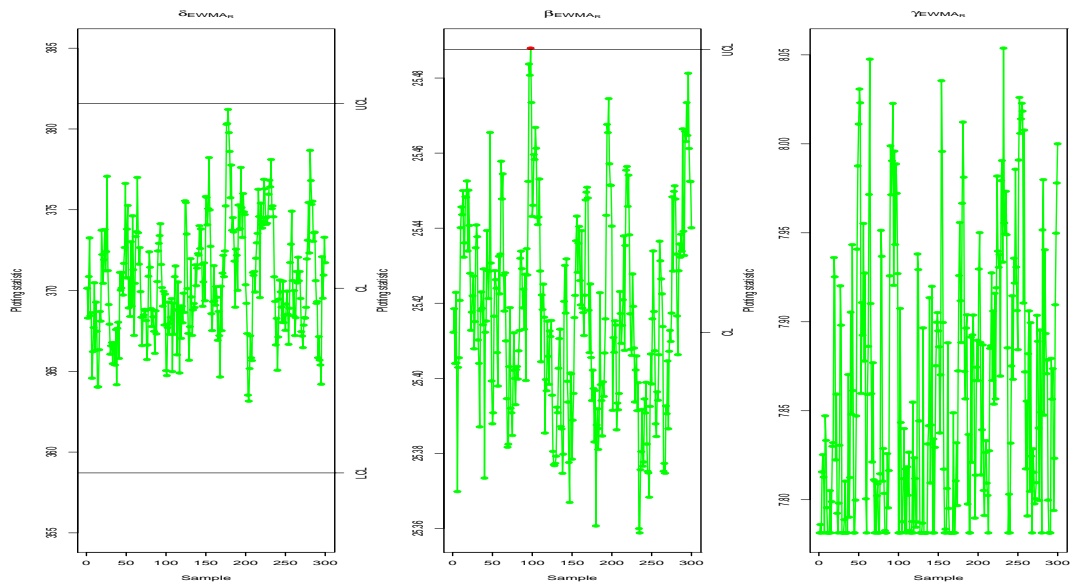


Figure 3.16: EWMA<sub>R</sub>

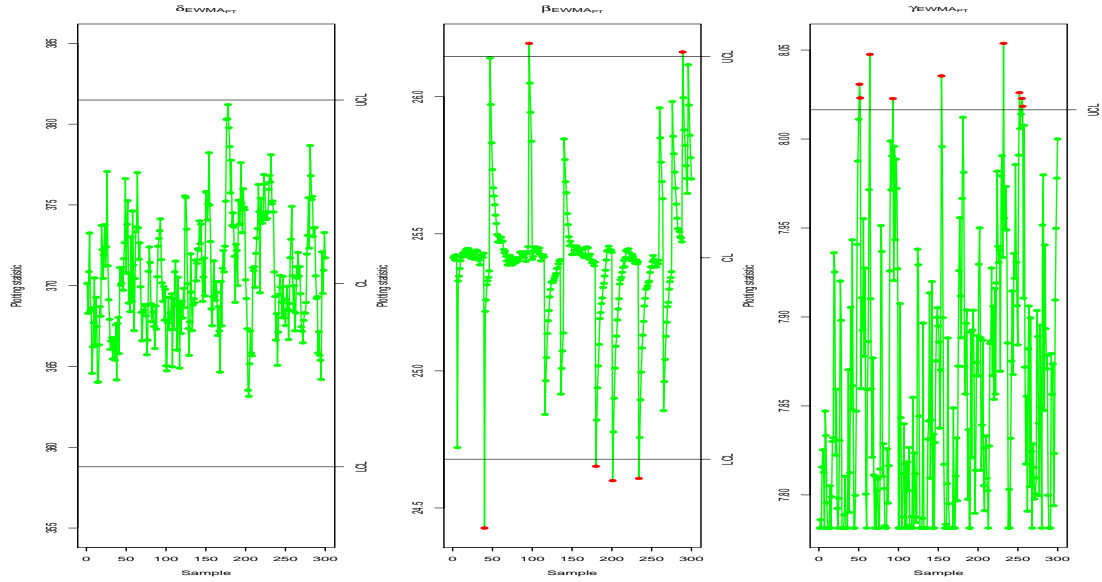


Figure 3.17:  $EWMA_{PT}$

similarly under the intercept shifts of the linear profile, that was due to the useless of the UPI that caused by the adjusted explanatory variable.

Overall,  $EWMA_R$  performs better under smaller values of  $d$  and small shifts, whereas  $EWMA_{PT}$  with smaller values of  $d$  was the worse. Under the larger values of  $d$ ,  $EWMA_R$  and  $EWMA_{PT}$  approach to EWMA\_3 and they perform similarly when  $d = 0$ .



## CHAPTER 4

# THE PERFORMANCE OF PHASE I COEFFICIENT OF VARIATION CONTROL CHARTS FOR PROCESS MONITORING

### 4.1 Introduction

In many cases, while the process is in-control, it has a constant mean and variance.

In such cases  $\bar{X}$  control chart can be used to monitor the mean and **S** or **R** control charts can be used to monitor the dispersion. Recently, control charting techniques have been adopted in many applications such as education, health, finance, etc.

where the mean and the standard deviation might be non constant even though the process is operating in-control. Hence, the situation urged us to introduce the CV control charts for monitoring relative dispersion.

In recent years, researchers investigated the monitoring of location and scale parameters in phase I, for example, Yang et al. (2006) studied Phase I sample size impact on the false signal rate of the  $\bar{X}$  chart. Schoonhoven and Does (2012) studied the influence of estimating the standard deviation in phase I on the behavior of the control chart in phase II for dispersion monitoring. Abbasi et al. (2015) investigated the efficiency of Shewhart chart in phase I to monitor the variability by considering normal and non-normal processes.

However, many literatures have investigated the CV control charts in phase II, the performance of CV control charts in phase I has not been investigated in SPC literature so far. Therefore, the purpose of this study is to evaluate and investigate the performance of different CV estimators to study the probability to signal (PTS) of the CV control charts in phase I, as similar to the studies of location and dispersion, done by Abbasi et al. (2015); Jensen et al. (2006); Jones-Farmer and Champ (2010).

The organization of this chapter is as follows: Section 4.2 presents monitoring of the CV in phase I. Section 4.3 describes the simulation study. Section 4.4 contains the results and discussion and gives comparisons of different charting structures.

The chapter is wrapped up by conclusions and recommendations in Section 4.6.

## 4.2 Monitoring of process CV in phase I

Assume that we have a process ( $\mathbf{X}$ ) with mean ( $\mu > 0$ ) and standard deviation ( $\sigma$ ). By definition, the CV of  $\mathbf{X}$  is defined as

$$\gamma = \frac{\sigma}{\mu}. \quad (4.1)$$

which is a standardized measure of dispersion of the process  $\mathbf{X}$ . More details about the CV properties are available in Calzada and Scariano (2013).

The CV estimator is a standardized measure of dispersion of the quality characteristic of  $X$ . According to Everitt (1998), the CV can be used in a variety of real world applications; for example, to express the precision of an assay in the analytical chemistry, conducting quality assurance studies in engineering and determining the volatility of bonds in economic. In addition, the CV has many advantages over the other dispersion estimators, such as the standard deviation, because the standard deviation of data is always understood in the context of the mean of the data. In contrast, it is unlike the standard deviation, it can not be used directly to establish confidence intervals for the process mean. For more details about the CV properties, the reader is referred to Calzada and Scariano (2013). From the practical aspects, the parameter in Equation (??) is inapplicable because it relies on parameters  $\sigma$  and  $\mu$ . Hence, it is more practical to use an

estimator of  $\gamma$  that will take the advantage of using a sample from the process.

Consider historical data containing a sample of size  $n$ , and let  $X_{ij}, i = 1, \dots, n; j = 1, \dots, m$  represents the  $i^{th}$  historical observation from the process  $\mathbf{X}$ , with standard deviation and mean  $\bar{X}_j$  and  $S_j$ , respectively. Then, the CV of the process  $\mathbf{X}$  is defined as

$$W_j = \frac{S_j}{\bar{X}_j}. \quad (4.2)$$

In many practical aspects, the estimator in Equation (4.2) might not be efficient estimator of CV for many reasons, such as, under very small sample sizes, the existence of extreme points inside the sample, the sample is heterogeneous, as well as when the sample follows non-normal distribution. For more details, the reader is referred to Sokal and Rohlf (1995). Phase I data sets are usually contaminated with extreme points. These contaminations may be a part of a particular sample or may be distributed across the historical dataset. The goal of Phase I analysis is to detect/remove any inconsistent observations so that the Phase II limits can be based on a clean dataset. In this study, we will also propose a new sensitive estimator of CV that is defined as

$$V_j = \frac{R_j}{\tilde{X}_j}, \quad (4.3)$$

where,  $\tilde{X}_j$  is the sample median and  $R_j$  is the usual range estimator defined as:

$R_j = x_{(n)_j} - x_{(1)_j}$ , where  $X_{(1)_j}$  and  $X_{(n)_j}$  represent the extreme observations in the data vector  $\mathbf{X}$ .

### 4.2.1 Control chart structure

In this subsection, we propose different control chart structures for monitoring the CV in Phase I. Similarly to the structure of R chart, we follow Montgomery (2009); Schoonhoven and Does (2012); Abbasi et al. (2015) to introduce our new charting structures. Suppose a historical dataset contains  $m$  samples each of size  $n$ . After estimating CV by using either  $W$  or  $V$ , different control chart structures are described below

$$\begin{aligned}
 UCL &= \bar{W} + L_{\bar{W}} \frac{d_{3\bar{W}}}{d_{2\bar{W}}} \bar{W} \\
 \bar{W}chart : \quad CL &= \bar{W} \\
 LCL &= \bar{W} - L_{\bar{W}} \frac{d_{3\bar{W}}}{d_{2\bar{W}}} \bar{W}
 \end{aligned} \tag{4.4}$$

$$\begin{aligned}
 UCL &= \tilde{W} + L_{\tilde{W}} \frac{d_{3\tilde{W}}}{d_{2\tilde{W}}} \tilde{W} \\
 \tilde{W}chart : \quad CL &= \tilde{W} \\
 LCL &= \tilde{W} - L_{\tilde{W}} \frac{d_{3\tilde{W}}}{d_{2\tilde{W}}} \tilde{W}
 \end{aligned} \tag{4.5}$$

$$\begin{aligned}
 UCL &= W_p + L_{W_p} \frac{d_{3W_p}}{d_{2W_p}} W_p \\
 W_pchart : \quad CL &= W_p \\
 LCL &= W_p - L_{W_p} \frac{d_{3W_p}}{d_{2W_p}} W_p
 \end{aligned} \tag{4.6}$$

For the monitoring purposes,  $W_j$  is used as a plotting statistics for the above three control charts.

$$\begin{aligned}
UCL &= \bar{V} + L_{\bar{V}} \frac{d_{3\bar{V}}}{d_{2\bar{V}}} \bar{V} \\
\bar{V} \text{ chart : } \quad CL &= \bar{V} \\
LCL &= \bar{V} - L_{\bar{V}} \frac{d_{3\bar{V}}}{d_{2\bar{V}}} \bar{V}
\end{aligned} \tag{4.7}$$

$$\begin{aligned}
UCL &= \tilde{V} + L_{\tilde{V}} \frac{d_{3\tilde{V}}}{d_{2\tilde{V}}} \tilde{V} \\
\tilde{V} \text{ chart : } \quad CL &= \tilde{V} \\
LCL &= \tilde{V} - L_{\tilde{V}} \frac{d_{3\tilde{V}}}{d_{2\tilde{V}}} \tilde{V}
\end{aligned} \tag{4.8}$$

$$\begin{aligned}
UCL &= V_p + L_{V_p} \frac{d_{3V_p}}{d_{2V_p}} V_p \\
V_p \text{ chart : } \quad CL &= V_p \\
LCL &= V_p - L_{V_p} \frac{d_{3V_p}}{d_{2V_p}} V_p
\end{aligned} \tag{4.9}$$

For the monitoring purposes,  $V_j$  is used as a plotting statistics for the above three control charts. In addition,  $\bar{W} = \sum_{i=1}^m \frac{W_i}{m}$ ,  $\bar{V} = \sum_{i=1}^m \frac{V_i}{m}$ , the pooled estimate of Connett and Wong Lee (1990) are  $W_p = \sqrt{\sum_{i=1}^m \frac{W_i^2}{m}}$  and  $V_p = \sqrt{\sum_{i=1}^m \frac{V_i^2}{m}}$ . Also,  $\tilde{W}$  and  $\tilde{V}$  are the median of m samples of  $W_i$  and  $V_j$ , respectively.

The constants  $d_{2\bar{W}}, d_{3\bar{W}}, d_{2\bar{V}}, d_{3\bar{V}}, d_{2\tilde{W}}, d_{3\tilde{W}}, d_{2\tilde{V}}, d_{3\tilde{V}}, d_{2W_p}, d_{3W_p}, d_{2V_p}, d_{3V_p}$  are available in Table A.1 .

### 4.3 Simulation study

To investigate the performance of the various control chart schemes that have been considered in Section 4.2, we performed a comprehensive simulation study considering Phase I of SPC. In practice, samples are collected from a process in a form of rational subgroups. As the historical data contains  $m$  subgroups each of size  $n$ , hence, in this study, we considered  $m = 30$  and  $n = 5, 10$  and  $15$ . The observations come from normal distribution  $\mathcal{N}(\mu, \mu * \gamma_0)$ , where  $\mu = 500$  and  $\gamma_0 = 0.05$ . It is frequent to get extreme observations/samples in Phase I data set and the aim of Phase I is to detect these contaminations efficiently and quickly. To check the detection ability of CV charts, we introduced two contaminated scenarios in Phase I following Schoonhoven et al. (2011); Schoonhoven and Does (2012); Abbasi et al. (2015), as given below.

- A model for localized CV disturbances in which observations in  $m_1$  samples are drawn from  $\mathcal{N}(\mu, \mu * \gamma_1)$  distribution, with  $\gamma_1 = \gamma_0 + \delta\gamma_0$ ,  $\delta$  represent the shift in  $\gamma_0$ , and  $m_1 = 3, 6, 9$ , or  $12$ .
- A model for diffuse symmetric CV disturbances in which each observation has  $(1 - p)\%$  probability of being drawn from the  $\mathcal{N}(\mu, \mu * \gamma_0)$  distribution and  $p\%$  probability of being drawn from the  $\mathcal{N}(\mu, \mu * \gamma_1)$  distribution, with  $p = 5\%, 10\%, 15\%$  or  $20\%$ .

The multipliers  $L$  of the control charts structure (described in Section 4.2) are appropriately chosen in order to give a constant false alarm probability (FAP) ( $\alpha$ ), where  $\alpha = 1 - (1 - \alpha^*)^m$ ,  $\alpha^*$  is the probability to signal from one sample.

More details about FAP can be found in Jones-Farmer and Champ (2010); Shiau and Sun (2010). Later, we use respective sample statistic (i.e.,  $W$  or  $V$ ) as the monitoring statistic to inspect any out-of-control signals. The values of  $L$  under the considered  $m$  and  $n$ , are chosen to fix the  $FAP(\alpha) = 0.01$  for all the control charts, as reported in Table 4.1. This procedure is repeated 100,000 times for getting the probability to signal.

Table 4.1: Control chart multiplier  $L$  to fix FAP at 0.01 for all the control charts.

$n$	$\bar{W}$	$\tilde{W}$	$W_p$	$\bar{V}$	$\tilde{V}$	$V_p$
5	3.873	4.287	1.209	4.07	4.48	1.256
10	3.72	3.99	0.818	4.25	4.61	0.922
15	3.63	3.88	0.66	4.53	5	0.81

## 4.4 Results and discussion

In this section, we provide a comprehensive report of the results from the simulation study conducted in Section 4.3. From the performance comparison perspective, the control chart that gives higher probability to signal is considered better than the other control charts. The findings are reported in the forthcoming paragraphs.

Figure 4.1 and Figure 4.2 show the probability to signal of the control charts in presence of localized CV disturbances with subgroup sizes  $n = 5$  and  $10$ . The results showed that the  $\tilde{W}$  and  $\tilde{V}$  control charts dominantly performed better than



the other control charts.  $W_P$  and  $V_P$  control charts showed the worst performance in detecting the localized disturbances. Addition to that, the larger subgroup size ( $n$ ) gave higher probability to signal with all the control charts.

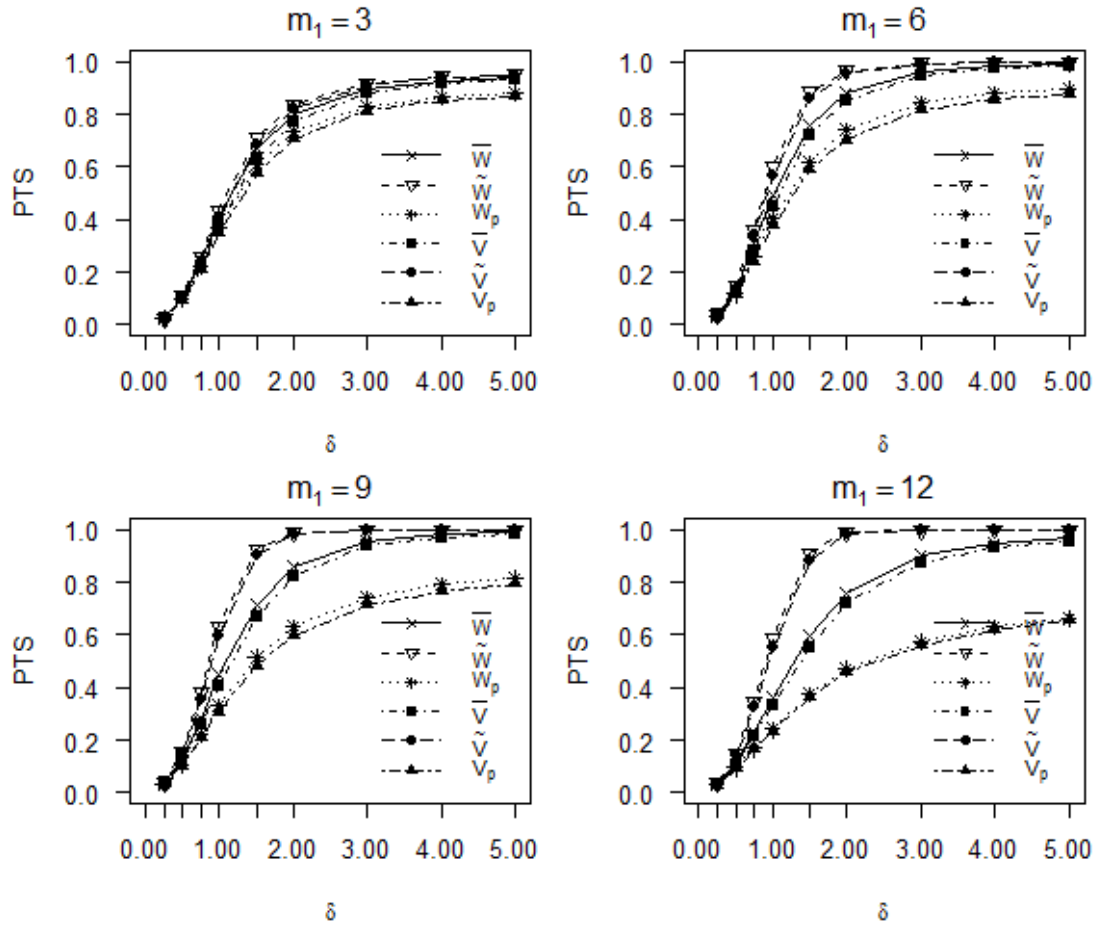


Figure 4.1: The PTS of CV charts with localized CV disturbances,  $n = 5, \gamma_0 = .05$  and  $m = 30$ .

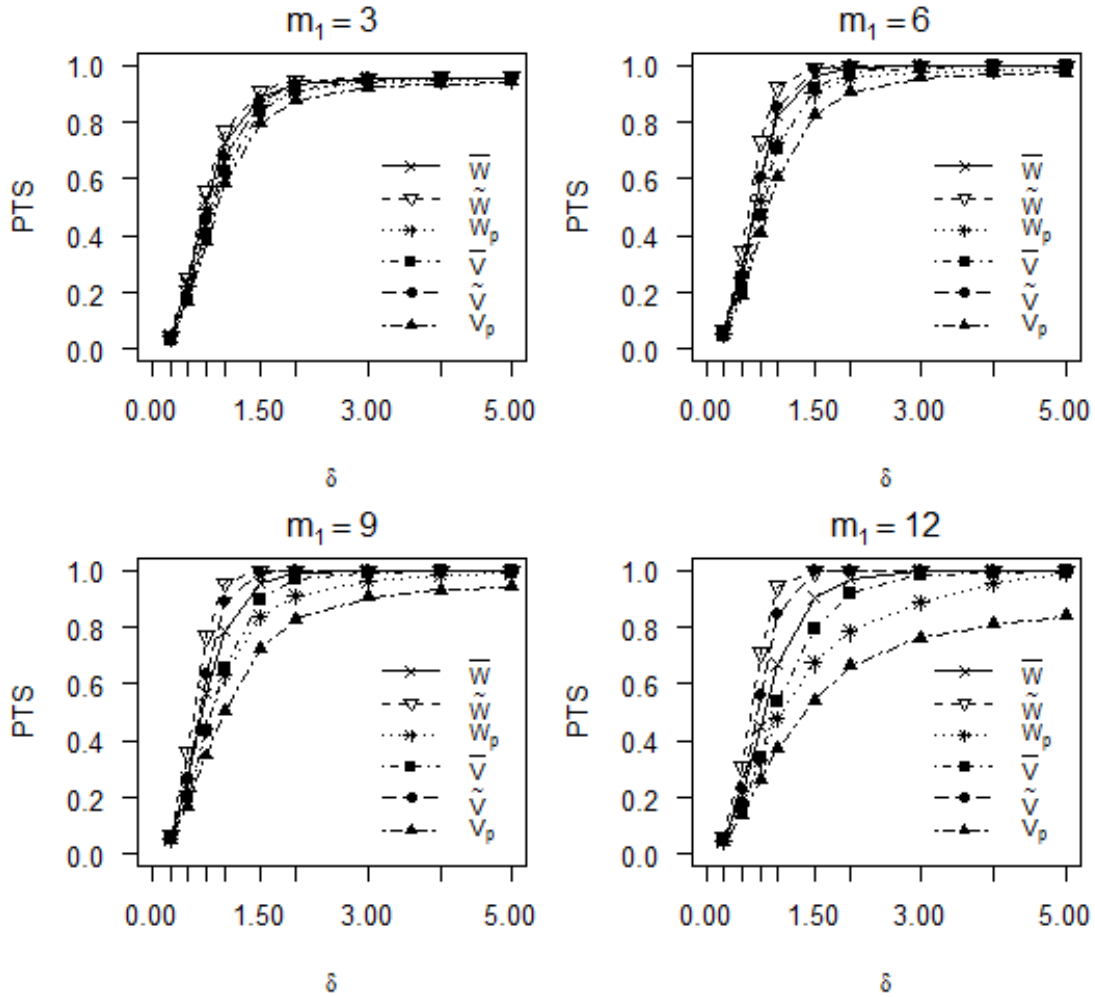


Figure 4.2: The PTS of CV charts with localized CV disturbances,  $n = 10, \gamma_0 = .05$  and  $m = 30$ .

Figure 4.3 and Figure 4.4 show the probability to signal of the control charts with diffuse symmetric CV disturbances for subgroup sizes  $n = 5$  and  $10$ . Relying on the depicted plots, it is clear that the  $W_p$  and  $\tilde{V}$  control charts are showing far higher PTS as compared to the other charts when  $n = 5$ . At this sample size  $V_p$  and  $\bar{W}$  are showing the worst performance at different level of  $p$ . For large sample sizes ( $n = 10$ ), again  $W_p$  and  $\tilde{V}$  are performing better as compared to the other charts for  $\delta < 3$ . For large values of  $\delta$ ,  $\bar{W}$  and  $\tilde{V}$  are better choices. In general

we can say that  $W_p$  and  $\tilde{V}$  are the best charts for the detection of the diffuse symmetric CV disturbances.

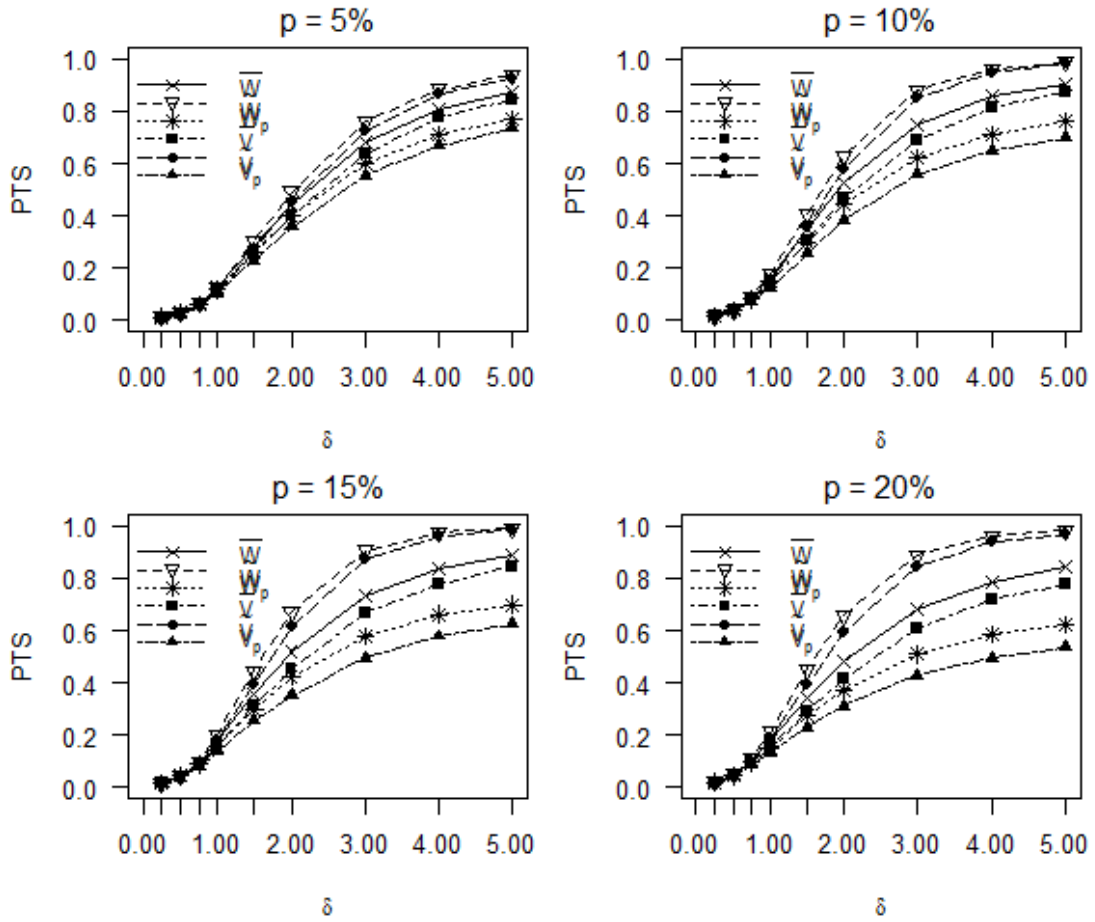


Figure 4.3: The PTS of the CV charts with diffuse symmetric CV disturbances,  $n = 5, \gamma_0 = .05$  and  $m = 30$ .

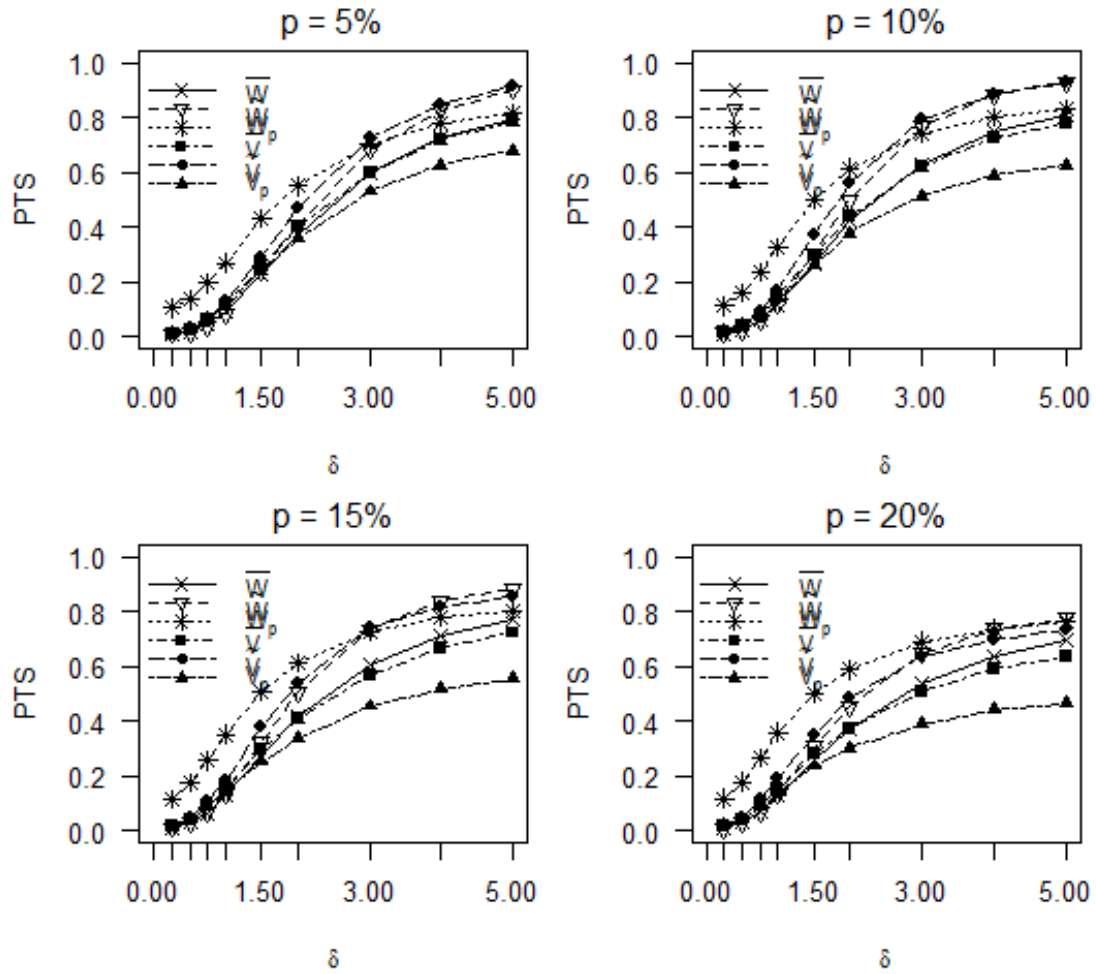


Figure 4.4: The PTS of the CV charts with diffuse symmetric CV disturbances,  $n = 10, \gamma_0 = .05$  and  $m = 30$ .

#### 4.4.1 The effect of $n$ , CV ( $\gamma$ ) and $m$ on PTS

We will investigate the effect of sample size ( $n$ ),  $\gamma$ , and number of subgroups ( $m$ ) on PTS. To save space, we will only investigate  $\tilde{W}$  chart for varying levels of  $m$ ,  $\gamma$  and  $n$ . similar investigations can be carried out for other charts.

##### Effect of the sample size ( $n$ )

The effect of the sample size ( $n$ ) on the performance of  $\tilde{W}$  has been depicted in Table 4.2. In order to be able to study the effect of the subgroup size, we considered the number of subgroups  $m = 30$ ,  $\gamma_0 = 0.05$ , localized CV disturbances  $m_1 = 6$  and the diffuse symmetric CV disturbances  $p = 10\%$ . By Calculating the PTS for the  $\tilde{W}$  control chart we observed that the probability of detecting more localized CV disturbance increase with the subgroup size.

Table 4.2: The effect of the size of subgroup in the PTS of  $\tilde{W}$  with localized CV disturbances,  $m = 30$ ,  $\gamma_0 = 0.05$

	$m_1 = 3$			$m_1 = 6$		
$\delta$	n = 5	n = 10	n = 15	n = 5	n = 10	n = 15
0.25	0.0235	0.044	0.0754	0.0359	0.0628	0.0933
0.5	0.1062	0.2488	0.4132	0.1468	0.3458	0.5583
0.75	0.2559	0.5583	0.7445	0.3619	0.7329	0.9098
1	0.4328	0.7691	0.8881	0.6026	0.9232	0.9845
1.5	0.7127	0.9114	0.9478	0.8838	0.9915	0.9977
2	0.8374	0.9442	0.9558	0.9644	0.9973	0.9986
3	0.9192	0.956	0.9577	0.9931	0.9986	0.9988
4	0.9415	0.9574	0.9578	0.9969	0.9987	0.9988
5	0.9496	0.9577	0.9578	0.998	0.9988	0.9988
	$m_1 = 9$			$m_1 = 12$		
Shift	n = 5	n = 10	n = 15	n = 5	n = 10	n = 15
0.25	0.0371	0.066	0.1021	0.0366	0.059	0.0947

0.5	0.1555	0.3556	0.5792	0.1432	0.3052	0.4998
0.75	0.3839	0.7699	0.9448	0.343	0.713	0.9221
1	0.6313	0.9559	0.9961	0.5878	0.942	0.9967
1.5	0.9245	0.9987	0.9999	0.9081	0.9993	1.0000
2	0.9872	0.9999	1.0000	0.988	1.0000	1.0000
3	0.9992	1.0000	1.0000	0.9998	1.0000	1.0000
4	0.9998	1.0000	1.0000	1.0000	1.0000	1.0000
5	0.9999	1.0000	1.0000	1.0000	1.0000	1.0000

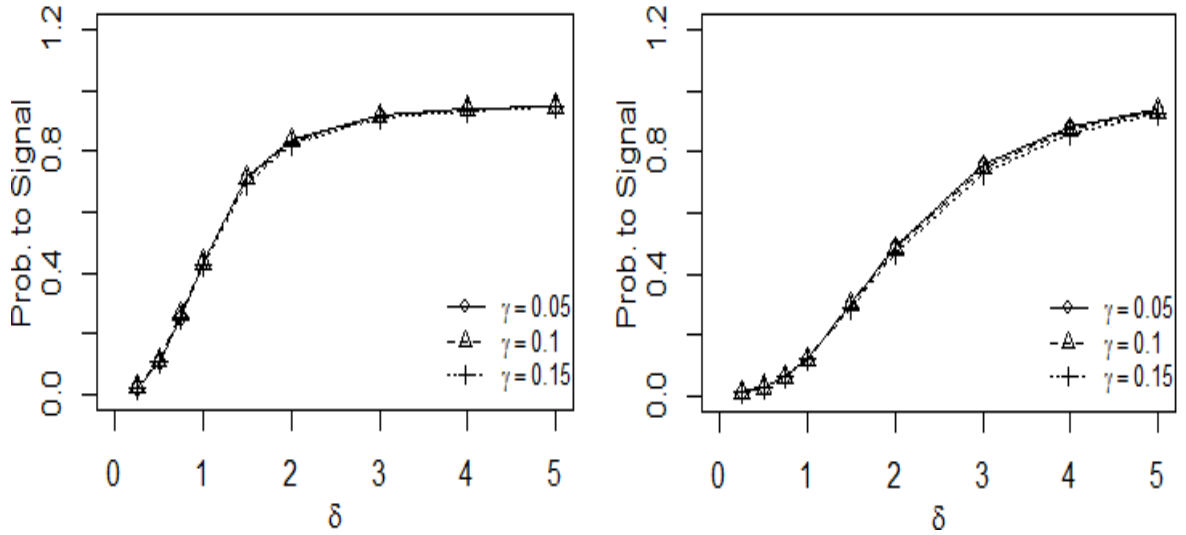
Table 4.3: The effect of the size of subgroup in the PTS of  $\tilde{W}$  with diffuse symmetric CV disturbances,  $m = 30$ ,  $\gamma_0 = 0.05$

	$p = 5\%$			$p = 10\%$		
Shift	n = 5	n = 10	n = 15	n = 5	n = 10	n = 15
0.25	0.0136	0.012	0.0102	0.0178	0.0131	0.0131
0.5	0.0283	0.0187	0.0205	0.0376	0.026	0.0266
0.75	0.0632	0.041	0.0374	0.0887	0.0584	0.0529
1	0.122	0.0859	0.0803	0.1783	0.1236	0.105
1.5	0.3037	0.2401	0.2043	0.4066	0.3039	0.2551
2	0.4923	0.4086	0.3574	0.6303	0.5007	0.4195
3	0.7602	0.6824	0.6171	0.8795	0.7663	0.6408
4	0.883	0.8269	0.7606	0.9628	0.8852	0.7528
5	0.9376	0.9009	0.839	0.9862	0.9303	0.8111

Shift	$p = 15\%$			$p = 20\%$		
	n = 5	n = 10	n = 15	n = 5	n = 10	n = 15
0.25	0.0168	0.0122	0.0131	0.0203	0.0115	0.0153
0.5	0.0462	0.0328	0.028	0.0511	0.0344	0.0308
0.75	0.0983	0.0672	0.0598	0.1129	0.069	0.0657
1	0.2023	0.1397	0.118	0.2108	0.1397	0.1239
1.5	0.446	0.3232	0.2618	0.45	0.3074	0.2432
2	0.6732	0.5069	0.3963	0.6569	0.4536	0.3464
3	0.9054	0.7353	0.5806	0.8878	0.6462	0.4893
4	0.9752	0.8375	0.6726	0.9621	0.7361	0.5781
5	0.9919	0.8819	0.7271	0.9831	0.7731	0.6315

### Effect of $\gamma$

To study the effect of  $\gamma$  on the performance of the  $\tilde{W}$  control chart, the values of  $\gamma_0 = 0.05, 0.1,$  and  $0.15$  have been examined. We considered the subgroup size ( $n=5$ ), number of subgroups ( $m = 30$ ) and the amount of disturbances ( $m_1 = 3$  and  $p = 5\%$ ), the results are summarized in Figure 4.5. The results showed that  $\gamma$  had a low impact on the performance of the  $\tilde{W}$  control chart. We can also observe that the PTS is higher in the detection of the localized CV disturbances as compared to the diffuse symmetric CV disturbances.



(a) Localized CV disturbances ( $m_1 = 3$ )      (b) Diffuse symmetric CV disturbances ( $p = 5\%$ )

Figure 4.5: The effect of the CV ( $\gamma$ ) in the PTS of  $\tilde{W}$  chart,  $m = 30, n = 5$

### Effect of the number of subgroups

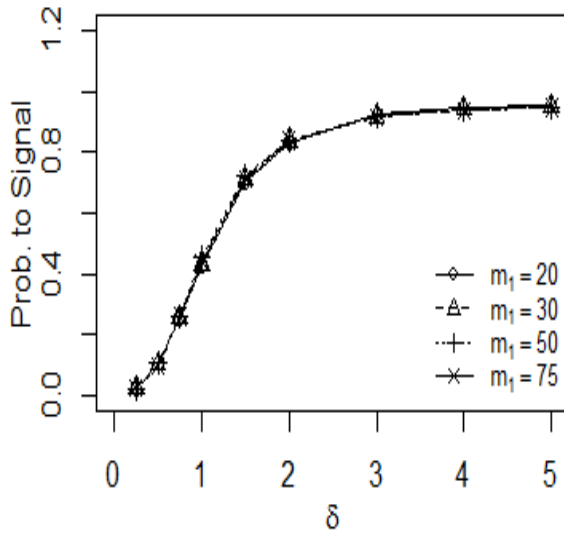
Finally, to evaluate the effect of the number of subgroups ( $m$ ) on the performance of the  $\tilde{W}$  chart, we studied the performance under  $n = 5, \gamma_0 = 0.05, m = 20, 30, 50$  and  $75$ . Hence, different amount of disturbances have been considered,  $m_1 = 3$  and  $9$  as the localized CV disturbances and  $p = 5\%$  and  $15\%$  as the diffuse symmetric CV disturbances.

As the results of the  $\tilde{W}$  control chart with different number of subgroups are depicted in Figures 4.6-4.7 with  $m_1 = 3$  and  $p = 5\%$ , the performance under the localized CV disturbances was resistant to the different values of  $m$ . In contrast, the performance under the diffuse symmetric CV disturbances was drastically affected by the number of subgroups, where the performance increased by increasing the number of subgroups.

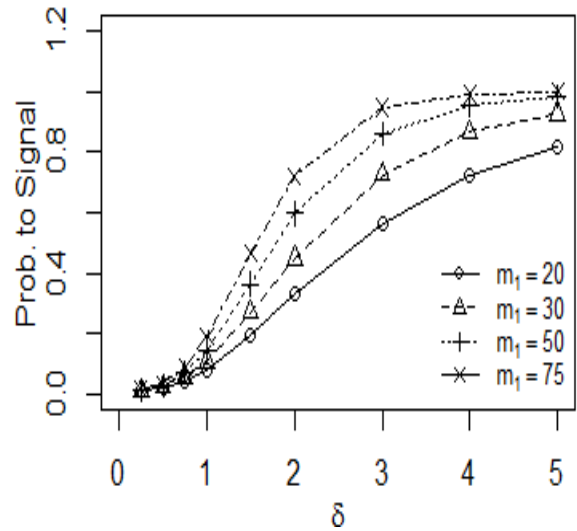


Figure 4.6 shows the effect of number of subgroups on detection of the localized CV disturbances. We can observe that when  $m_1$  is small ( $m_1 = 3$ ), there seems no effect on the PTS at different levels of  $m$ . When  $m_1 = 9$  the probability increase as  $m$  increases.

Similarly, the PTS for the detection of diffuse symmetric CV disturbances is plotted in Figure 4.7. Again we can observe that the PTS of the  $\tilde{W}$  chart increases as number of subgroups ( $m$ ) increases.

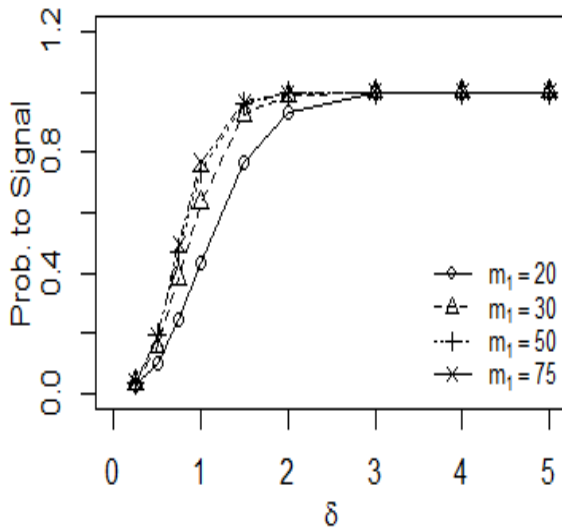


(a) Localized CV disturbances ( $m_1 = 3$ )

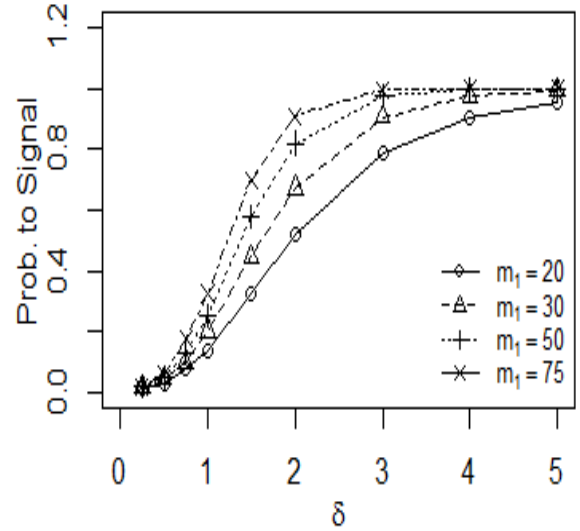


(b) Diffuse symmetric CV disturbances ( $p = 5\%$ )

Figure 4.6: The effect of the number of subgroups in the PTS of  $\tilde{W}$  with  $\gamma_0 = 0.05, n = 5$ .



(a) Localized CV disturbances ( $m_1 = 9$ )



(b) Diffuse symmetric CV disturbances ( $p = 15\%$ )

Figure 4.7: The effect of the number of subgroups in the PTS of  $\tilde{W}$  with  $\gamma_0 = 0.05, n = 5$

#### 4.4.2 Simulation experiment

In this part we formulated a numerical experiment to examine our control charting structures. We considered 30 subgroups each with size 5. We considered the in-control  $CV(\gamma_0)$  is 0.05 and  $\mu = 500$ . Besides, the consideration of the two types of sample contamination: i) Localized CV disturbances with  $m_1 = 9$ , ii) diffuse symmetric CV disturbances  $p=20\%$  both with  $\delta = 2.5$ . The experiment was conducted as follow

1. Generated a sample of 30 subgroups each of size 5. Then, estimate the control limits as they have been discussed previously by fixing  $FAP(\alpha) = 0.01$ .

2. Generate a new sample for plotting purposes, 30 subgroups each of size 5.

The contamination was introduced as:

- Localized disturbances: 21 subgroups from  $\mathcal{N}(\mu, \mu * \gamma_0)$  and the last 9 subgroups as contaminated from  $\mathcal{N}(\mu, \mu * (\gamma_0 + \gamma_0 * \delta))$ .
- Diffuse symmetric disturbances: 150 observations, 85% (128) from  $\mathcal{N}(\mu, \mu * \gamma_0)$  and 15% (22) from  $\mathcal{N}(\mu, \mu * (\gamma_0 + \gamma_0 * \delta))$ , then distribute these observations randomly into 30 subgroups.

3. Estimate 30 plotting statistics ( $W_j$ ) from the samples estimated in the previous step regarding to the disturbance technique.

Figure 4.8 shows the case of samples contaminated with localized CV disturbances. It is clear that  $\tilde{W}$  charting structure was able declare out-of-control signal at sample points as soon as the process goes out-of-control where 7 points are supposed to be out-of-control. The second charting structure was  $\bar{W}$ , it was able to detect 3 points out-of-control while it failed on detecting the other out-of-control points.  $W_p$  was the less performance control chart, it was able just to detect only one point out-of-control.

The case of the diffuse symmetric CV disturbances is depicted in Figure 4.9. The results show less number of out-of-control points has been detected,  $\tilde{W}$  is still the preference control chart but it detected 3 points out-of-control, then followed by  $\bar{W}$  chart and it was able to detect only one point out-of-control.  $W_p$  was failed to detect any out-of-control that our dataset contained.

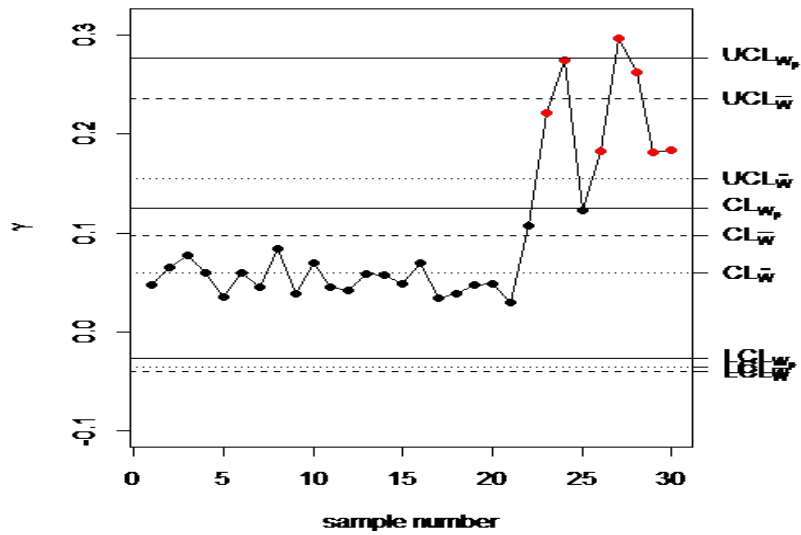


Figure 4.8: The CV Control Charts of the numerical experiment with localized CV disturbances.

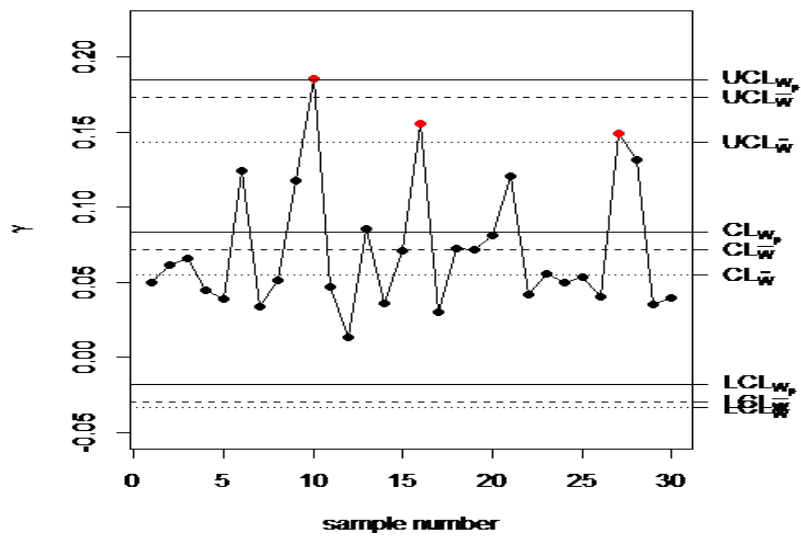


Figure 4.9: The CV Control Charts of the numerical experiment with diffuse symmetric CV disturbances.

## 4.5 Real life example

A manufacturing process has been considered as an illustrative example. A Tunisian company manufacturing zinc alloy parts for the sanitary sector had provided a dataset of a die-casting hot chamber process. The dataset is available in Castagliola et al. (2013). The characteristic of interest is the weight of scrap zinc alloy (in grams) to be removed between the molding process and continuous-coating for the surface.

Phase I has been investigated by Castagliola et al. (2013) and others, their results revealed that the proportion between the standard deviation ( $s$ ) and the mean ( $\mu$ ) of the scrap alloy weight is constant. Their preliminary results were based on a dataset of 30 samples each of size 5.

We utilized the same dataset to initiate the control limits of  $\bar{W}$ ,  $\tilde{W}$  and  $W_p$  charts as they have been discussed in Section 4.2. To estimate the in-control CV ( $\gamma_0$ ), we followed Connett and Wong Lee (1990); Castagliola et al. (2013), the associated estimates are reported as

$$\bar{\gamma}_0 = \sum_{i=1}^{30} \frac{\hat{\gamma}_i}{30} = 0.00974$$

$$\tilde{\gamma}_0 = \text{median}(\hat{\gamma}_i) = 0.00935$$

$$W_p = \sqrt{\sum_{i=1}^{30} \frac{\hat{\gamma}_i}{30}} = 0.01085$$

To fix  $FAP(\alpha) = 0.01$ , the values of the multiplier  $L$  and  $d_{\bar{W}_2}, d_{\bar{W}_3}, d_{\tilde{W}_2}, d_{\tilde{W}_3}, d_{W_p}$  and  $d_{W_p}$  are given in Table 4.4.

Table 4.4: The values of the constant multipliers of die casting hot chamber process.

Chart	L	$d_2$	$d_3$
$\bar{W}$	3.853	0.9366	0.3415
$\tilde{W}$	4.31	0.9177	0.3514
$W_p$	1.21	0.502	0.5042

The graphical display of the considered control charts is provided in Figure 4.10. The sample numbers are shown on the horizontal axis, whereas the sample statistic  $W_j$  is plotted on the vertical axis. The figure shows the lower control limit (LCL), upper control limit (UCL) and the central line (CL) of each chart of  $\bar{W}$ ,  $\tilde{W}$  and  $W_p$  charts are represented by the dashed (— — — —), dotted (. . . . .) and solid (—) horizontal lines, respectively.

It is evident from Figure 4.10 that there is no charting structure was able to declare any out-of-control signal at sample points, this might be due to the symmetry in our dataset and there is no contamination in the dataset. As a result, we can conclude that under the normal conditions when the dataset is symmetric all the charting structures perform similarly.

It is an evident from Figure 4.10 that there is no charting structure was able

to declare any out-of-control signal at sample points, this might be due to the symmetry in our dataset and there is no contamination in the dataset. As a result, we can conclude that under the normal conditions when the dataset is symmetric all the charting structures perform similarly.

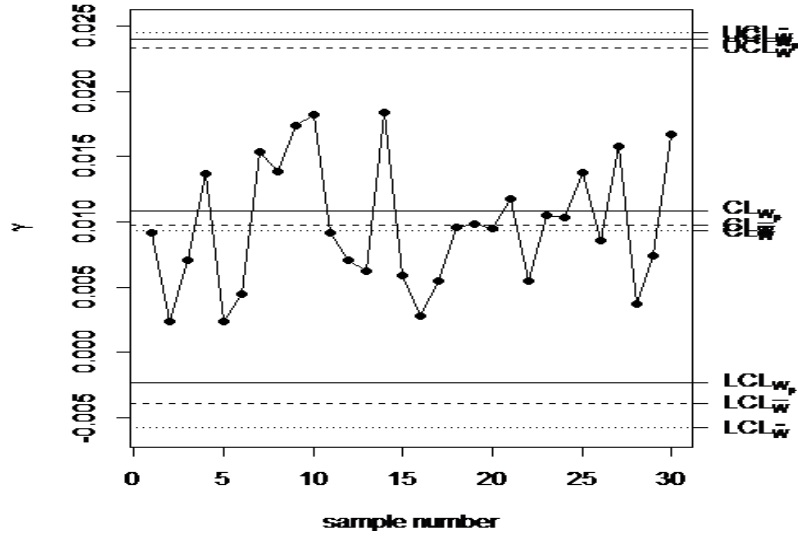


Figure 4.10: The CV Control Charts of die casting hot chamber process.

## 4.6 Summary and conclusion

This study has investigated the choice of an appropriate control charting structure for efficient monitoring of process CV parameter in phase I. We studied the performance of different CV control charting structures under the effect of two types of CV disturbances. However, all the estimators performed almost similarly under small disturbances, the results showed that the  $\tilde{W}$  and  $\tilde{V}$  control charts performed better than the other control charts. The results showed that,  $\gamma$  did not have a significant impact on the performance of  $\tilde{W}$  control chart, the localized

CV disturbances with large subgroup size gave the highest PTS and the diffuse symmetric CV disturbances with small subgroup size gave the highest PTS. Regarding to the impact of the number of subgroups ( $m$ ), the PTS with the large values of the localized CV disturbances did not vary with the different values of  $m$ . In contrast, the PTS under the diffuse symmetric CV disturbances was drastically been effected by  $m$ . Finally, the  $\tilde{W}$  and  $\tilde{V}$  control charts have shown the best ability of detecting the out-of-control subgroups in phase I under the different types of disturbances. It might be used as a powerful tool by quality control practitioners and researchers for efficient monitoring and decision making in their practice.



## CHAPTER 5

# CONCLUSION AND FUTURE RESEARCH

In this thesis, we studied different estimation strategies for some statistical models. Particularly, we considered ARCH model, simple linear regression models with applications in statistical quality control and the CV parameter under different environments.

The following estimation strategies are discussed in this thesis

1. Application and comparison of restricted ( $\beta_1^R$ ), pretest ( $\beta^{PT}$ ), James-Stein shrinkage ( $\beta^S$ ) and positive James-Stein shrinkage ( $\beta^{S+}$ ) estimators for the ARCH model.
2. Application and comparison of restricted and pretest estimators of the simple linear regression model that was carried out by Khan and Hoque (2002); Khan et al. (2005), then they have been used to construct efficient control charts for simultaneous linear profiling.

3. We studied the effect of different CV estimators in the performance of the CV control charts in phase I.

We compared the performance of the proposed estimators with the classical MLE estimate when a UPI is available. We extracted the UPI by using model selection criteria, particularly we used AIC and BIC criteria.

We summarize the findings as follow:

In Chapter 2, we proposed restricted, pretest and shrinkage estimators for a vector of parameters  $\boldsymbol{\theta}$  in the ARCH model, the estimators were driven under the general linear restriction  $R\boldsymbol{\theta} = \boldsymbol{r}$ . We drove the joint asymptotic distribution of the unrestricted and restricted estimator then, we obtained the asymptotic quadratic risks, the quadratic biases and the asymptotic quadratic mean square error of the proposed estimators. We conducted analytical comparisons of the relative dominance of these estimators with respect to the unrestricted estimator of  $\boldsymbol{\theta}$ . We also carried out an intensive Monte Carlo simulation study by considering different scenarios to compare these estimators in terms of their relative mean squared errors. A real world problem has been considered as a case study, we tried to forecast the volatility in Standard & Poor 500 (SP500) stock market data, we selected the sub-model via stepwise selection procedures based on the AIC and BIC criteria. Our findings indicate that, it is better to use the positive James-Stein estimator as it outperforms all other estimators.

In chapter 3, we introduced the idea of the Bayesian statistics in the SPC by involving the available UPI into the parameters estimation, we adopted the restricted and the pretest estimators of the simple linear regression model to constructed the control charts of linear profile under EWMA structure. As a result, we came up with two control charts  $EWMA_R$  and  $EWMA_{PT}$ . The results showed that, the  $EWMA_R$  control chart outperforms all the other control charts under the different values of shifts in the slope and the error variance of the considered linear profile. In contrast, the traditional control chart (EWMA\_3) and the proposed control charts performed similarly under the shifts in the linear profile intercept, that was due to the useless of the UPI that caused by the adjusted explanatory variable. Overall,  $EWMA_R$  performed better under smaller values of *distrust constant*  $d$  and small shifts, whereas  $EWMA_{PT}$  with the smaller values of  $d$  was the worse. Under the larger values of  $d$ , the performance of  $EWMA_R$  and  $EWMA_{PT}$  dropped towards the performance of EWMA\_3 and they performed similarly when  $d = 0$ .

In chapter 4, we investigated the choice of an appropriate control charting structure for efficient monitoring of process CV parameter in phase I. We studied the performance of different CV control chart structures under the effect of two types of CV disturbances, and three location estimators where used in the control charts structures. The probability to signal was used as the performance measure. The  $\tilde{W}$  and  $V_p$  charts showed the best ability for detecting the out-of-control subgroups

in phase I under different types of disturbances.  $\tilde{W}$  can be used as a powerful tool by quality control practitioners and researchers for efficient monitoring of the CV in phase I.

## 5.1 Future Research

There is an urgent demand to extend the shrinkage estimation strategy to the other models in GARCH family. In addition, we will consider more sophisticated cases of the corresponding errors term in each model.

For our future research in Chapter 3, we may consider the linear profile with variable values for the predictor instead of taking constant values. Researchers may also consider the linear profile of multiple linear regression in order to take the advantage of shrinkage estimation strategies. However it is complicated to use the simultaneous linear profiling without removing the correlation between the intercept and the slope, we may investigate the structures of the control charts without removing their correlation in order to take the advantage of the restricted and the pretest under the shifts in the intercept.

In Chapter 4, it is recommended to investigate the performance of the proposed control charts with the CV disturbances generated from fat-tailed probability distributions.

# Appendix

## A.1 Courant Theorem

**Theorem A.1** (*Courant Theorem*). Let  $\lambda_1, \dots, \lambda_n$  be the characteristic roots of an  $n \times n$  matrix  $A$  such that  $\min \lambda_i = \lambda_1$ ,  $\max \lambda_i = \lambda_n$ , and let  $v_1, \dots, v_n$  be the characteristic vectors. Then  $\mathbf{A} = \lambda_1 v_1 v_1' + \dots + \lambda_n v_n v_n'$ ,  $\mathbf{I} = v_1 v_1' + \dots + v_n v_n'$ :  
 $\text{Sup} \left( \frac{x'Ax}{xx'} \right) = \lambda_n$  and  $\text{Inf} \left( \frac{x'Ax}{xx'} \right) = \lambda_1$ . Hence,

$$Ch_{\min}(A) \leq \frac{x'Ax}{xx'} \leq Ch_{\max}(A), \quad (\text{A.1})$$

where

$$\min_i \lambda_i = Ch_{\min}(A) \quad \text{and} \quad \max_i \lambda_i = Ch_{\max}(A). \quad (\text{A.2})$$

## A.2 Adjustment Constants ( $d_2$ and $d_3$ )

Table A.1: Control chart coefficients  $d_2$  and  $d_3$  for different CV control charts.

	5			10			15		
$\gamma$	0.05	0.1	0.15	0.05	0.1	0.15	0.05	0.1	0.15
$d_{2\bar{W}}$	0.9451	0.9439	0.9483	0.97	0.9735	0.9743	0.9844	0.9843	0.9834
$d_{3\bar{W}}$	0.3423	0.3427	0.3499	0.2315	0.2343	0.2368	0.1889	0.1892	0.192
$d_{2\bar{W}_p}$	0.921	0.9132	0.9158	0.9613	0.9634	0.9621	0.9768	0.9772	0.9765
$d_{3\bar{W}_p}$	0.3474	0.3433	0.3504	0.2336	0.2351	0.2412	0.1878	0.187	0.1894
$d_{2W_p}$	0.4999	0.5009	0.5025	0.4999	0.5001	0.5014	0.5	0.4999	0.5007
$d_{3W_p}$	0.502	0.5031	0.5048	0.5009	0.5011	0.5024	0.5006	0.5006	0.5014
$d_{2\bar{V}}$	2.3395	2.3366	2.3506	3.0690	3.0811	3.0895	3.4829	3.4789	3.4790
$d_{3\bar{V}}$	0.8692	0.8736	0.8983	0.7970	0.8042	0.8191	0.7625	0.7668	0.7802
$d_{2\bar{V}_p}$	2.2682	2.2497	2.2584	3.0200	3.0197	3.0268	3.4239	3.4185	3.4204
$d_{3\bar{V}_p}$	0.8717	0.8639	0.8902	0.8030	0.7952	0.8184	0.7503	0.7462	0.7635
$d_{2V_p}$	1.2405	1.2448	1.2512	1.5892	1.5908	1.5955	1.7763	1.7774	1.7814
$d_{3V_p}$	1.2459	1.2506	1.2573	1.5928	1.5946	1.5994	1.7792	1.7805	1.7845

# REFERENCES

# REFERENCES

- S. A. Abbasi, M. Riaz, A. Miller, and S. Ahmad. On the Performance of Phase I Dispersion Control Charts for Process Monitoring. *Quality and Reliability Engineering International*, 31(8):1705–1716, 2015. ISSN 10991638. doi: 10.1002/qre.1703.
- R. Aggarwal, J. F. Lawless, and R. J. Mackay. Analysis of variation transmission in manufacturing processes II. *Journal of Quality Technology*, 31(2):143–154, 1999.
- S. E. Ahmed, a. Hussein, and M. Al-Momani. Efficient estimation for the conditional autoregressive model. *Journal of Statistical Computation and Simulation*, 85(13):2569–2581, 2015. ISSN 0094-9655. doi: 10.1080/00949655.2014.893346.
- M. Al-Momani. *Shrinkage and Penalty Estimation Strategies in Some Spatial Models*. PhD thesis, University of Windsor, Ontario, Canada, 2013.
- M. Al-Momani, A. A. Hussein, and S. E. Ahmed. Penalty and related estimation strategies in the spatial error model. *Statistica Neerlandica*, 2016. ISSN 00390402. doi: 10.1111/stan.12098.



- T. A. Bancroft. On biases in estimation due to the use of preliminary tests of significance. *The Annals of Mathematical Statistics*, 15(2):190–204, 1944.
- T. Bollerslev. Generalized autoregressive conditional heteroskedasticity. *Journal of econometrics*, 31(3):307–327, 1986.
- M. E. Calzada and S. M. Scariano. A synthetic control chart for the coefficient of variation. *Journal of Statistical Computation and Simulation*, 83(5):853–867, 2013.
- P. Castagliola, L. Universit, and G. Celano. Monitoring the Coefficient of Variation Using EWMA Charts. *Journal of Quality Technology*, 43(3):249–265, 2011. ISSN 0022-4065.
- P. Castagliola, A. Achouri, H. Taleb, G. Celano, and S. Psarakis. Monitoring the coefficient of variation using a variable sampling interval control chart. *Quality and Reliability Engineering International*, 29(8):1135–1149, 2013. ISSN 07488017. doi: 10.1002/qre.1465.
- J. E. Connett and W. Wong Lee. Estimation of the coefficient of variation from laboratory analysis of split specimens for quality control in clinical trials. *Controlled Clinical Trials*, 11(1):24–36, 1990. ISSN 01972456. doi: 10.1016/0197-2456(90)90029-2.
- S. V. Crowder and M. D. Hamilton. An EWMA for monitoring a process standard deviation. *Journal of quality technology*, 24(1):12–21, 1992. ISSN 0022-4065.
- H. Darcy. Les fontaines publique de la ville de dijon. *Dalmont, Paris*, 647, 1856.

- D. Ding, F. Tsung, and J. Li. Ordinal profile monitoring with random explanatory variables. *International Journal of Production Research*, 55(3):736–749, 2017. ISSN 0020-7543. doi: 10.1080/00207543.2016.1204476.
- Z. Ding, C. W. Granger, and R. F. Engle. A long memory property of stock market returns and a new model. *Journal of empirical finance*, 1(1):83–106, 1993.
- M. O. Elobeid, L. M. Alhems, A. Al-Sarkhi, A. Ahmad, S. M. Shaahid, M. Basha, J. Xiao, R. Lastra, and C. E. Ejim. Effect of inclination and water cut on venturi pressure drop measurements for oil-water flow experiments. *Journal of Petroleum Science and Engineering*, 147:636–646, 2016.
- R. F. Engle. Autoregressive conditional heteroscedasticity with estimates of the variance of united kingdom inflation. *Econometrica: Journal of the Econometric Society*, pages 987–1007, 1982.
- R. F. Engle. Estimates of the variance of us inflation based upon the arch model. *Journal of Money, Credit and Banking*, 15(3):286–301, 1983.
- R. F. Engle and T. Bollerslev. Modelling the persistence of conditional variances. *Econometric reviews*, 5(1):1–50, 1986.
- B. Everitt. *The Cambridge Dictionary of Statistics Cambridge University Press*. Cambridge University Press, UK New York, 1998. ISBN ISBN 0521593468.
- E. F. Fama. The behavior of stock-market prices. *The journal of Business*, 38(1):34–105, 1965.

- C. Francq and J.-M. Zakoïan. Strict stationarity testing and estimation of explosive and stationary generalized autoregressive conditional heteroscedasticity models. *Econometrica*, 80(2):821–861, 2012.
- C. Francq and J. Zikoïan. Garch models: Structure, statistical inference and financial applications, 2010.
- C. Francq, J.-M. Zakoïan, et al. Maximum likelihood estimation of pure garch and arma-garch processes. *Bernoulli*, 10(4):605–637, 2004.
- D. A. Freedman et al. Bootstrapping regression models. *The Annals of Statistics*, 9(6):1218–1228, 1981.
- S. Gupta, D. C. Montgomery, and W. H. Woodall. Performance evaluation of two methods for online monitoring of linear calibration profiles. *International Journal of Production Research*, 44(10):1927–1942, 2006. ISSN 0020-7543. doi: 10.1080/00207540500409855.
- L. P. Hansen. Large sample properties of generalized method of moments estimators. *Econometrica: Journal of the Econometric Society*, pages 1029–1054, 1982.
- E. P. Hong, C. W. Kang, J. W. Baek, and H. W. Kang. Development of CV control chart using EWMA technique. *Journal of the society of Korea Industrial and Systems Engineering*, 31(4):114–120, 2008.
- L. Huwang, C. J. Huang, and Y. H. T. Wang. New EWMA control charts for

- monitoring process dispersion. *Computational Statistics and Data Analysis*, 54 (10):2328–2342, 2010. ISSN 01679473. doi: 10.1016/j.csda.2010.03.011.
- W. a. Jensen, L. A. Jones-farmer, C. W. Champ, and W. H. Woodall. Effects of Parameter Estimation on Control Chart Properties : A Literature Review. *Journal of Quality Technology*, 38(4):349–364, 2006. ISSN 0022-4065.
- L. A. Jones-Farmer and C. W. Champ. A Distribution-Free phase I control chart for subgroup scale. *Journal of Quality Technology*, 42(4):373–387, 2010. ISSN 00224065.
- C. W. Kang, M. A. N. S. Lee, and D. M. Hawkins. A Control Chart for the Coefficient of Variation. *Journal of Quality Technology*, 39(2):151–158, 2007.
- L. Kang and S. Albin. On-line monitoring when the process yields a linear. *Journal of Quality Technology*, 32(4):418–426, 2000.
- M. S. Khan. The variability of expectations in hyperinflations. *The Journal of Political Economy*, pages 817–827, 1977.
- S. Khan and Z. Hoque. Estimation of the slope parameter for linear regression model with uncertain prior information. *Journal of Statistical Reserach*, 36: 55—73, 2002.
- S. Khan, Z. Hoque, and A. K. M. E. Saleh. Estimation of the intercept parameter for linear regression model with uncertain non-sample prior information. *Statistical Papers*, 46(3):379–395, jul 2005. ISSN 0932-5026. doi: 10.1007/BF02762840.

- K. Kim, M. Mahmoud, and W. Woodall<sup>1</sup>. ASQ: On The Monitoring of Linear Profiles. *Journal of Quality Technology*, 35(3):317–328, 2003. ISSN 0361-0926. doi: 10.1080/03610920701653136.
- B. Klein. The demand for quality-adjusted cash balances: Price uncertainty in the us demand for money function. *The Journal of Political Economy*, pages 691–715, 1977.
- J. F. Lawless. *Statistical models and methods for lifetime data*. 2002. ISBN 0471372153.
- P. E. Maravelakis and P. Castagliola. An EWMA chart for monitoring the process standard deviation when parameters are estimated. *Computational Statistics and Data Analysis*, 53(7):2653–2664, 2009. ISSN 01679473. doi: 10.1016/j.csda.2009.01.004.
- S. K. McNees. *The forecasting record for the 1970s*. Federal Reserve Bank of Boston, 1980.
- D. Montgomery. *Introduction to statistical quality control*. 2009. ISBN 9780470169926. doi: 10.1002/1521-3773(20010316)40:6;9823::AID-ANIE9823;3.3.CO;2-C.
- R. Noorossana, M. Eyvazian, and A. Vaghefi. Phase II monitoring of multivariate simple linear profiles. *Computers and Industrial Engineering*, 58(4):563–570, 2010. ISSN 03608352. doi: 10.1016/j.cie.2009.12.003.

- M. Riaz, T. Mahmood, S. A. Abbasi, N. Abbas, and S. Ahmad. Linear profile monitoring using EWMA structure under ranked set schemes. *The International Journal of Advanced Manufacturing Technology*, 2017. ISSN 0268-3768. doi: 10.1007/s00170-016-9608-y.
- R. W. Rich, J. Raymond, and J. Butler. Generalized instrumental variables estimation of autoregressive conditional heteroskedastic models. *Economics Letters*, 35(2):179–185, 1991.
- A. M. E. Saleh. *Theory of preliminary test and Stein-type estimation with applications*, volume 517. John Wiley & Sons, 2006.
- S. Satchell and J. Knight. *Forecasting Volatility in the Financial Markets*. Butterworth-Heinemann, 2002.
- M. Schoonhoven and R. J. Does. A Robust Standard Deviation Control Chart. *Technometrics*, 54(1):73–82, 2012. ISSN 0040-1706. doi: 10.1080/00401706.2012.648869.
- M. Schoonhoven, M. Riaz, and R. J. M. M. Does. Design and Analysis of Control Charts for Standard Deviation with Estimated Parameters. *Journal of Quality Technology*, 43(4):307—333, 2011. ISSN 00224065.
- J. J. H. Shiau and J. H. Sun. A new strategy for Phase I analysis in SPC. *Quality and Reliability Engineering International*, 26(5):475–486, 2010. ISSN 07488017. doi: 10.1002/qre.1075.

- R. R. Sokal and F. J. Rohlf. Biometry, 3rd edn New York. NY: *WH Freeman and Company*, 1995.
- S. L. Soo, J. J. Stukel, and J. M. Hughes. Measurement of mass flow and density of aerosols in transport. *Environmental Science & Technology*, 3(4):386–393, 1969.
- H. S. Stefan. EWMA Control Charts with Time-Varying Control Limits and Fast Initial Response. *Journal of Quality Technology*, 31(1):75, 1999. ISSN 00224065.
- C. Stein. Inadmissibility of the usual estimator for the mean of a multivariate normal distribution. *Proceedings of the Third Berkeley symposium on . . .*, 1956.
- C. Stein. An approach to the recovery of interblock information in balanced incomplete block designs. *Research paper in statistics: Festschrift for J. Neyman*, pages 351–366, 1966.
- C. Stein et al. Inadmissibility of the usual estimator for the mean of a multivariate normal distribution. In *Proceedings of the Third Berkeley symposium on mathematical statistics and probability*, volume 1, pages 197–206, 1956.
- F. S. Stover and R. V. Brill. Statistical quality control applied to ion chromatography calibrations. *Journal of Chromatography A*, 804(1-2):37–43, apr 1998. ISSN 00219673. doi: 10.1016/S0021-9673(98)00094-6.
- S. Taylor. Modelling financial time series, 1986.

Tsay. *Analysis of Financial Time Series*, volume 48. 2006. ISBN 0471415448.

doi: 10.1198/tech.2006.s405.

R. S. Tsay. *Analysis of financial time series*. John Wiley & Sons, 2002.

A. A. Weiss. Asymptotic theory for arch models: estimation and testing. *Econometric theory*, 2(01):107–131, 1986.

D. Wuertz, Y. Chalabi, and M. Miklovic. fgarch: Rmetrics-autoregressive conditional heteroskedastic modelling, r package version 290.76, 2008.



# Vitae

- Name: Abdaljbbar Babiker Abdaljbbar Dawod
- Nationality: Sudanese
- Date of Birth: MARCH-13-1987
- Permanent Address: Giad Industrial City, Mobile: (+249) 913440501, email: *abdaljbbar@gmail.com/abdaljbbar@uofk.edu*, Khartoum, Sudan.
- **Education:** B.Sc.(honour) in Statistics & Computer Sciences, Division I class II, Faculty of Mathematical Sciences, University of Khartoum, Sudan (2010).
- **Experience**
  - Full time teaching assistant, Faculty of mathematical sciences, University of Khartoum, April 2013 - Present.
  - Software developer, Soba University Hospital, Khartoum, Sudan, February 2012 - February 2014.
  - Statistician, Statistical Consulting Unit, University of Khartoum, August 2010 - December 2011.
- **PUBLICATIONS**

- Dawod, A., Riaz, M. and Abbasi, S.A., 2016. *On Model Selection for Autocorrelated Processes in Statistical Process Control*. Quality and Reliability Engineering International. DOI: 10.1002/qre.2063
- Dawod, A. and Al-Momani, M. *Efficient Estimation Strategies in ARCH Model*. Journal of the Korean Statistical Society (submitted).
- Dawod, A., Abbasi, S.A. and Al-Momani, M., *On the Performance of Coefficient of Variation Control Charts in Phase I*. Quality and Reliability Engineering International.(submitted).
- Dawod, A., Al-Momani, M. and Abbasi, S.A., *On Efficient Estimation Strategies in Monitoring of Linear Profiles*. The International Journal of Advanced Manufacturing Technology.